

2022

Characterization of biochar as a carbon regulator in manure and environmental management applications

Josephine Getz

Technological University Dublin, d17125048@mytudublin.ie

Follow this and additional works at: <https://arrow.tudublin.ie/built/doc>

 Part of the [Civil and Environmental Engineering Commons](#)

Recommended Citation

Getz, J. (2022). Characterization of biochar as a carbon regulator in manure and environmental management applications. Technological University Dublin. DOI: 10.21427/5WRK-4P11

This Theses, Ph.D is brought to you for free and open access by the Built Environment at ARROW@TU Dublin. It has been accepted for inclusion in Doctoral by an authorized administrator of ARROW@TU Dublin. For more information, please contact arrow.admin@tudublin.ie, aisling.coyne@tudublin.ie, vera.kilshaw@tudublin.ie.



This work is licensed under a [Creative Commons Attribution-NonCommercial-Share Alike 4.0 International License](#).

Characterization of biochar as a carbon regulator in manure and environmental management applications

Josephine Getz

Supervised by:

Dr. Alan Gilmer

Prof. John Cassidy

Dr. Vivienne Byers

PhD thesis

School of Architecture, Building & Environment

Technological University Dublin

October 2022

Abstract

Biochar is a product of pyrolysis, which is the thermal decomposition of materials at elevated temperatures (300 - 900 °C) in an oxygen-limited atmosphere. Biochar has been recognized as a potentially vital tool to help reduce the climate change impact. It has been used in the agricultural sector as an addition to reduce greenhouse gas emissions in several animal husbandry settings. The application in the animal sector is an important point to reduce the overall amount of greenhouse gases released as this sector produces many greenhouse gases. Though not in every case a reduction of emissions was the result of the addition of biochar. This study analysed five feedstocks (peat, peat fibre, fine urban green waste and two types of brewery waste) and the resulting biochars to evaluate how pyrolysis at various temperatures affects the properties of the resultant biochars and how those different properties influence the potential of biochars to adsorb emissions from manure. Increasing pyrolysis temperature has been noted to lead to a decrease in volatile matter content for all feedstocks used, whereas the surface area and the fixed carbon content of the resultant biochars were shown to lead to an increase. This suggests that higher production temperatures are optimal to produce more stable biochars, which makes biochars an excellent material to sequester carbon, but this comes at a cost in energy demand and environmental terms. The study has examined the application of the resultant biochars in the regulation of greenhouse gas emissions associated with piggery manure management and was able to demonstrate the optimal configurations of biochar type and production process in regulating associated GHG emissions from the manure used in this study, which came from Germany. In addition, the biochars were used and able to adsorb dissolved organics from water. The results found here broaden the knowledge about the characterisation of biochars, and their applications and can potentially be used to include more biochar applications into policy.

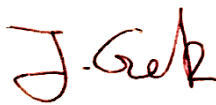
Declaration

I certify that this thesis which I now submit for examination for the award of PhD, is entirely my own work and has not been taken from the work of others, save and to the extent that such work has been cited and acknowledged within the text of my work.

This thesis was prepared according to the regulations for graduate study by research of the Technological University Dublin and has not been submitted in whole or in part for another award in any other third level institution.

The work reported on in this thesis conforms to the principles and requirements of the TU Dublin's guidelines for ethics in research.

TU Dublin has permission to keep, lend or copy this thesis in whole or in part, on condition that any such use of the material of the thesis be duly acknowledged.

Signature: 

Date: 16.10.2022

Candidate

Acknowledgements

I would like to thank my supervisors Dr Alan Gilmer, Professor John Cassidy and Dr Vivienne Byers for their support during the last years, and Scott Banks from Energy & Bioproducts Research Institute at Aston University, Birmingham, UK for the help with elemental analysis. Dr.-Ing. habil Dirk Weichgrebe and Karen Kock from the Leibniz University Hanover, Germany for their support and cooperation during my time at the university and Dr.-Ing. Corinna Lorey from the Leibniz University Hanover, Germany for help with the gas chromatograph. Furthermore, I want to thank Denise Denning and Luke O'Neill from the FOCAS Institute, TU Dublin for the help with the scanning electron microscope and RAMAN spectroscopy as well as Filipe Rego and Stelios Stefanidis from Energy & Bioproducts Research Institute at Aston University, Birmingham, UK for the support with Brunauer–Emmett–Teller and thermogravimetric analysis.

List of Abbreviations

As	arsenic
ATR	Attenuated total reflection
BET	Brunauer–Emmett–Teller
B	boron
B black	brewery grain black
B white	brewery grain white
Br	bromine
C	Carbon
Ca	calcium
Cd	cadmium
CH ₄	methane
Co	Cobalt
Cu	copper
CO ₂	carbon dioxide
CO ₂ -eq	carbon dioxide equivalent
CR	Congo red
CV	crystal violet
daf	dry basis, ash-free
db	dry basis
DM	dry matter
EF _{CH₄}	emission factor for methane
FC	fixed carbon
Fe	iron
Fine ugw	fine urban green waste
FM	fresh matter
FTIR	Fourier-transform infrared spectroscopy
GC	gas chromatograph
GHG	greenhouse gas

H	hydrogen
ICP-MS	inductively-coupled-plasma mass-spectrometry
K	potassium
MB	methylene blue
MG	malachite green
Mg	magnesium
Mn	manganese
MO	methyl orange
N	nitrogen
Na	sodium
Ni	nickel
NH ₃	ammonia
NH ₄	ammonium
N ₂ O	nitrous oxide
O	oxygen
P	phosphorus
P fibre	peat fibre
PAH	polycyclic aromatic hydrocarbon
Pb	lead
PFO	Pseudo-first order
PSO	Pseudo-second order
S	sulphur
SEM	scanning electron microscope
TGA	thermogravimetric analysis
VM	volatile matter
w/v	weight to volume
wt	weight total
Zn	zinc

Table of content

Table of tables.....	3
Table of figures.....	5
1. Introduction.....	8
1.1 Rationale	9
1.2 Aim & objectives	10
2. Literature review.....	11
2.1 Manure management and emission reduction.....	11
2.1.1 Animal husbandry and the influence on greenhouse gas emissions	11
2.1.2 Manure management.....	12
2.1.3 Emission reduction through biochar application.....	14
2.2 Adsorption of organics from water	19
2.3 Biochar.....	21
2.4 Applications of biochar.....	23
2.5 Production and characterisation of biochars	27
2.5.1 Pyrolysis.....	27
2.5.2 Characterisation of biochars.....	29
2.6 Biochar feedstocks and applications	34
2.7 Peat and brewery grain.....	42
2.7.1 Peat.....	42
2.7.2 Brewery grain.....	47
3. Methodology and methods.....	48
3.1. Origin of organic feedstocks.....	49
3.2. Preparation of materials	51
3.3. Production of biochars	52
3.4. Chemical analysis – pH, dry matter and moisture content.....	52
3.5. Thermo-gravimetric analysis (TGA)	53
3.6. Nitrogen physisorption (BET)	54
3.7. Scanning electron microscopy (SEM)	54
3.8. Fourier Transform Infrared spectroscopy/Attenuated total reflection (FT-IR/ATR)..	56
3.9. Polycyclic aromatic hydrocarbons (PAH)	56
3.10. RAMAN spectroscopy.....	57
3.11. Elemental analysis (CHNS)	57

3.12.	ICP-MS	57
3.13.	Manure emission experiments	58
3.13.1.	Manure	58
3.13.2.	Gas emission experiment set-up.....	59
3.14.	Dye adsorption experiments.....	60
3.14.1.	Experimental arrangement	60
3.14.2.	Adsorption isotherm models	61
3.14.3.	Adsorption kinetics – Pseudo-First Order and Pseudo-Second Order	62
3.15.	Statistical analysis	63
4.	Results.....	64
4.1.	Biochar yield.....	64
4.2.	Feedstock analysis – dry matter & moisture content, pH	66
4.3.	TGA results.....	69
4.4.	BET results.....	74
4.5.	SEM results.....	77
4.6.	ATR / FT-IR results	80
4.7.	PAH results	84
4.8.	RAMAN spectroscopy results	85
4.9.	CHNS results	90
4.10.	ICP-MS results.....	99
4.11.	Gas emission experiment results.....	103
4.12.	Adsorption results of dye onto biochars.....	107
5.	Discussion	112
5.1.	Chemo-physical analysis of biochar produced from waste materials in comparison to a peat-based feedstock from drained Irish ombrotrophic peatlands	112
5.2.	Potential control of CO ₂ , CH ₄ and NH ₃ from swine manure	124
5.3.	Potential adsorption of organics like dye and therefore potentially other contaminants from water.....	127
5.4.	Future work.....	129
6.	Conclusion	130
	References.....	133
	Appendix.....	151

Table of tables

Table 1: Summary of results found in the literature regarding emission reduction after biochar application.....	16
Table 2: Production parameter of biochars produced using a muffle furnace	29
Table 3: Costs and benefits of biochar feedstocks (McCarl et al., 2009)	37
Table 4: Comparison of the elemental composition of feedstocks and biochars (Taherymoosavi et al., 2017; Hu et al., 2019) (%db = % on a dry basis)	39
Table 5: properties of hardwood biochar and manure used in the study (Ippolito et al., 2016)..	41
Table 6: peatlands in Finland, Ireland, the UK and the whole of Europe (Tanneberger et al., 2017)	42
Table 7: peat-based biochar analysis done by UKBRC (%db = % dry basis), data provided by Bord na Móna	44
Table 8: metal analysis results of moss peat samples (UKBRC), data provided by Bord na Móna	44
Table 9: Proximate and ultimate analysis of peat (0.5-2.0mm sieve size) and biochars obtained from varying heating rates (df, %) (Sutcu, 2007)	45
Table 10: properties of peat biochar produced at 400°C for 4h.....	47
Table 11: Overview of methods and equipment used to analyse the biochars	49
Table 12: Feedstocks used in the project as well as their sample date and origin	50
Table 13: Feedstocks used for biochar production and exemplarity biochars produced from these feedstocks	51
Table 14: Conditions of biochar production ranging from 450 – 750 °C	52
Table 15: Analytical methods used for the chemical characterisation of feedstocks and biochars	52
Table 16: biochar - slurry mixtures for emission reduction trials.....	58
Table 17: Ingredients of pig feed.....	58
Table 18: Weender Analysis of ingredients of the pig feed.....	58
Table 19: chemical analysis of pig manure used for emission trials.....	59
Table 20: dilutions used in the adsorption experiments with the respective initial concentration of dye in mg L ⁻¹ (ppm).....	61
Table 21: Biochar yield (%FM) calculated for different production temperatures as described in section 3.3	64
Table 22: Biochar yield of fresh materials (%DM) calculated for different production temperatures as described in section 3.3.....	65
Table 23: Biochar yield (%DM) calculated for different production temperatures as described in section 3.3	65
Table 24: dry matter, moisture content and pH results obtained from feedstocks used for biochar production	67
Table 25: pH values of feedstocks in comparison to biochars produced at 450 - 750 °C from fresh material	68
Table 26: pH values of biochar produced from pre-dried material.....	68
Table 27: results obtained by thermo-gravimetric analysis of all five materials	71
Table 28: Fixed carbon content calculated on a dry ash-free basis using the formula published by (Riley, 2007)	72
Table 29: CHNS results from all twenty biochars	91

Table 30: H/C and O/C ratios of biochars produced between 450-750°C from five different materials.....	96
Table 31: ICP-MS results of all biochars analysed in a 1:1000 dilution, part 1	99
Table 32: ICP-MS results of all biochars analysed in a 1:1000 dilution, part 2	99
Table 33: Adsorption of malachite green onto biochars at different dilutions.....	108
Table 34: Adsorption kinetics of malachite green onto biochars at different dilutions	110
Table 35: sixteen PAHs which have been designated High Priority Pollutants by the Environmental Protection Agency (EPA); in no specific order	118
Table 36: a schematic overview of the impact of rising production temperatures on the characteristics of biochar	124
Table 37: D- and G- band values of biochars obtained through Raman analysis	152

Table of figures

Figure 1: Greenhouse gas emissions by source sector in the EU in 2020 (Eurostat, 2020).....	12
Figure 2: GHG emissions from cattle manure from the a) low emitting, b) reference and c) high emitting scenarios per farm size and management practise (Aguirre-Villegas and Larson, 2017)	13
Figure 3: Conversion efficiency of biomass, C, N and P during pyrolysis ((data from Enders et al. (2012); typical losses followed by range in brackets) by Lehmann and Joseph, 2015).....	23
Figure 4: The 17 sustainability and development goals as stated by the United Nations (The global goals, 2022).....	24
Figure 5: carbon cycle with and without biochar application (Lehmann, 2007; Bahuguna, Sharma and Dadarwal, 2021).....	26
Figure 6: Conversion of biomass into biochars, fuels and other products presented by Richard L. Bain at the DOE/NASLUGC Biomass and Solar Energy Workshops in 2004 (Bain, 2004)	30
Figure 7: Van Krevelen diagram showing changes in O/C and H/C ratios from feedstocks to biochars (Oliveira et al., 2017).....	31
Figure 8: methodological flowchart of the thesis.....	48
Figure 9: Reaction after the incident beam reaches the sample	55
Figure 10: Scheme of a scanning electron microscope	55
Figure 11: Experimental set-up of the emission trials run with swine manure and biochar	60
Figure 12: Dry matter (DM) and moisture content of feedstocks used for biochar production in %FM	67
Figure 13: Volatile matter content of biochars produced from pre-dried materials obtained from samples heated up to 900°C under nitrogen flow	69
Figure 14: Fixed carbon content of biochars produced from pre-dried materials obtained at 900°C under nitrogen flow.....	70
Figure 15: Ash content of biochars produced from pre-dried materials obtained at 900°C under airflow.....	70
Figure 16: TGA plot of biochar produced from b black at 450°C; Graph goes till the end of N ₂ run at the TGA	73
Figure 17: TGA plot of biochar produced from fine ugw at 750°C; Graph goes till the end of N ₂ run at the TGA	74
Figure 18: surface area of biochars produced from pre-dried materials	75
Figure 19: micropore area of biochars produced from pre-dried materials	75
Figure 20: average pore size of biochars produced from pre-dried materials.....	76
Figure 21: total pore volume of biochars produced from pre-dried materials	76
Figure 22: SEM picture of dried peat without treatment showing a smooth surface.....	77
Figure 23: SEM picture of biochar produced from peat at 750 °C with the porous surface.....	78
Figure 24: SEM image of dried brewery grain white showing a smooth surface before pyrolysis	78
Figure 25: SEM image of biochar produced from brewery grain white at 550°C with the porous and irregular surface	79
Figure 26: SEM image of dried fine urban green waste showing a smooth surface.....	79
Figure 27: SEM image of biochar produced from fine urban green waste at 650°C.....	80
Figure 28: ATR results of biochars produced from b black at various temperatures	82
Figure 29: ATR results of biochars produced from peat at various temperatures	83

Figure 30: chromatograph of 16 PAHs reference with total ion count mass spectrometer detector	84
Figure 31: PAH results of GC chromatograph of peat 750 biochar sample	85
Figure 32: RAMAN results overview of all 20 biochars	86
Figure 33: D and G band changes throughout the samples.....	87
Figure 34: D/G intensity ratio in relation to production temperature for b white biochars	88
Figure 35: D/G intensity ratio in relation to production temperature for b black biochars.....	88
Figure 36: D/G intensity ratio in relation to production temperature for peat fibre biochars	89
Figure 37: D/G intensity ratio in relation to production temperature for peat biochars.....	89
Figure 38: Carbon content of biochars produced at four different temperatures from five different materials (**** p<0.0001, *** p<0.001, ** p<0.01, * p<0.05 for samples which are significantly different from the biochar produced at 450 °C; ++++ p<0.0001, +++ p<0.001, ++ p<0.01, + p<0.05 for samples which are significantly different from the biochar produced at 550 °C; and ---- p<0.0001, --- p<0.001, -- p<0.01, - p<0.05 for samples which are significantly different from the biochar produced at 650 °C).....	92
Figure 39: hydrogen content of biochars produced at four different temperatures from five different materials (**** p<0.0001, *** p<0.001, ** p<0.01, * p<0.05 for samples which are significantly different from the biochar produced at 450 °C; ++++ p<0.0001, +++ p<0.001, ++ p<0.01, + p<0.05 for samples which are significantly different from the biochar produced at 550 °C; and ---- p<0.0001, --- p<0.001, -- p<0.01, - p<0.05 for samples which are significantly different from the biochar produced at 650 °C).....	93
Figure 40: nitrogen content of biochars produced at four different temperatures from five different materials (**** p<0.0001, *** p<0.001, ** p<0.01, * p<0.05 for samples which are significantly different from the biochar produced at 450 °C; ++++ p<0.0001, +++ p<0.001, ++ p<0.01, + p<0.05 for samples which are significantly different from the biochar produced at 550 °C; and ---- p<0.0001, --- p<0.001, -- p<0.01, - p<0.05 for samples which are significantly different from the biochar produced at 650 °C).....	94
Figure 41: oxygen content of biochars produced at four different temperatures from five different materials (**** p<0.0001, *** p<0.001, ** p<0.01, * p<0.05 for samples which are significantly different from the biochar produced at 450 °C; ++++ p<0.0001, +++ p<0.001, ++ p<0.01, + p<0.05 for samples which are significantly different from the biochar produced at 550 °C; and ---- p<0.0001, --- p<0.001, -- p<0.01, - p<0.05 for samples which are significantly different from the biochar produced at 650 °C).....	95
Figure 42: Van Krevelen diagram of all twenty biochars produced from five materials at four temperatures with EBC and IBI limits for H/C and O/C molar ratios (International Biochar Initiative, 2015; EBC (2012-2022), 2022).....	97
Figure 43: Van Krevelen Diagram trends throughout the materials for biochars produced at four temperatures.....	98
Figure 44: ICP-MS results for 1:1000 dilution of low concentrations elements in mg kg ⁻¹	101
Figure 45: ICP-MS results for 1:1000 dilution of high concentration elements in mg kg ⁻¹	101
Figure 46: ICP-MS results of the 1:10 dilution for P in mg kg ⁻¹	102
Figure 47: ICP-MS results of the 1:10 dilution for Mn and Zn in mg kg ⁻¹	102
Figure 48: ICP-MS results of the 1:10 dilution.....	103
Figure 49: NH ₄ remaining in the filtered manure/biochar including the amount of NH ₄ remaining in the control (black line); tested with cuvette test	103
Figure 50: A screenshot of one of the chromatographs taken during GC analysis of the gas emission samples; 1 st peak air (N ₂ and O ₂), 2 nd peak CH ₄ , 3 rd peak CO ₂ (two repetitions).....	105

Figure 51: GC results for the CH ₄ content of gases released from biochar manure mixtures after three days in mg/L	105
Figure 52: GC results for the CO ₂ content of gases released from biochar manure mixtures after three days in mg/L	107
Figure 53: Milligram of malachite green adsorbed onto one gram of biochar	108
Figure 54: Langmuir plots of adsorption experiments conducted with biochars produced at 750 °C	109
Figure 55: Freundlich plots of adsorption experiments with biochars produced at 750 °C	109
Figure 56: PFO kinetics calculated for fine ugw 450 in a 1-10 dilution of malachite green	111
Figure 57: PSO kinetics calculated for fine ugw 450 in a 1-10 dilution of malachite green	111
Figure 58: Schematic showing what is needed to reduce GHG emissions through biochar application.....	Fehler! Textmarke nicht definiert.

1. Introduction

Climate change is a natural process influenced by factors such as changes in the sun's intensity and processes within the climate system including changes in ocean and atmospheric circulation. More recently, due to emissions of greenhouse gases through human activities, climate change is being accelerated (Allen *et al.*, 2018; Eyring *et al.*, 2021). In 2018, the Intergovernmental Panel on Climate Change (IPCC), stated that human influence on climate has been the dominant cause of observed warming since the mid-20th century (Allen *et al.*, 2018). Examples of human activities contributing to climate change include carbon dioxide (CO₂) emissions through burning fossil fuels such as coal, oil, gas and peat, as well as methane (CH₄) and nitrous oxide (N₂O) emissions from agriculture (EPA, 2018).

EU directives require the member states to reduce their GHG emissions by more than 40% in 2030 (European Commission, 2020). An estimated 23% of total anthropogenic GHG emissions (2007-2016) derive from Agriculture, Forestry and Other Land Use (AFOLU) (Shukla *et al.*, 2020). AFOLU activities account for around 13% of CO₂, 44% of CH₄, and 81% of N₂O emissions from human activities globally during 2007 – 2016, making up the estimated 23% of total net anthropogenic emissions of GHGs (Shukla *et al.*, 2020). In the past decades, there have been many attempts to find the best solution to reduce GHG emissions in many fields of everyday life (e.g., transport, agriculture, and housing). A summary of negative emissions technologies (NETs) describes biochar as a biogenic removal and storage strategy with a low biodiversity risk and medium cost as well as a medium rating for carbon removal (McGeever *et al.*, 2018). To give an example, GHG management of agricultural wastes such as manure associated with Ireland's intensive animal production sector presents a special challenge. In 1990, 1904.53 kilotonnes of CO₂ equivalent were produced in Irish manure management, whereas in

2018, 1969.73 kilotonnes were emitted. The levels were decreasing until 2011 (1736.19 kilotonnes) but started rising afterwards. Therefore, optimal GHG management of manure-mediated emissions for this sector is important to reduce the emissions as required by law without cutting productivity. This is an example which applies to a lot of countries and could therefore have a great impact.

1.1 Rationale

The literature presents a broad range of materials used for pyrolysis as well as possible applications. Though it does leave a gap regarding biochar production from peat compared to defined other sources as well as their specific end applications, the regulation of GHG in manure management or their use in the field of adsorption of organics. Peat-based biochar and biochars produced from other waste sources can be added to manure management systems to reduce GHG emissions. However, the mechanisms behind this process are highly variable and very much case-dependent. Understanding the processes at play is a challenge, yet this understanding remains critical to developing tailor-made solutions to GHG control in these settings. This work seeks to explore the processes in biochar production in a way that aids understanding of the relationship between feedstock, production processes and specified end-use applications. The literature in this area remains incomplete. Hence, this project will provide new knowledge and insights into the use of Irish peat, spent brewery grains and urban green waste materials as a feedstock in the production of biochar. The project explores and contextualises the production of biochar and its application in agriculture in terms of GHG efflux regulation from swine manure management systems by way of example. The project defines the chemo-physical nature of the biochar production system using defined organic waste feedstocks (green waste and brewery waste) and compares this to biochars produced using peat from Irish peatlands.

1.2 Aim & objectives

This work aims to provide a deeper understanding of how slow pyrolysis changes a range of defined feedstocks. It also seeks to explore the potential to develop applications of the biochars in regulating GHG emissions from manure and the adsorption of model organic compounds. The research questions helping to achieve this aim are the following:

- How does the chemo-physical nature of the Biomass-Biochar production system change using waste materials like brewery grain or fine green waste in comparison to a peat-based feedstock from drained Irish ombrotrophic peatlands?
- Do Peat-based Biochars and Biochar produced from other biomass feedstocks have the potential to control the efflux of carbon dioxide (CO₂), methane (CH₄) and ammonia (NH₃) from swine manure and what are the processes controlling this potential?
- Are the biochars used in this study able to adsorb organic pollutants that are present in the run-off waters from the manure management cycle?

To address this aim and answer the questions the following objectives were identified:

- Develop protocols for biochar production from fresh and dried material
- Undertake extensive chemo-physical analysis of biochars
- Apply biochars to swine manure of defined composition in different concentrations to measure the effect on GHG emissions
- Apply biochars to organic dye-water mixes to evaluate the potential ability of the biochars to adsorb organic pollutants

2. Literature review

2.1 Manure management and emission reduction

Taking action on climate change is increasingly urgent, and sequestration in biomass and soil could play an important role. The conversion of biomass to biochar is a C sequestration strategy that can contribute to "negative emissions" (Cowie *et al.*, 2015).

2.1.1 Animal husbandry and the influence on greenhouse gas emissions

The EU-27 has a substantial population of livestock with 143 million pigs, 77 million bovine animals and 74 million sheep and goats in 2019 (Eurostat, 2020). Most of those pigs and bovine animals are located in just a few member states. The EU produced a provisional 22.8 million tonnes of pig meat in 2019 (Eurostat, 2020), with an output from the agricultural industry of 418 billion Euro. About two-fifths (38.6 %) of total output came from animals and animal products (EUR 161.4 billion), a majority coming from just milk and pigs (9.5 %) (Eurostat, 2020). These numbers indicate the importance of research looking into the impact of pig farming on climate change and greenhouse gas emissions. Within the EU the agricultural sector produced 11.4 % of the total GHGs produced (Figure 1). As an example, in 2019, the agricultural sector was responsible for 35.4% of GHG emissions in Ireland, out of which 10.6% came from manure management (Duffy *et al.*, 2021).

Greenhouse gas emissions by source sector, EU, 2020

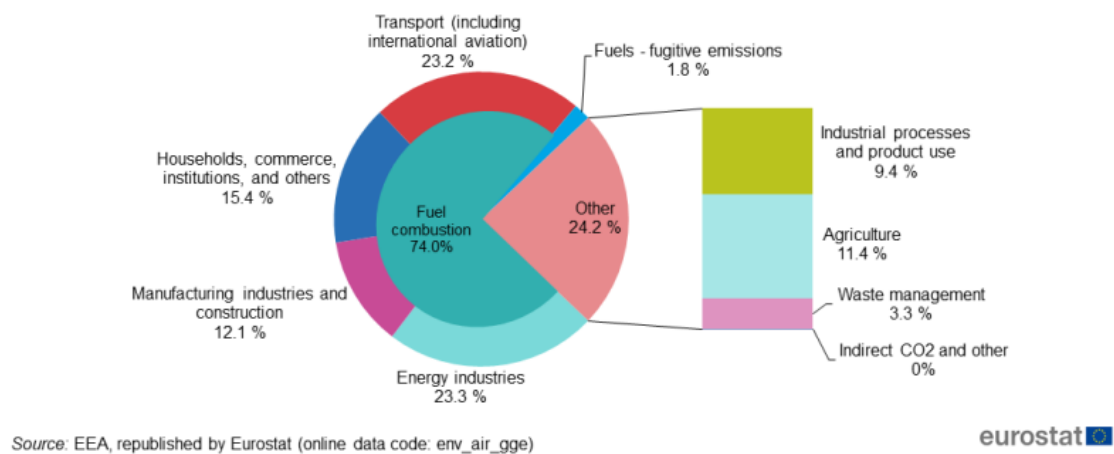


Figure 1: Greenhouse gas emissions by source sector in the EU in 2020 (Eurostat, 2020)

2.1.2 Manure management

Manure is the second-largest source of GHG emissions from dairy farms (Aguirre-Villegas and Larson, 2017). Aguirre-Villegas and Larson (2017) also compared practices based on farm size and related these practices to GHG emissions. Their findings suggest that manure systems and management practise vary depending on farm size with larger farms handling liquid manure and using long-term storage, while smaller farms tend to deal with solid manure and land-apply daily (Aguirre-Villegas and Larson, 2017). They also report that storing liquid manure for long periods without processing is one of the major contributors to GHG emissions from this waste source. When implementing manure processing, permitted techniques can reduce emissions significantly, mostly through anaerobic digestion. Small farms keep their emissions lower than large farms due to the daily handling of solid manure and land-application manure (Aguirre-Villegas and Larson, 2017). Depending on the practice of storing and spreading the manure and farm size, GHG emissions per ton of manure range from 2200 to 12,000 g CO₂-eq for collection, 200 to 2400 g CO₂-eq for transportation, 16,000 to 84,000 g CO₂-eq for storage, and 16,400 to 33,500 g CO₂-eq for land application. They concluded that GHG

and NH_3 emissions occur mostly during manure land application in small farms, but during manure storage in large and permitted facilities (concentrated animal operations that are regulated due to their size of >1000 animal units), highlighting the importance of adopting further mitigation practises in these manure handling stages (Figure 2).

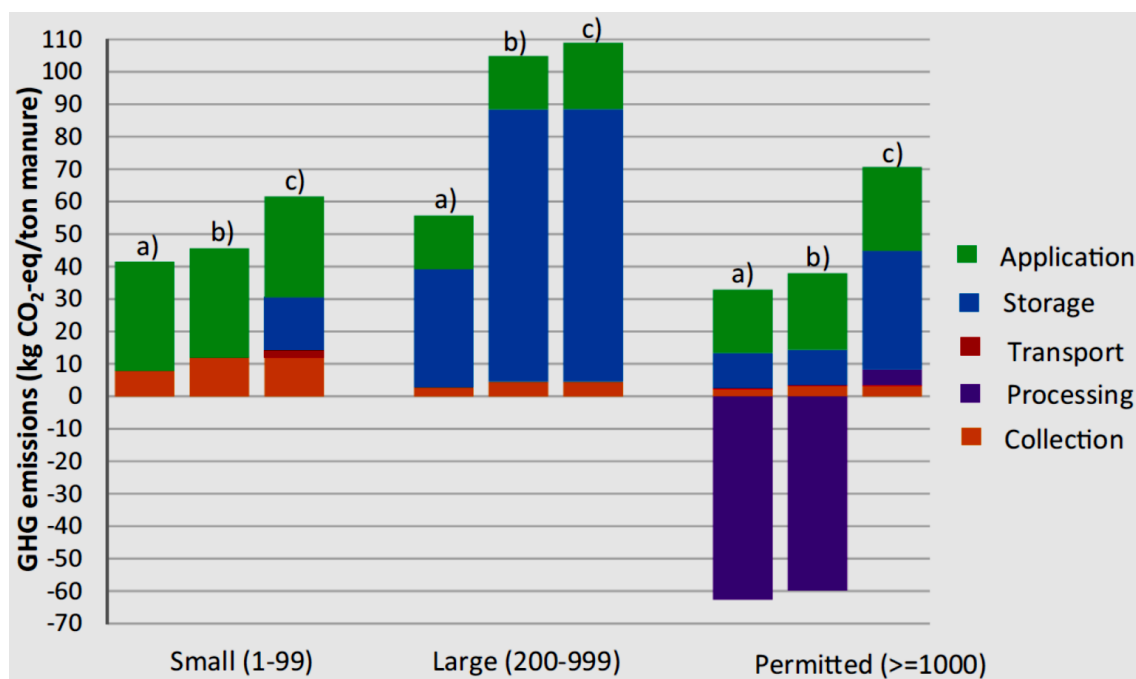


Figure 2: GHG emissions from cattle manure from the a) low emitting, b) reference and c) high emitting scenarios per farm size and management practise (Aguirre-Villegas and Larson, 2017)

As an example, pig farms are required to have 26 weeks' storage capacities in Ireland to make sure that pig manure will not be spread on land during the prohibited spreading period and is not permitted outside of the prohibited period if weather or ground conditions are unsuitable and there is a risk that the nutrients in the fertilisers might run off into surface water and groundwater (Department of Agriculture, 2018). The same storage capacity is applied for digestate. Similar requirements are in place in other European countries (Bundesministerium für Ernährung und Landwirtschaft, 2021).

A study from Ireland (Zhang *et al.*, 2021) calculated the CH₄ emission factor (EF_{CH₄}) for pig manure storage for a farm in Ireland. The EF_{CH₄} for pig manure storage was calculated according to IPCC guidelines (IPCC, 2019).

$$EF_{CH_4} = VS \times 365 \times B_0 \times 0.67 \text{ kg m}^{-3} \times MCF \times MS$$

where EF_{CH₄} is the emission factor of CH₄ during pig manure storage in kg CH₄/sow/yr. VS is volatile solids excreted by breeding pigs on farms in kg VS/sow/d. B₀ is the maximum pig manure methane production capacity in m³ CH₄/kg VS, which is 0.26 m³ CH₄/kg VS (Dennehy *et al.*, 2016). 0.67 is the factor converting CH₄ from m³ to kg. MCF is the manure methane conversion factor during storage in %, which is 10% at an annual average temperature of 10 °C in Ireland. And MS is the fraction of pig manure handled by storage (dimensionless). The calculated EF_{CH₄} is 9.38 kg CH₄/sow/yr, corresponding to 15.8% of the total CH₄ produced from mono-digestion of pig manure (Xie *et al.*, 2017).

Possible ways to reduce GHG and NH₃ emissions are anaerobic digestion and solid-liquid separation, which have been shown to reduce GHG emissions for storage and land application by 25 % and 31 % respectively in comparison to untreated manure (Holly *et al.*, 2017). Another possibility is the use of biochar in the abatement of GHG effluxes in the manure management cycle (Hani *et al.*, 2012; Troy *et al.*, 2013; Gai *et al.*, 2014).

2.1.3 Emission reduction through biochar application

Woolf *et al.* (2010) present an analysis which shows that sustainable global implementation of biochar can potentially compensate a maximum of 12 % of current anthropogenic CO₂ -C equivalent (CO₂ -C_e) emissions (i.e., 1.8 Pg CO₂ - C_e per year of the 15.4 Pg CO₂ -C_e emitted annually) (Woolf *et al.*, 2010). The relative climate-mitigation potentials of biochar depend on the fertility of the soil amended as well as the type of biomass used (Woolf *et al.*, 2010). A study published in 2017 reports that biochar's

global maximum carbon sequestration potential is 2.27 Pg C year⁻¹ (M.R. Yadav *et al.*, 2017).

Brennan *et al.* evaluated the impact of land-spreading of biochars on GHG emissions (Brennan *et al.*, 2015). Biochar was derived from wood shavings (2 mm diameter), pyrolysed in a muffle furnace at 650 °C for 4.5 h and applied at a rate equivalent to 3.96 m³ ha⁻¹. The amendments were added to the slurry and mixed rapidly using a blender before simulated land application. Slurry and amended slurry were applied directly to the surface of the intact grassed soil at a rate equivalent to 33m³ slurry ha⁻¹ (Brennan *et al.*, 2015). Significant reductions in CO₂ efflux were observed upon biochar addition, with an 84 % reduction in cumulative CO₂ emissions. Biochar addition resulted in a reduction of 63 % in cumulative N₂O loss and a reduction of NH₃ emissions by 77 % compared to the slurry control which could lead to a reduction of atmospheric pollution and eutrophication after deposition caused by loss of reactive nitrogen. Only the CH₄ emissions did not show a significant change compared to the slurry control after the addition of biochar (Brennan *et al.*, 2015). It was concluded that the amendment of slurry with biochar can significantly reduce global warming potential following land application of dairy cattle slurry (Brennan *et al.*, 2015). This point could also apply to pig manure, as the result showed an emission reduction during manure composting after adding biochars (Wang *et al.*, 2013; Vu *et al.*, 2015; Yang *et al.*, 2020). These studies found that the addition of biochar, either on its own or in a mix, to pig manure during composting can lead to a reduction in CO₂, N₂O, NH₃ or CH₄ emissions.

Table 1 presents a range of studies that used biochars produced from various biomasses for emission reduction in different agricultural settings. Table 1 also presents the potential emission reductions. They have been derived from application in manure lagoons, in soil, as well as for (co-)composting.

Table 1: Summary of results found in the literature regarding emission reduction after biochar application

Author	Feedstock	Addition to biochar	Target	Applied to	Result
(Martin <i>et al.</i> , 2015)	Bought from BioRegional HomeGrown, Surrey, UK	Anaerobic digestates (different feedstocks)	Ammonification, nitrification and N ₂ O flux	Sandy loam soil	Reduced N ₂ O emissions by around half with higher biochar concentration
(Janczak <i>et al.</i> , 2017)	Willow woodchips		NH ₃ reduction in composting	Poultry manure mixed with wheat straw	Reduced NH ₃ emissions of up to 44% wet weight
(Troy <i>et al.</i> , 2013)	1.Pig manure after anaerobic digestion, Sitka Spruce sawdust 2.Sitka Spruce wood	Pig manure	Quantify effect of CO ₂ , N ₂ O and CH ₄	acid brown earth	Increased CO ₂ and N ₂ O emissions from manure-amended treatments
(W. Chen <i>et al.</i> , 2017)	Cornstalk, bamboo, wood, layer manure, coir	sawdust	CH ₄ and NH ₃ mitigation	Layer hen manure composting	NH ₃ production (up to -24.8%) and CH ₄ emissions (up to -26.1%) reduced

The use of biochar to counter nitrogen pollution was investigated by Gai *et al.* This was done under the aspect of the effects of various feedstocks and temperatures on characteristics of biochars and their adsorption ability for ammonium N (NH₄⁺-N) and nitrate N (NO₃⁻-N) being present in different concentrations (10, 30, 50, 70, 100, 150, 300, 500 mg NH₄⁺ (or NO₃⁻)L⁻¹ (Gai *et al.*, 2014). Their results showed that biochar yield and contents of N, H and O decreased as pyrolysis temperature increased from 400 °C to 700°C, whereas contents of ash, pH and carbon increased with higher pyrolysis temperature. All biochars could sorb considerable amounts of NH₄⁺-N, and the adsorption amount decreased with higher pyrolysis temperature (Gai *et al.*, 2014). In comparison to

that, none of NO_3^- -N was adsorbed to biochars at different NO_3^- concentrations. Instead, some NO_3^- -N was even released from the biochar materials (Gai *et al.*, 2014).

GHG reduction with the help of biochar was not only investigated in terms of its application to the soil but to manure and animal husbandry as well. A review article published in 2017 considered biochar as a tool to reduce the agricultural GHG burden in multiple areas such as composting additives, and feed in husbandry, to name just a few (Kammann *et al.*, 2017). In Germany, Austria and Switzerland about 90% of the traded biochar is used in animal husbandry as a feed additive using a dosage of 1% of the animal feed (Kammann *et al.*, 2017). Studies to date have focused on toxin adsorption, digestion, blood values, feed-use efficiency and so forth (Kammann *et al.*, 2017). They suggest that there are limited published studies on GHG emissions in animal housing and in terms of the emissions of manure pits associated with animals where biochar is in the food mix. It was shown that biochar amendment can reduce NH_3 volatilisation, especially in materials containing a high level of nitrogen such as sludge or manure (Steiner *et al.*, 2010; Malińska *et al.*, 2014). Beyond that, it is concluded that biochar, depending on the rate of application (10 or 20 % w/w) can reduce CH_4 and N_2O emissions by up to > 50 % subject to the material on which it is used (chicken manure, organic waste, municipal solid waste) (Kammann *et al.*, 2017). Co-composting is the addition of biochar to the initial composting feedstock (Kammann *et al.*, 2017).

The effect of the amendment of biochar to slurry and its mitigation of NH_3 emissions was investigated. In the study, three biochars were used out of which two were untreated and the third was treated with a phosphoric acid solution. They mixed 5 L of dairy cow slurry with 200 g of biochar. Before the experiments, the slurry was diluted with water at a ratio of 1:2, slurry to water. The measurements were carried out using a Dynamic Chamber (DC) system in a large environmental chamber with regulated temperature (20

°C) and humidity (60 %) (Hani *et al.*, 2012). The inflowing and outgoing gas concentrations of the dynamic chamber were measured and recorded. It was found that the untreated biochars changed the emissions to 75-105 % of the control and the treated one reduced the emission down to < 3 % of the control sample, showing that not just the pH of the biochar but combinations of characteristics determine the results (Hani *et al.*, 2012). This suggests that a variety of NH₃ emission reduction behaviours can be expected depending on the feedstock, pyrolysis process and post-treatment of the biochar (Hani *et al.*, 2012).

A short report on the effects of biochar addition on manure composting and associated N₂O emissions was published (Jia, Yuan and Ju, 2015), which indicated that reduced N₂O emissions were primarily attributed to high porosity and surface area of biochar which enables absorption/adsorption and retention of water, NH₃ or water-soluble NH₄⁺. This study was focused on solid manure but similar dynamics are to be expected regardless of the source of NH₃ / NH₄⁺.

The influence of biochar in regulating emissions from manure has been considered in several settings. Inter alia the role of biochar in chicken manure composting and the associated methane and carbon dioxide emission was investigated (Jia *et al.*, 2016). It was found that the addition of biochar reduced the CH₄ emission peak by 54.9 % but increased the CO₂ emission peak by 148 % when compared to the control without biochar. Calculating the global warming potential of these results (CH₄: 25, CO₂: 1) (UNFCCC Process, 2007), it can be said that the emissions were reduced by around 1500 CO₂ equivalents (CO_{2eq}). Furthermore, it was found that the addition of biochar increased the pH as well as the composting rate. Adding to the above, Gronwald *et al.* found no evidence of a clear and consistent reduction of NH₃ volatilization from cattle slurry or poultry manure through the addition of biochar (Gronwald *et al.*, 2018).

2.2 Adsorption of organics from water

Biochar can not only be used in liquid manure management but also the treatment of other liquid environments. One example of the usage of biochar for liquid environmental purposes is wastewater remediation. The adsorption of dyes onto biochars can be used as a proxy indicator of the efficacy of biochars in removing a range of organics from water as might be relevant in the water discharges in manure management. If biochar can reduce emissions in manure management, it might also help to reduce the amount of other organics leaching from manure. Various dyes and concentrations have been used as chemical proxies to examine the ability of biochars produced from varied materials to adsorb chemicals. The ability of biochars and activated carbon to adsorb dye has been well recognised (Chan *et al.*, 2012; Leng *et al.*, 2015; Rawat and Singh, 2018; Sumalinog, Capareda and de Luna, 2018).

Studies published on dye adsorption investigated their behaviour using the Freundlich and Langmuir isotherms as well as Pseudo-first and Pseudo-second order (PFO, PSO) kinetics. The Langmuir isotherm accounts for the surface coverage by balancing the relative rates of adsorption and desorption (Ayawei, Ebelegi and Wankasi, 2017). It is used to describe the equilibrium between adsorbate and adsorbent, where the adsorbate adsorption is limited to one molecular layer (Liu *et al.*, 2019). It states that each site can hold only one adsorbate species and all sites are energetically equivalent. This model suggests that there are no relationships between the adsorbate species (Chen *et al.*, 2018). The Freundlich isotherm on the other hand is used to explain adsorption processes onto heterogenous surfaces (Chan *et al.*, 2012; Sewu, Boakye and Woo, 2017). This model describes multilayer adsorption where the energy is distributed unevenly over the heterogeneous surface and where the adsorption ability will increase along with the increase of adsorbate concentration (Chen *et al.*, 2018). The PFO is based on the

assumption that physical adsorption limits the rate of adsorption of compounds onto the adsorbent (PFO), while the PSO sets the chemisorption as the limiting mechanism for the process (Sumalinog, Capareda and de Luna, 2018).

Dyes used for adsorption are cationic and anionic dyes like Congo red (CR), malachite green (MG), methylene blue (MB), crystal violet (CV) or methyl orange (MO) (Leng *et al.*, 2015; Sewu, Boakye and Woo, 2017; Rawat and Singh, 2018; Sumalinog, Capareda and de Luna, 2018). It was found in some studies that cationic dyes seem to have higher adsorption onto biochars than anionic dyes (Leng *et al.*, 2015; Sewu, Boakye and Woo, 2017; Wang and Wang, 2019; Li *et al.*, 2020). Results for maximum adsorptive capacity (Q_m) for the Langmuir isotherm ranges from around 4.2 – 1153.8 mg g⁻¹ for different dyes used with biochars produced from various materials and applied at different concentrations (Leng *et al.*, 2015; Sewu, Boakye and Woo, 2017; Chen *et al.*, 2018) and from around 10.0 – 4117.7 mg g⁻¹ for the malachite green in particular (Leng *et al.*, 2015; Chen *et al.*, 2018; Rawat and Singh, 2018). Studies show that Langmuir seems to be more suitable than Freundlich for some biochars, whereas others report a better fit using the Freundlich isotherm (Sewu, Boakye and Woo, 2017; Chen *et al.*, 2018). This indicates that biochars provide one-layer adsorption as well as adsorption to heterogeneous surfaces depending on which feedstock is used for biochar production.

Throughout the literature, the PFO values for the amount of adsorbate adsorbed at equilibrium (Q_e) range from 4.44 to 379.9 mg g⁻¹ (Sewu, Boakye and Woo, 2017; Park *et al.*, 2019). The Q_e of PSO results varies between 4.37 and 390.9 mg g⁻¹ (Sewu, Boakye and Woo, 2017; Park *et al.*, 2019). R^2 values reported in the literature range from 0.449 to 1.0, showing that not all results calculated using PFO or PSO equations are a good fit for the kinetic models used (Sewu, Boakye and Woo, 2017; Park *et al.*, 2019). The results show that for dyes like MG, CV or MB, the PSO is a better fit, which means adsorption

is driven by chemical interactions between the dye and the biochar (Leng *et al.*, 2015; Sewu, Boakye and Woo, 2017; Chen *et al.*, 2018; Rawat and Singh, 2018; Sumalinog, Capareda and de Luna, 2018; Park *et al.*, 2019).

2.3 Biochar

Biochar is a product generated through a process in which biomass is heated with limited or no air to above 250°C (Lehmann and Joseph, 2015). The temperature conversion efficiency of biomass to biochar ranges across different mixtures of materials and heating rates (Figure 3). Biochar is commonly enriched in carbon (C) and other elements such as phosphorus (P), calcium (Ca) or nitrogen (N) (Lehmann and Joseph, 2015). Pyrolysis, gasification and hydrothermal carbonization are three major thermochemical processes used to produce biochar (Lehmann and Joseph, 2015; Singh *et al.*, 2022). Carbonisation is the process of converting a feedstock into biochar through reductive thermal processing. The process involves a combination of time, heat and pressure exposure factors that can vary between processors, equipment, and feedstocks. There are two main processes of carbonisation of dry feedstocks: pyrolysis and gasification (International Biochar Initiative, 2018). If the feedstock has a high moisture content, hydrothermal carbonisation (HTC) can be used to produce biochar. HTC is also working with high pressure in an aqueous environment, whereas the pyrolysis process does not work with pressure and in a “dry” environment (Rodriguez Correa *et al.*, 2019; Zhou *et al.*, 2021). Furthermore, pyrolysis and gasification produce biochars in a temperature range of 400 – 1000 °C and HTC in a range of 180 – 250 °C (Rodriguez Correa *et al.*, 2019). Here the focus will be on the pyrolysis of biomass or other feedstocks to obtain biochar. To produce biochar, any material such as organic waste, wood or manure can be used (Lehmann and Joseph, 2015). A European Biochar Certificate (EBC) was established in 2012 to provide a standard and definition regarding the name, method

of production and quality, as well as properties of the final material. The EBC certificate defines these standards and regulates the production of biochar. Producers wishing to produce an EBC-certified biochar have to go through the certification programme provided by q.inspecta (EBC, 2012).

Globally the International Biochar Initiative (IBI) has produced a separate set of standards (International Biochar Initiative, 2015). The standards include terms and definitions, feedstock material and best management practices for biochar production, material tests, as well as general protocols and restrictions (International Biochar Initiative, 2015). These standards serve as the basis for the IBI Biochar Certification Program and are intended for use and adaptation to local conditions and regulations by any nation or region. Standards are used to establish a common definition for biochar, and standardised testing and measurement methods for selected physicochemical properties of biochar materials have been developed (International Biochar Initiative, 2015). The IBI standards as well as the standards used for the EBC are informed by the latest research findings and updated regularly and therefore are similar to each other. Though not each testing method is required for both, such as bulk density, germination inhibition or the water holding capacity.

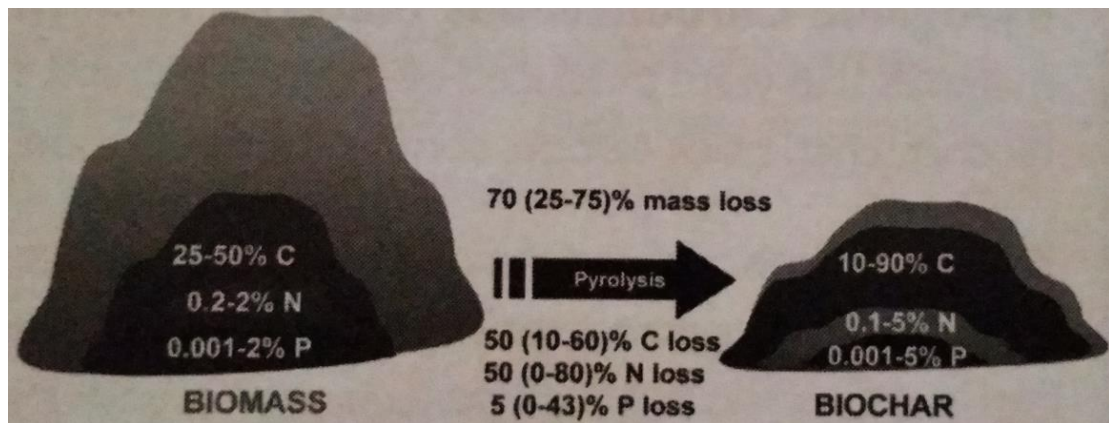


Figure 3: Conversion efficiency of biomass, C, N and P during pyrolysis ((data from Enders *et al.* (2012); typical losses followed by range in brackets) by Lehmann and Joseph, 2015)

2.4 Applications of biochar

Per definition circular economy is a model of production and consumption, which involves sharing, leasing, reusing, repairing, refurbishing and recycling existing materials and products as long as possible. In this way, the life cycle of products is extended (European Parliament, 2022). In practice, this implies reducing waste to a minimum, which is where biochar can help. When a product reaches the end of its life, its materials are kept within the economy wherever possible (e.g. biochar production), thereby creating further value (European Parliament, 2022). The aim of a circular economy is aligned with achieving many of the sustainability goals, set by the United Nations (Figure 4) (The global goals, 2022). As the topic of the circular economy becomes more and more important, it becomes evident to also see biochar as a potential part of it. Biochar has gained popularity in the environmental sector as it is a versatile material for waste reduction and increasing the efficacy of the circular economy (Singh *et al.*, 2022). It has demonstrated possibilities towards environmental impact, battling climate change, and creating an efficient circular economy model (Singh *et al.*, 2022). Biochar can upcycle waste materials and then use them towards the betterment of the environment. It can be used in agriculture, wastewater treatment, anaerobic digestion and various other sectors

thereby proving its multidimensional role towards the protection of the environment and successfully building up a circular economy-based environmental management model (Singh *et al.*, 2022). As biochar can be an example of a circular economy, it can play an important role in reaching sustainability goals as well.



Figure 4: The 17 sustainability and development goals as stated by the United Nations (The global goals, 2022)

In recent years there has been considerable interest in the various environmental applications of biochar (BC), such as carbon sequestration, soil amendment or pollutant removal (Oliveira *et al.*, 2017). It was stated that pyrolysis is one of the most promising technologies for the conversion of biomass into high-value products such as syngas, bio-oil or biochar (Qambrani *et al.*, 2017). The durable nature of biochar captures carbon from the atmosphere, providing a carbon sink to terrestrial ecosystems while improving water and soil quality (Lehmann *et al.*, 2009). Its stable nature leads to a slower degradation of the biochar, which slows the rate at which photosynthetically fixed carbon (FC) is returned to the atmosphere (Woolf *et al.*, 2010). Carbon in biochar can persist in soils over long time scales (International Biochar Initiative, 2018), therefore, being able to reduce carbon released to the atmosphere in comparison to carbon sequestration by photosynthesis (Figure 5).

Beyond the carbon sequestered in the form of biochar itself, biochar incorporated in soils also offers numerous other potential climate benefits. Biochar can improve soil fertility, stimulating plant growth, which then consumes more CO₂ in a positive feedback effect as well as reducing emissions of N₂O and CH₄ from agricultural soils (International Biochar Initiative, 2018). Apart from the positive effects on the soil, converting agricultural and forestry waste into biochar can avoid CO₂ and CH₄ emissions otherwise generated by the natural decomposition or burning of this waste (International Biochar Initiative, 2018). Biochar can reduce the need for chemical fertilisers, resulting in reduced emissions of GHG from fertiliser manufacture and application (International Biochar Initiative 2018). Another benefit is the potential to increase the biomass of soil microbial life, resulting in more carbon storage in soil (International Biochar Initiative 2018). In addition, biochar yields several potential co-benefits (Woolf *et al.*, 2010). It is a source of renewable bioenergy; it can improve agricultural productivity, particularly in low-fertility and degraded soils; it reduces the losses of nutrients and agricultural chemicals in run-off; it can improve the water-holding capacity of soils (Johannes Lehmann and Joseph, 2009; Lehmann and Joseph, 2015). Additionally using feedstocks that are waste material means biochar production represents an effective waste management strategy which can prevent further land-use change to produce energy.

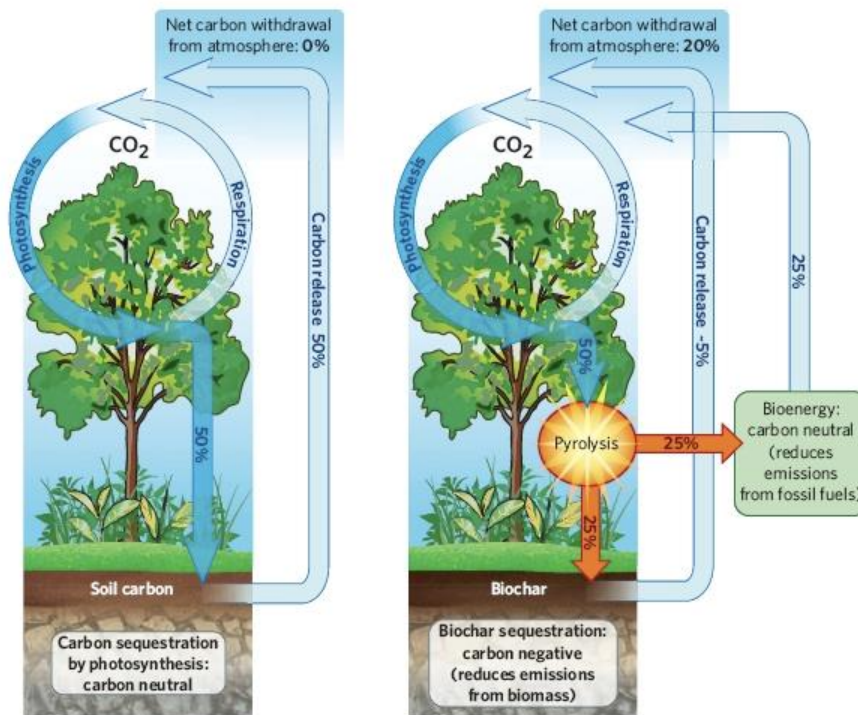


Figure 5: carbon cycle with and without biochar application (Lehmann, 2007; Bahuguna, Sharma and Dadarwal, 2021)

Of the possible strategies to remove CO₂ from the atmosphere, biochar is notable, if not unique, in this regard. It can store CO₂ in the soil and when applied to soil, landfill covers or manure, biochar can reduce GHG emissions from these sources as well (Johannes Lehmann and Joseph, 2009; Brennan *et al.*, 2015; Sadasivam and Reddy, 2015). Biochar can be produced at scales ranging from large industrial facilities down to individual farm units (Johannes Lehmann and Joseph, 2009), making it applicable to a variety of socioeconomic situations. Various pyrolysis technologies are commercially available that yield different proportions of biochar and bioenergy products, such as bio-oil and syngas (Woolf *et al.*, 2010). The outputs of the pyrolysis process serve to provide energy, avoid emissions of GHG such as CH₄ and N₂O, and amend agricultural soils and pastures. Bioenergy is used to offset fossil-fuel emissions while returning about half of the C fixed by photosynthesis to the atmosphere (Woolf *et al.*, 2010). The biochar stores

carbon in a resistant form that can increase soil water- and nutrient-holding capacities, which typically results in increased plant growth. The intensified production further enhances the amount of CO₂ removed from the atmosphere (Woolf *et al.*, 2010).

Although the literature presents a wide range of feedstocks and applications for biochar, there remains limited information on the use of peat as a feedstock and consequently the use of this type of biochar as an additive to slurry or liquid manure management. Yet the demands for new ways to reduce the emissions of GHG in the agricultural sector remain as pressing as ever. Various feedstocks have been used and do show promise in terms of emission reduction when applied to soil or during composting (Vu *et al.*, 2015; Kammann *et al.*, 2017; Gronwald *et al.*, 2018; Yang *et al.*, 2020).

2.5 Production and characterisation of biochars

2.5.1 Pyrolysis

The pyrolysis process is described as a transformation of organic materials into their gaseous components, a solid residue (biochar), and a liquid called bio-oil. Pyrolysis systems use kilns, retorts, and other specialized equipment to contain the baking biomass while excluding oxygen. The reaction vessel is vented to allow pyrolysis gases to escape. Pyrolysis gases are often called “syngas”. The process becomes self-sustaining as the syngas produced is combusted, and heat is released (International Biochar Initiative, 2018). Pyrolysis itself can be divided into two types of processes: slow and fast pyrolysis.

Slow pyrolysis is usually carried out within a range of 350 – 400 °C and residence times of minutes up to hours while fast pyrolysis is carried out between 450 – 550 °C with a residence time of seconds (Shackley and Sohi, 2010). The biochar yields of the processes vary between 25 – 35 % oven-dry feedstock mass for slow and 10 – 25 % for

fast pyrolysis (Shackley and Sohi, 2010). The yield varies depending on the heating rate, maximum temperature, type and composition of the feedstock, particle size and reactor conditions (Qambrani *et al.*, 2017). Low heating rates and long residence times favour high yields of biochar while high heating rates and short residence times result in a higher oil yield and therefore less biochar (Shackley and Sohi, 2010). Another important factor is the final carbonisation temperature or the highest treatment temperature (Babinszki *et al.*, 2021). This was found to be the most important factor influencing the biochar yield when comparing yields for the same feedstock. A biochar yield of 21 – 29% was obtained when using milled debarked spruce and birch samples at temperatures between 400 – 700 °C (Babinszki *et al.*, 2021). Generally, it can be said that higher treatment temperatures result in lower biochar yields (Mašek *et al.*, 2013; Ronsse *et al.*, 2013; Greco *et al.*, 2020; Zhang *et al.*, 2020; Babinszki *et al.*, 2021). It was found that to obtain one kilogram of biochar produced from green waste, around 1 – 5 kg of feedstock would be needed (Ronsse *et al.*, 2013). For peat, it would be around 2 – 3 kg (Sutcu, 2007) and from brewery grain 1.2 – 5 kg would be needed (Olszewski *et al.*, 2019).

Production methods vary throughout the literature as widely as materials used. Biochars can be produced using a furnace, a fixed-bed reactor, a rotary furnace, a fluidised bed reactor, a tube furnace or a muffle furnace (Qambrani *et al.*, 2017). All these different ways of producing biochar require adaptations depending on the required outcome. The muffle furnace is one of the more common methods used in biochar production (Abrishamkesh *et al.*, 2015; Zhao, Coles and Wu, 2015; Hernandez-Soriano *et al.*, 2016; Domingues *et al.*, 2017; Xiaofeng *et al.*, 2017). Production parameters of particular significance include the heating rates (change of temperature with time), residence times (minutes to hours) as well as final temperatures (Table 2). Crucibles are the preferred

container used for biochar production in a (muffle) furnace (Jindo *et al.*, 2014; Abrishamkesh *et al.*, 2015; Hernandez-Soriano *et al.*, 2016; Xiaofeng *et al.*, 2017).

Table 2: Production parameter of biochars produced using a muffle furnace

	(Xiaofeng <i>et al.</i> , 2017)	(Abrishamkesh <i>et al.</i> , 2015)	(Zhao, Coles and Wu, 2015)	(Hernandez-Soriano <i>et al.</i> , 2016)
Heating rate ($^{\circ}\text{C min}^{-1}$)		0.25-0.3	20	7.5
Final temperature ($^{\circ}\text{C}$)	250-650	250-500	450	450
Residence time (min)	120	30-225	60	120

2.5.2 Characterisation of biochars

The properties of the biochar obtained vary depending on the feedstock as well as on the process conditions used during production (Figure 6). To characterise the biochars, chemical and physical properties need to be measured. Although the chemical properties such as pH, elemental composition, ash content and fixed carbon (FC) are not presented in every study a more complete understanding requires this information to be available. This also applies to physical properties such as density or CEC.

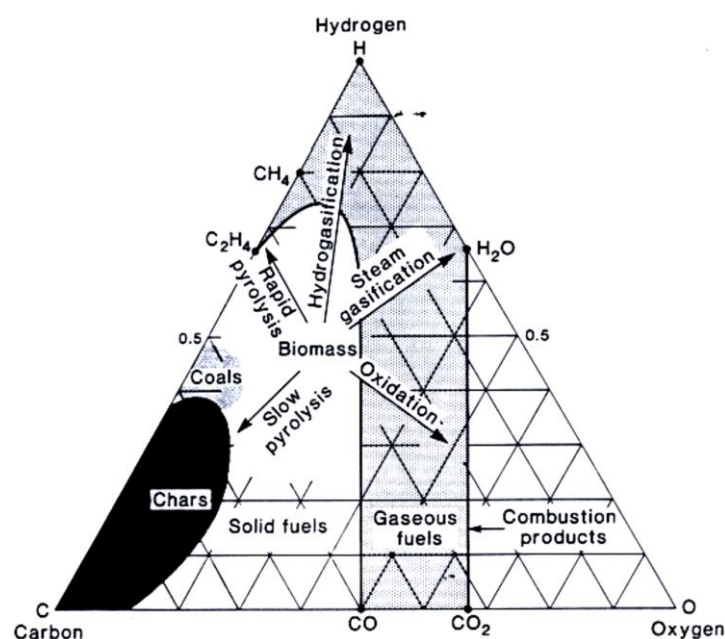


Figure 6: Conversion of biomass into biochars, fuels and other products presented by Richard L. Bain at the DOE/NASLUGC Biomass and Solar Energy Workshops in 2004 (Bain, 2004)

It was found that variations in the physical properties of the biochars are obvious and can be easily observed with visualisation, particularly when the biochar is in a loose, granular, or pelleted form (Amin *et al.*, 2016). The range of chemical properties is as wide as the variation of physical properties but not as visible and only detectable through careful laboratory analysis (Amin *et al.*, 2016). To determine the chemical characteristics of biochar, various analytical techniques can be used such as elemental analysis, thermogravimetric and derivative thermogravimetric analysis (TGA-DTG), Fourier transform infrared spectroscopy (ATR-FTIR), scanning electron microscopy (SEM), and analytical techniques for PAHs analysis. A van Krevelen diagram is often used to underline the selective loss of elements during pyrolysis by comparing atomic ratios of H/C and O/C (Oliveira *et al.*, 2017) (Figure 7). Typically, the formation of biochar results in a decrease in H/C and O/C ratios (Figure 7).

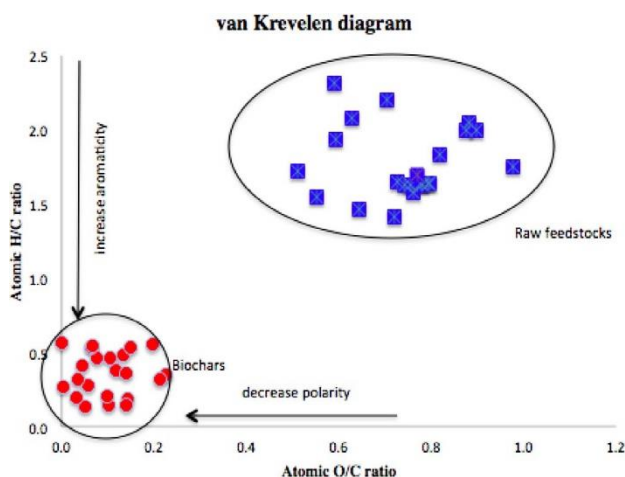


Figure 7: Van Krevelen diagram showing changes in O/C and H/C ratios from feedstocks to biochars (Oliveira *et al.*, 2017)

As noted earlier biochar properties are influenced by the process parameters such as particle size, residence time, heating rate and pyrolysis temperature among others (Amin *et al.*, 2016; Zhao *et al.*, 2018). Depending on these parameters as well as on the input material, different yields and qualities of biochar can be expected. Generally, it has been reported that temperature is one of the more significant influential factors affecting the morphology, structural surface area and functional chemistry of biochars (Amin *et al.*, 2016). At the same time, a higher lignin content within the feedstock used leads to a higher yield which can be explained by the structural stability of lignin itself (Cantrell *et al.*, 2012).

In terms of elemental composition, Zhang *et al.* (2017) reviewed several biochars produced at temperatures from 350°C up to 900°C and from four different feedstocks (oak and pine chips, sugarcane residue and peanut shell) through slow pyrolysis. The biochars concerned were analysed by proximate analysis, for their elemental composition, pH and electrical conductivity (Zhang *et al.*, 2017). Results showed that yield and volatile matter (VM) were reduced whereas fixed matter and electrical conductivity were increased for the samples produced with higher temperatures. The biochars from all four feedstocks showed a general rise in carbon content with higher temperatures although this

was not that clearly visible above 750°C. The hydrogen (H) and oxygen (O) content of all biochars behave in an opposite way to the carbon (C) content (Zhang *et al.*, 2017). However, even if pyrolysis temperature has a big influence on biochar composition, the most important factor is the feedstock. Feedstocks with a similar CHO content will produce biochars with similar contents if pyrolysed at the same temperature (Zhang *et al.*, 2017). The oak and pine chip samples pyrolysed in the study proved this statement by starting with a carbon content of 71 and 72 % respectively after being pyrolysed at 350 °C and ending with a content of 83 and 84 % at 900 °C (Zhang *et al.*, 2017).

Residues from biogas production were pyrolysed and characterised (Stefaniuk and Oleszczuk, 2015). The biochars were produced at a range of 400 – 800 °C and analysed for their physicochemical and surface properties such as moisture and ash content, elemental composition and surface properties. Depending on the temperature conditions during the biogas process and the type of residue (separated/ unseparated), as well as the substrate used to feed the biogas plant, the individual parameters such as surface area varied. Separated residues from biogas production presented higher values for the surface area ($2.4 - 2.8 \text{ m}^2 \text{ g}^{-1}$) than unseparated residues ($1.6 \text{ m}^2 \text{ g}^{-1}$). No significant differences were found within the separated materials, even when using different types of feedstock digestion including thermophilic or mesophilic processes, (Stefaniuk and Oleszczuk, 2015). The surface areas of the biochars generated did not demonstrate a visible trend. Despite no trend being found for the surface area, it was generally found that pH, ash and macro- and micronutrient content increased with higher temperatures while the yield and quantity of H, N and O decreased (Stefaniuk and Oleszczuk, 2015).

Wood samples were pyrolysed within a temperature range of around 350 – 600 °C and 190 °C min^{-1} for 30 min (Suliman *et al.*, 2016). These were analysed using a wide range of methods like elemental and proximate analysis (TGA), SEM, pH, EC and CEC

among others to assess how feedstock source and pyrolysis temperature affect surface properties of biochars (Suliman *et al.*, 2016). Results show increased ash and fixed carbon content with increasing temperatures and a declining yield at the same time. As the temperature increased it was noted that the surface area also increased (up to 250 %) as well as both the pore size volume (up to 200 %) and the mineral content (50 - 300 %). No clear thermally related trend was visible across all three feedstocks in terms of pH. However, EC did show an increased value with higher process temperatures ranging from around 0.0 - 0.1 dS m⁻¹ to around 0.05 - 0.35 dS m⁻¹ depending on the sample (Suliman *et al.*, 2016). It is concluded that physicochemical properties are affected by feedstock and pyrolysis temperature and that by using combinations of temperature and feedstock source it is possible to produce biochars with a wide range of physicochemical properties (Suliman *et al.*, 2016). Therefore, in designing biochars with desirable end qualities or for specific treatment scenarios the challenge remains to coordinate the most appropriate production protocol using the most appropriate feedstock source.

The influence of feedstock type and the rate of pyrolysis and associated conditions has been evaluated in several settings. (Ronsse *et al.*, 2013) reported that the fixed carbon (FC) content (wt%) strongly depended on the duration and temperature of treatment. They noted increased amounts of FC with higher temperatures as well as with longer residence times for wood, straw and green waste samples. The pH was also reported to rise with treatment temperature, like the total carbon content (wt%).

It can be concluded that biochar properties such as pH, FC or surface area can be influenced by controlling the production conditions of pyrolysis. Higher temperatures lead to higher pHs, more FC and slightly higher surface area (Shackley and Sohi, 2010). The resulting biochars are more stable and demonstrate a higher potential to interact with the environment within which they are set.

2.6 Biochar feedstocks and applications

As biochar can be made from biomass waste materials; biochar production should not create competition for land with any other land-use options, such as food production or leaving the land in its original state (Johannes Lehmann and Joseph, 2009). Biochar can be made from any source material or feedstock with high carbon content (Jirka and Tomlinson, 2014). Biomass can be subdivided into unprocessed feedstocks (for example, wood chips or corn stover) and processed feedstocks (Jirka and Tomlinson, 2014). The latter are those feedstocks that have undergone chemical (e.g., paper pulp sludge) or biological (e.g., digestion to produce animal manures or sludge from waste effluent treatment) processing (Jirka and Tomlinson, 2014). Biomass waste materials appropriate for biochar production include crop residues (field residues and processing residues such as nutshells, fruit pits, and bagasse), yard, food and forestry wastes, and animal manures (International Biochar Initiative, 2018). Large amounts of agricultural, municipal and forestry biomass are currently burned or left to decompose and release CO₂ and CH₄ back into the atmosphere (Brassard, Godbout and Raghavan, 2016; Kern *et al.*, 2017; Panwar, Pawar and Salvi, 2019).

Using these materials to make biochar not only removes them from a pollution cycle – but biochar also produces energy-like heat from this biomass during pyrolysis. Feedstocks must not contain unacceptable levels of toxins such as heavy metals, which can be found in sewage sludge and industrial or landfill waste (Johannes Lehmann and Joseph, 2009). The chemical composition of biochar (i.e. the amount of carbon, nitrogen, potassium, calcium, etc.) depends on the feedstock used and the duration and temperature of pyrolysis (International Biochar Initiative, 2018). However, pyrolysis conditions greatly affect the nutrient content of the biochars and so biochar should be tested on a batch-by-batch basis to determine specific properties (Chan and Xu, 2009). While a wide

range of feedstocks can be converted into biochar, several issues limit the practicality of using some feedstocks (Jirka and Tomlinson, 2014). Firstly, feedstock conversion challenges can arise due to the physical properties of the feedstock such as size or moisture content, or chemical properties such as high silica content. While the feedstock can be mechanically or chemically processed to facilitate the conversion, the added expense of pre-processing makes the cost prohibitive (Jirka and Tomlinson, 2014). Secondly, serious safety concerns can arise from the presence of contaminants in the feedstock. For example, municipal solid waste (MSW) or biomass grown on contaminated soils may contain plastics or heavy metals which can lead to the concentration, formation, or emission of environmental pollutants during the conversion process and in the final product (Jirka and Tomlinson, 2014).

The feedstocks offering the best chance of financial viability are derived from biomass residues such as by-products from agriculture, forestry, livestock rearing, food production and processing, and related industries. In many cases, residues present waste management challenges (in terms of disposal) – therefore, their use in biochar production can be viewed as a win-win solution. Indeed, many municipalities around the world currently pay to incinerate and landfill urban green waste with all the associated environmental and GHG impacts. Yet the use of urban green waste in biochar production represents a viable feedstock source and would greatly offset these negative impacts (Jirka and Tomlinson, 2014). Perhaps the greatest limitation to using any feedstock is the ability to procure it in large and continuous quantities and at a viable cost, including harvesting and transport costs. While biochar producers may find feedstocks that are low cost, free, or even bring in money due to tipping fees, as soon as the demand for feedstocks increases, – as it would with an established biochar industry – the price of feedstocks can be expected to rise in line with the economic principles of supply and demand. Biochar producers will have to

factor this into their business models until feedstocks reach equilibrium price points (Jirka and Tomlinson, 2014). Therefore, it is important to study all the aspects of feedstock supply before setting up a biochar operation. Feedstock availability can vary from year to year and within years (J. Lehmann and Joseph, 2009). The choice of feedstock will be affected by the biomass resources in the immediate area and availability and of course the intended end use. Due to the associated collection, transport, and storage costs of feedstocks, local sources are often seen as the best economic option. There is a wide range of costs and benefits to consider with feedstock choices (Table 3) (McCarl *et al.*, 2009).

Table 3: Costs and benefits of biochar feedstocks (McCarl et al., 2009)

sector	cost	benefit
Feedstock production and collection	<ul style="list-style-type: none"> • Economic issue? → waste or purposely grown for the production of biochar (e.g., switchgrass) • possible costs and inputs needed for the growing and harvesting of the crop 	<ul style="list-style-type: none"> • Revenue/tipping fees from certain waste feedstocks?
Use Trade-off	<ul style="list-style-type: none"> • Nutrient value lost? → biochar production vs. Fertiliser use 	<ul style="list-style-type: none"> • Biochars can add and help retain nutrients • Bio-oil and syngas could be sold
Feedstock transport	<ul style="list-style-type: none"> • transportation costs can be very high 	<ul style="list-style-type: none"> • Densifying the biomass by chipping or pelletising before transport as a solution?
Feedstock storage and pre-treatment	<ul style="list-style-type: none"> • feedstocks might need drying 	<ul style="list-style-type: none"> • drying process could occur passively through careful storage or may need more intervention (drier → requiring energy and labour)

Biochar can be applied and used in many different fields of everyday life including agriculture, the building sector, as a decontamination agent and in biogas production as well as applications in textiles (Schmidt, 2012). Here, the focus will be on the agricultural sector in particular manure management applications in animal farming. Many of the effects of adding biochar in agricultural settings are considered positive. These typically include aspects such as an improvement in soil condition, plant growth promotion, remediation of contaminated soil or as a factor helping to reduce GHG emissions. However, there are also some potentially negative consequences such as being a source of soil contamination, altering soil biota or causing a rise in CO₂ emissions due to soil priming or the extra decomposition of native soil organic matter (Qadeer *et al.*, 2017).

Notwithstanding the potential limitations associated with the application of biochar in agriculture, it has been well-recognised that one of the more significant roles of biochar is environmental remediation (Oliveira *et al.*, 2017). Indeed, Oliveira *et al.* (2017) have described biochar applications for remediation in solid, liquid and gaseous phases, remediation of toxic gases, removal of miscellaneous pollutants from the liquid and solid phases, as well as kinetic studies associated with environmental applications of biochar and the possibility of climate change mitigation.

The organic compounds of biochars were analysed and it was found that their interactions with the mineral compounds of biochars, like amalgamation, carbon structures or distribution of minerals inside the porous structure of biochars, were significantly influenced by thermal treatment (Taherymoosavi *et al.*, 2017). Interactions like the distribution of mineral phases, which are rich in Ca, P and Fe, inside the porous structure and Si/Al-based phases on the surface of the biochar particle would suggest considerable interactivity between these phases at higher pyrolysis temperatures (Taherymoosavi *et al.*, 2017). They also analysed the change in elemental composition

and found that the carbon and nitrogen content increases after pyrolysis while the hydrogen content decreases (Table 4). As has already been noted the elemental composition of the feedstock has a significant bearing on the quality of the resulting biochar. This is particularly significant for C/H ratios in feedstocks commonly associated with different wood species. Indeed, the C/H ratios that occur in these feedstocks are heavily linked to the yield of biochar and the resulting by-products. A higher C/H content in wood has been associated with a higher yield of biochar and a reduced tar yield, whereas a feedstock wood species with a lower C/H ratio tends to produce lower biochar yields and higher gas and tar yields (Hu *et al.*, 2019).

Table 4: Comparison of the elemental composition of feedstocks and biochars (Taherymoosavi *et al.*, 2017; Hu *et al.*, 2019) (%db = %on a dry basis)

		(Hu <i>et al.</i> , 2019)					(Taherymoosavi <i>et al.</i> , 2017)
		Poplar	Acacia	Pine	Cedar	Ailanthus altissima	Municipal solid waste
C	Feedstock	46.6	46.3	47.3	16.4	45.8	54.6
(%db)	Biochar	79.7	72.9	80.6	81.5	76.6	68.6-80.7
H	Feedstock	6.1	6.4	6.6	6.2	6.3	5.88
(%db)	Biochar	5.2	5.0	5.4	4.9	8.6	4.33-2.64
N(%db)	Feedstock	0.30	0.61	0.27	0.49	0.37	5.36
	Biochars		-	0.57	-	0.57	6.09-5.79

Different combinations of applications of biochars with various materials are possible. In this case, hardwood biochar combined with dairy manure (Table 5) was applied to soil in a laboratory incubation experiment to determine the effect of biochar–manure co-application on soil water content, nutrient concentrations, and other effects in relation to the priming effect (Ippolito *et al.*, 2016). It was found that the application improved the soil water content, and increased soil organic carbon content as well as

plant-available iron (Fe) and manganese (Mn). Though the CO₂ respiration rate was not greatly influenced by increasing biochar application rates and stable manure rates. Regarding this project, the soil application, and the effects it creates are of less interest than the chemical analysis of the hardwood biochar as well as the dairy cattle manure (55.3% solids) (Table 5) as they are not part of the project. The more or less similar respiration rates with rising biochar application rates could indicate that biochar applications do not influence CO₂ emissions from manure.

Table 5: properties of hardwood biochar and manure used in the study (Ippolito *et al.*, 2016)

	Units	Biochars	Manure
pH		6.8	8.8
Ash	%	14	Not determined
Total C	%	66.2	26.4
Total N	%	0.32	2.15
Surface area	m ² g ⁻¹	0.75	Not determined
NO ₃ -N	mg kg ⁻¹	1.5	80.6
NH ₄ -N	mg kg ⁻¹	1.2	220
K	mg kg ⁻¹	3400	13,500
Ca	mg kg ⁻¹	3700	22,000
Mg	mg kg ⁻¹	1500	8230
Na	mg kg ⁻¹	200	3750
P	mg kg ⁻¹	300	4080
Fe	mg kg ⁻¹	1400	4480
Zn	mg kg ⁻¹	14.1	167
Mn	mg kg ⁻¹	118	169
Cu	mg kg ⁻¹	16.8	76.5
Ni	mg kg ⁻¹	4.9	3.4
Cd	mg kg ⁻¹	<0.05	0.34
Pb	mg kg ⁻¹	2.0	1.9
B	mg kg ⁻¹	12.3	27.3

The focus of a study from 2014 was on polycyclic aromatic hydrocarbons (PAHs), heavy metals and mineral elements (Luo *et al.*, 2014). Biochars were produced from corn stalks and sewage sludge using slow pyrolysis within a temperature range of 200 – 700 °C with 100 °C increments, a heating rate of 5 °C min⁻¹ and a peak temperature being held for 6 hours. The total concentration of PAHs and heavy metals in most of the biochars was below the control standards (e.g. IBI standards, EBC) of sludge for

agricultural use in China, the USA, and Europe (Luo *et al.*, 2014). These findings are inconsistent with results obtained from biochars produced using residues of biogas production (Stefaniuk, Oleszczuk and Bartmiński, 2016). Stefaniuk *et al.*, (2016) used separated or unseparated residues from thermo- or mesophilic operating biogas plants to produce the biochars. Their findings revealed that with increasing pyrolysis temperature the content of PAHs and certain heavy metals increased as well (Stefaniuk, Oleszczuk and Bartmiński, 2016).

2.7 Peat and brewery grain

2.7.1 Peat

Peat is defined as sedentarily accumulated material of which at least 30% (dry mass basis) is dead organic matter (Tanneberger *et al.*, 2017). It is an organic material with < 25% by weight mineral matter that ranges in colour from blond to black (Girardello *et al.*, 2013). The deposit of organic matter can reach thicknesses of several metres and occupy large areas, forming a peatland (Girardello *et al.*, 2013). Ireland is covered with peatlands, making up around 21% of its country area (Tanneberger *et al.*, 2017). The country with the highest percentage of peatland area per country area is Finland, followed by Ireland (Table 6) (Tanneberger *et al.*, 2017).

Table 6: peatlands in Finland, Ireland, the UK and the whole of Europe (Tanneberger *et al.*, 2017)

Country	Country area (km ²)	Peatland area estimate (km ²)	Peatland area % of the country area
Finland	337010	90000 ¹	26.71
Ireland	69825	14664.7 ²	21.00
UK	242495	26838.3	11.07
Total		≈ 593727	

¹ > 0 cm of peat, ² ≥ 45 cm of peat if undrained and ≥ 30 cm of peat if drained

The largest areas of peatlands are found in Canada, Alaska, Northern Europe, Western Siberia, Southeast Asia and parts of the Amazon basin (Kern *et al.*, 2017). In 2013, 13.2 % of these peatlands were in Europe, covering an area of around 525,668 km². Peatlands are a naturally occurring carbon sink but due to anthropogenic impact, this system is altered. The removal of peat can lead to increased CH₄ or organic carbon release if the water table drops (Kern *et al.*, 2017). Most of the extracted peat is used for energy generation or growing media production.

Peat samples from an ombrotrophic peat bog in Switzerland were analysed by Zacccone et al.. The ash contents vary from around 0.41-6.83 %, while the C content ranges from around 48.18 to 57.77 %. As the samples were taken from different depths, it is shown that ash content stays more or less constant while the C and H content increases and the O content decreases with depth, indicating a higher microbial activity in the upper layers (Zacccone, Miano and Shotyky, 2007).

Samples of ombrotrophic peat coming from Bord na Móna have already been pyrolysed and analysed by the UK Biochar Research Centre (UKBRC). Two types of peat were pyrolysed at two different temperatures (450 °C, and 600 °C). The feedstock itself was analysed for metal content (Table 8). Comparing the CHO analysis for the two pyrolyzed Irish peat samples (Table 7) with other pyrolyzed peat (Sutcu, 2007) (Table 9), for example, shows that the carbon content can vary between 51.85 and 92.45 % depending on the origin and composition of the material used. The results shown in the tables below were provided by Bord na Móna.

Table 7: peat-based biochar analysis done by UKBRC (%db = % dry basis), data provided by Bord na Móna

	Yield (%)	Carbon (%db)	Hydrogen (%db)	Oxygen (%db)	PAH (total EPA 16)
Hort peat 450°C	33	68.37	2.10	2.72	0.36
Hort peat 600°C	30	74.46	1.80	1.85	0.62
Fuel peat 450°C	50	51.85	2.02	2.62	0.7
Fuel peat 650°C	29	68.32	1.92	1.94	0.26

Table 8: metal analysis results of moss peat samples (UKBRC), data provided by Bord na Móna

	Moss peat sample 1	Moss peat sample 2
Metals	mg kg ⁻¹	mg kg ⁻¹
Arsenic	0.81	0.49
Cadmium	0.09	0.11
Chromium	1.15	16
Copper	2.37	4.69
Mercury	0.05	0.06
Nickel	0.72	7.12
Lead	8.47	7.39
Selenium	0.02	>0.01
Zinc	12.6	15.7
Molybdenum	<0.01	1.57
Fluoride	<10	16

A study focussing on pyrolysis of peat, biochar yield and characterisation was published in 2007 (Sutcu, 2007). In the study, the samples were air-dried, ground and sieved into different groups before being pyrolysed at 350, 450, 550 and 650 °C at heating rates of 5 and 20°C min⁻¹, and a residence time of one hour. For both heating rates, the results showed a decline in the biochar yield from around 50% to 35% with lower yields for the 20°C min⁻¹ heating rate. The proximate and ultimate analysis (Table 9) revealed

the chemical properties of the biochars, produced at two different heating rates to show high similarity (Sutcu, 2007).

Table 9: Proximate and ultimate analysis of peat (0.5-2.0mm sieve size) and biochars obtained from varying heating rates (df, %) (Sutcu, 2007)

	Peat	5°C min ⁻¹				20°C min ⁻¹			
		350°C	450°C	550°C	650°C	350°C	450°C	550°C	650°C
Ash ^a	6.51	10.88	11.47	12.57	13.34	10.35	11.85	13.54	14.33
VM ^a	69.15	33.67	27.05	18.49	15.21	35.26	28.14	19.16	17.08
FC ^a	24.34	55.45	61.21	68.94	71.45	54.39	60.01	67.30	68.59
C ^b	56.38	76.30	80.19	85.30	91.04	77.80	80.93	84.50	92.45
H ^b	5.98	3.85	3.18	2.99	2.65	3.71	3.20	2.87	2.51
N ^b	1.43	1.23	1.21	1.15	1.15	1.22	1.21	1.18	1.14
S ^b	0.52	0.31	0.35	0.37	0.36	0.32	0.33	0.37	0.37
O ^c	35.69	18.31	15.07	10.19	4.80	16.95	14.33	11.08	3.53

a= df%, b= daf%, c= 100- (C+H+N+S)

Furthermore, it was found that as the particle size of the peat increased, so did the yield (Sutcu, 2007). Increases in the sweeping gas flow rate led to a slightly decreased biochar yield but it was stated that neither the increased flow rate nor the particle size had an explicit effect on the results of proximate and ultimate analysis of the biochars (Sutcu, 2007). Nevertheless, one difference noted was that biochars obtained by pyrolysis of peat at 450 °C, and a heating rate of 20°C min⁻¹ for the four varying sizes (0.5, 0.5-1.0, 1.0-

2.0, above 2.0 mm) had lower ash contents than those obtained in other pyrolysis conditions (Sutcu, 2007).

The effects of CO₂ on the pyrolysis of peat instead of using N₂ as a sweeping gas have also been investigated (Lee *et al.*, 2017). The samples were ground and dried before pyrolysis which was carried out at 700°C with a heating rate of 10°C min⁻¹ and a gas flow rate of 500 ml min⁻¹ for N₂ and CO₂. Proximate and ultimate analysis and morphological and spectral analysis were conducted for peat and biochar, while thermo-gravimetric analysis was carried out for peat on its own. Elemental analysis showed that biochar produced in the N₂ environment contained more C, H, and S than biochar produced in the CO₂ environment. On the other hand, they contained more O and N than the ones from the N₂ environment, indicating that the pyrolysis atmosphere affects the elemental composition of biochars. Additionally, biochar produced in CO₂ has a larger surface area than in N production, suggesting that CO₂ had a distinct role in promoting pore formation on the biochar surface (Lee *et al.*, 2017). A larger surface might lead to higher adsorption and if applied in manure GHG emission reduction.

The amelioration of soil acidity and P scarcity of weathered soils using manure biochar was addressed by using peat biochar produced from peat collected from Fushun in Liaoning Province, China (Kamran *et al.*, 2018). The peat was then air-dried at room temperature and ground to pass a 2 mm sieve. To produce the char the peat was placed in ceramic crucibles, covered with a fitting lid and pyrolysed under oxygen-limited conditions in a muffle furnace. The furnace temperature was raised to 400 °C at 20 °C min⁻¹, and then kept constant for 4 h. Afterwards, the biochars were cooled at room temperature and then passed through a 0.2 mm sieve giving a C/N value of 15.6 (Table 10).

Table 10: properties of peat biochar produced at 400°C for 4h

	pH	EC (mS min ⁻¹)	VM (g kg ⁻¹)	Ash	FC	Total C (%)	Total N (%)	Total H (%)	C/N
Peat	6.43±0.04	0.359±0.01	185.4±0.9	678.2±1.1	136.4	22.1	1.4	1.4	15.6

Studies using peat as a feedstock solely focused on the use of peat as a single feedstock without using multiple feedstocks in the same study, leaving a gap in the literature.

2.7.2 Brewery grain

Brewery grain could present a possible, more eco-friendly alternative to the use of peat as a biochar feedstock. Beer was the fifth most consumed beverage in the world in 2017 (Sperandio *et al.*, 2017). In 2020, global beer production amounted to about 1.82 billion hectoliters. And it still has a rising popularity in the last years around the world and is therefore producing tons of spent grain, which could be used for biochar production. Biochars from brewery grain have already been produced to increase the value of the spent grain. The biochars were produced for energy purposes, wastewater treatment, to study pyrolysis kinetics and to develop screen-printed electrodes (Yinxin, Jishi and Yi, 2015; Sperandio *et al.*, 2017; Cancelliere *et al.*, 2019; Olszewski *et al.*, 2019). Spent grain is a resource usually given to animals as feed or to improve the texture of compost to avoid having to send it to a landfill. Using the grain for biochar production could give another use to the quantities of spent grains produced as a by-product of the brewing industry.

3. Methodology and methods

This chapter specifies the methodological approach used as well as the methods used (Figure 8, Table 11). The biochars were produced and analysed using qualitative methods. The interpretation of the data was done using statistical analysis (section 3.15). To investigate the influence of biochar on the release of carbon dioxide, methane and ammonia emissions from manure, laboratory-scale emission trials were carried out. The same applies to the adsorption of dye trials.

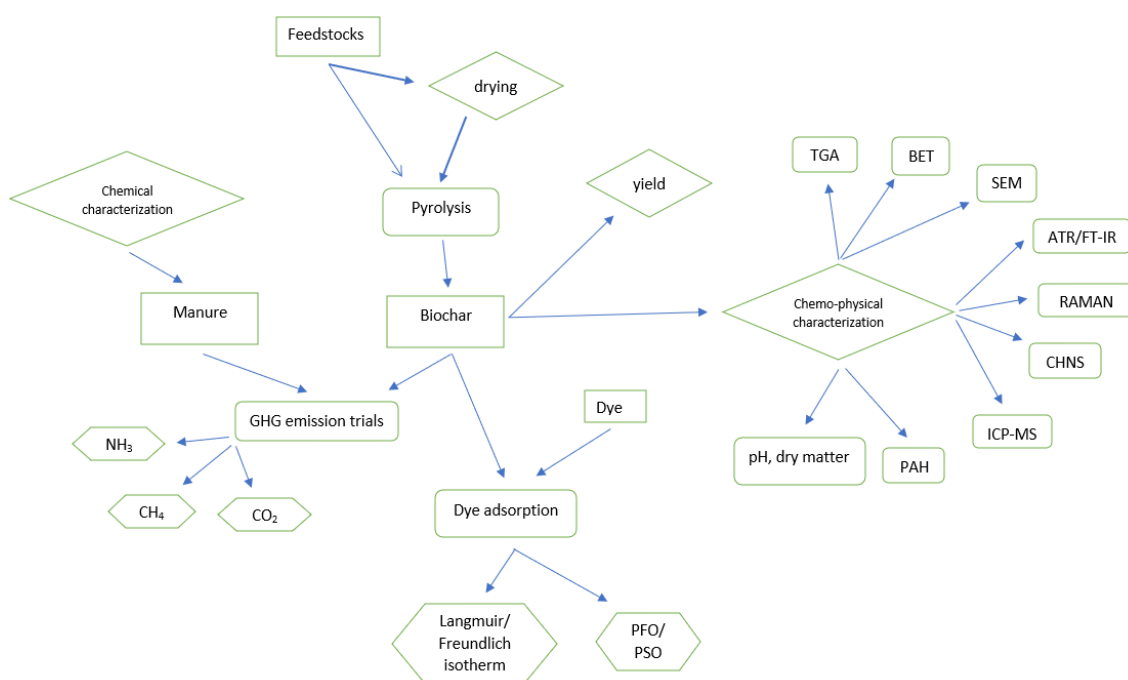


Figure 8: methodological flowchart of the thesis

Table 11: Overview of methods and equipment used to analyse the biochars

Analysis	Software/ equipment	Protocol
Dry matter content	Oven (UN55, memmert, Lennox)	VDLUFA Method Handbook Vol. 3, DIN EN12880:2001-02, chapter 3.1
pH	pH meter (pH700, EUTECH Instruments)	VDLUFA Method Handbook Vol. 3, DIN EN12880:2001-02, chapter 3.1
TGA	Mettler-Toledo TGA/DSC2	established protocol from the literature (Buss and Mašek, 2014)
BET	Quantachrome NOVATouch LX4	
SEM	Hitachi SU6600 FESEM	
FT-IR / ATR	Perkin Elmer Spectrum 100 FTIR with a Perkin Elmer Universal ATR accessory (Perkin Elmer, USA)	
PAH content		established protocols from the literature (Hilber <i>et al.</i> , 2012; Buss <i>et al.</i> , 2016; Frišták, Pipíška and Soja, 2018)
Raman	Horiba Jobin Yvon LabRAM HR 800	
CHNS	Carlo-Erba 1108 elemental analyser EA1108	
ICP	ICP – MS (7900 ICP-MS, Agilent Technologies)	Microwave digestion: US Environmental Protection Agency (EPA) Method 3051A

3.1. Origin of organic feedstocks

In this study, five different materials were used (Table 12, Table 13). The materials were obtained from the Bord na Móna (BnM) facility in Kilberry, Co. Kildare. The feedstocks used in this study were all defined by the research partner (BnM). This research was designed to assess and examine the potential use of defined sources available to the industry partner.

Table 12: Feedstocks used in the project as well as their sample date and origin

Material	Date of sampling	Origin
Raw peat	14.03.2018	Bord na Móna composting facility, Kilberry, Ireland
Peat fibre	14.03.2018	Bord na Móna composting facility, Kilberry, Ireland
Fine urban green waste	14.03.2018	Bord na Móna composting facility, Kilberry, Ireland
Brewery grain black	20.03.2018	Bord na Móna composting facility, Kilberry, Ireland
Brewery grain white	20.03.2018	Bord na Móna composting facility, Kilberry, Ireland

The peat and the peat fibre came from a drained Irish ombrotrophic peatland in the Midlands. The peat was used as the producer (BnM) wanted to explore the extent to which value could be added to mid-profile peat from a drained raised-bog mid-way through its extraction cycle. The peat fibre was obtained by separating the finer peat, used for growing media, from fibrous materials or chunks of organic material present in the peat. Both spent brewery grains were delivered to the composting facility in a pre-dried state carried out by the brewery. The difference between the two grains is their treatment during the brewing process. While the fine urban green waste was the result of a separation of composted green waste into different sections sorted by size, carried out at the composting facility.

Table 13: Feedstocks used for biochar production and exemplarity biochars produced from these feedstocks

Feedstock	Material name	Biochar
	peat	
	Peat fibre	
	Fine urban green waste	
	Brewery grain black	
	Brewery grain white	

3.2. Preparation of materials

A part of each feedstock was dried in an oven (UN55, memmert, Lennox) at 105 °C for 24 hrs before being used for the production of biochars. The other part was used as collected to determine the influence of pre-treatment on feedstocks. Before being used the materials were stored in a cold room at around 4 °C to ensure the continuity of the properties of the feedstocks.

3.3. Production of biochars

Biochars were produced using a muffle furnace (SNOL 13/1100) and ceramic crucibles with lids. The biochars were produced at 450 – 750 °C using fresh or pre-dried material with a residence time of 20 min and a heating rate of 7.5 °C min⁻¹ (Table 14). After production, the biochars were left to cool down overnight in a desiccator (250 mm Desiccator, Vacuum - Lennox) before their weight was recorded. The yield was determined on a fresh and dry matter basis as a product of the biochar weight in relation to the weight of the materials before pyrolysis. Around 20 – 61 g of fresh and around 7 – 30 g of dried feedstock was used per crucible for biochar production.

Table 14: Conditions of biochar production ranging from 450 – 750 °C

Material	Temperature (°C)				Residence time (min)
	450	550	650	750	20
Raw peat	X	X	X	X	X
Peat fibre	X	X	X	X	X
Fine urban green waste	X	X	X	X	X
Brewery grain black	X	X	X	X	X
Brewery grain white	X	X	X	X	X

3.4. Chemical analysis – pH, dry matter and moisture content

Chemical characterisation of the feedstocks and biochars was performed with the following methods (Table 15).

Table 15: Analytical methods used for the chemical characterisation of feedstocks and biochars

Parameter	Method
pH	According to VDLUFA Method Handbook Vol. 3, DIN EN12880:2001-02, chapter 3.1
Dry matter (DM)	According to VDLUFA Method Handbook Vol. 3, DIN EN12880:2001-02, chapter 3.1

pH was measured with de-ionised water. Biochar and feedstock pH values are obtained in triplicate using a ratio of 1g of biochar and feedstock in 10 mL deionised water (1:10 w/v). The solution is placed on a shaker (MaxQ2000, Thermo Scientific) and left there for 60 min at 150 rpm to ensure sufficient equilibration between solution and material surfaces. After shaking, the solution was left standing for 30 min before measuring using a pH meter (pH700, EUTECH Instruments).

To determine the dry matter (DM) content of the feedstocks, they were placed in an oven (UN55, memmert, Lennox) at 105 °C for 24 h. The weights were recorded before and after drying to calculate the DM and moisture content of each feedstock. DM was calculated as an equation of dry weight to the total weight. The moisture content is the difference in the weight before and after drying. To confirm that 24 h was sufficient time for drying, the feedstocks were dried for around 48h as well and it was seen that DM content stayed the same.

3.5. Thermo-gravimetric analysis (TGA)

Thermo-gravimetric analysis (TGA) was used to quantify fixed carbon in the biochars with a Mettler-Toledo TGA/DSC2. The samples were ground using a quartz mortar and pestle before storage in small glass containers. To start the analysis, 2.0 - 2.5 mg were put in a crucible (Buss and Mašek, 2014). First, the moisture was evaporated by heating the sample to 110 °C at 25 °C min⁻¹. Then, the temperature was held at 110 °C for 10 min. Next, the volatiles were driven off by heating to 900 °C using the same heating rate as before. This temperature is also held for 10 min. Both steps are performed using a nitrogen gas flow rate of 30 ml min⁻¹. As the machine (TGA/DSC2 STARe System, Mettler Toledo) conducting the analysis could not switch automatically from nitrogen to air a second run was performed using air as a flow gas to oxidise the carbon left in the sample and thereby determine the ash content. The amount of carbon combusted is the amount

of fixed carbon present in the sample. In this run, the steps were similar to the nitrogen flow, but the samples were held for 20 min at 900 °C and not for 10 min, as described in the original method. Each sample was processed in triplicate using 2.0 - 2.5 mg. A blank sample was run before the experiment to account for weight changes in the crucible.

To convert some properties (here the fixed carbon (FC) content) from one basis to another, the following general formula was used (Riley, 2007):

$$P_{wanted} = P_{given} * f_c$$

where P_{wanted} is the property based on a wanted basis, P_{given} is the property based on a given basis, and f_c is the conversion factor. To calculate the conversion factor for a conversion from a dry basis to a dry ash-free basis the FC content on a dry basis is divided by the difference of FC (wt%, db) – ash (% , db) (Cai *et al.*, 2017).

3.6. Nitrogen physisorption (BET)

Nitrogen physisorption was used to determine the surface and pore properties of the biochar samples. Physisorption was carried out in a Quantachrome NOVATouch LX4 at - 196 °C. Before analysis, the samples were degassed in a vacuum oven at 200 °C overnight and then in the instrument degassing stations at 300 °C for 12 h. The surface area of the samples was determined by the Brauner-Emmet-Teller (BET) method. The micropore surface area and volume were determined by the t-plot method. The total pore volume was determined from the total nitrogen adsorption at $P/P_0 = 0.99$.

3.7. Scanning electron microscopy (SEM)

Images are produced using a beam of electrons generated at the top of the microscope (Hitachi SU6600 FESEM). The beam passes through electromagnetic fields and lenses, which focus and shape the beam down towards a sample. Once the beam hits the sample, electrons and X-rays are ejected from it (Figure 9, Figure 10). Detectors collect these X-

rays, backscattered electrons and secondary electrons and convert them into a signal that is sent to a screen, where the image appears. The microscope is held under a vacuum throughout the process. SEM pictures from the samples were taken to characterise their surfaces. To do so, a few milligrams were placed on a conducting sticky pad and placed into the sample chamber of the SEM.

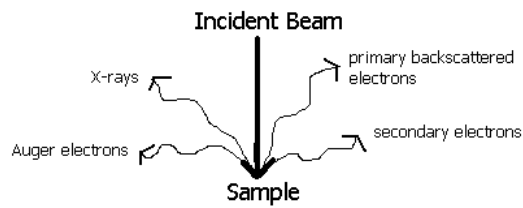


Figure 9: Reaction after the incident beam reaches the sample

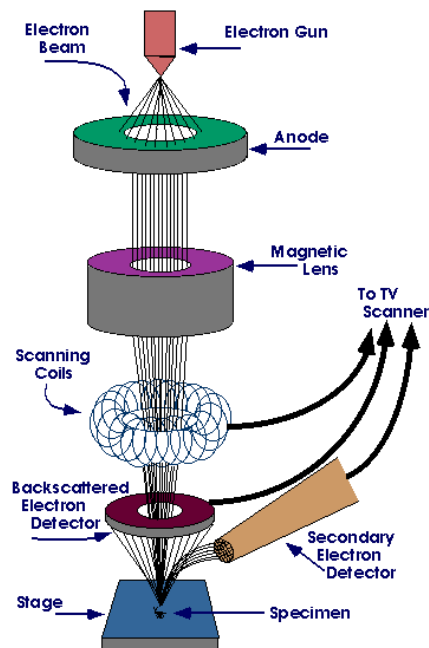


Figure 10: Scheme of a scanning electron microscope

3.8. Fourier Transform Infrared spectroscopy/Attenuated total reflection (FT-IR/ATR)

The FTIR spectra were collected using a Perkin Elmer Spectrum 100 FTIR with a Perkin Elmer Universal ATR accessory (Perkin Elmer, USA). For the ATR, first, a background was measured before applying the sample to the measuring crystal. Transmission and absorption were measured for each run, conducted in duplicate. 250 mg of each sample was placed on top of the ATR accessory.

3.9. Polycyclic aromatic hydrocarbons (PAH)

Polycyclic aromatic hydrocarbon (PAH) extraction of the biochars was carried out using established protocols (Hilber *et al.*, 2012; Buss *et al.*, 2016; Frišták, Pipiška and Soja, 2018). The biochars were first dried at 40 °C overnight and then ground to 0.75 mm with mortar and pestle and sieved to the correct size. Toluene (100%) was used as a starting solvent for the Soxhlet extractions. The extractions were run for 36 h and the sample size was 1g. After the extractions, the resulting liquid was run through a rotary evaporator to recover the toluene. The remaining liquid was run through a gas chromatograph (GC) to detect the PAHs. The GC – MS used was an Agilent 6890N gas chromatograph and an Agilent 5975 mass spectrometer.

A standard containing 16 EPA PAHs, which are designated High Priority Pollutants (HPP) by the Environmental Protection Agency (EPA), was used as a reference to identify the PAHs in the biochars. A blank of pure toluene was run to exclude any signs of toluene or its chemical components from the GC chromatograms.

3.10. RAMAN spectroscopy

The RAMAN analysis was performed using a Horiba Jobin Yvon LabRAM HR 800. A 532 nm laser line (max power 50 mW) was employed at 10% power to avoid sample degradation. Spectra were recorded with an x50 objective (spot size of approx. 4µm) with an acquisition time of 10s and averaging 3 accumulations. The internal optical set-up consisted of a 600 ln/mm grating with a 532 nm edge filter.

3.11. Elemental analysis (CHNS)

The biochars were also analysed for their CHNS content using a Carlo-Erba 1108 elemental analyser EA1108. All samples were ground before the analysis. Samples for CHNS analysis were prepared by adding 1-2 mg sample and 3-5 mg oxidiser (vanadium pentoxide, V₂O₅) to a tin crucible which was then closed and inserted into the analyser. Before analysis, sulphanilamide was used as a calibration standard. The oxygen content was calculated as the difference (O = 100-C-H-N-S-ash).

3.12. ICP-MS

Samples were digested, filtered and diluted before being inserted into the ICP-MS. Microwave digestion was carried out according to US Environmental Protection Agency (EPA) Method 3051A (Jeong, Lee and Kim, 2020). In the method, 0.5 g of biochar was inserted into a microwave vessel and mixed with 10 ml of concentrated nitric acid. The microwave digestion programme included a ramp of 5.5 min up to 175 °C, a holding time of 4.5 min and a cooling-down time of 30 min. After cooling, the vessels were vented in a fume hood before uncapping. The samples were quantitatively transferred to a 100 ml volumetric flask and topped up with ultra-pure water. This mix was then filtered into another acid-cleaned flask. 5 ml of the filtered sample was made up to 50 ml in a volumetric flask (1:10) and 1 ml of the diluted sample was made up to 100 ml with diluent

(1:1000). These dilutions were made to account for the different concentrations of the tested elements. The diluent contains 2% HNO₃ and 0.5% HCl in ultra-pure water.

The samples were analysed for As, B, Ca, K, Mg, P, S, Pb, Ni, Cu, Co, Cd, Na, Zn, Fe, and Mn using ICP – MS (7900 ICP-MS, Agilent Technologies).

3.13. Manure emission experiments

To determine the CH₄ and CO₂ emission reduction potential of the biochars they were mixed with slurry in different ratios to see which combination leads to the best results (Table 16). Each mixture was against a blank control (0 % biochar).

Table 16: biochar - slurry mixtures for emission reduction trials

	Mixture			
	0 %	0.25 %	0.5 %	1.0 %
Biochar	X	X	X	X

3.13.1. Manure

The manure used in this study was collected from a pig farm in Flegessen, Germany. The pigs were fed with single feed for carrying sows (12,2 MJ ME / 13,5 % XP) (see tables below).

Table 17: Ingredients of pig feed

feedstock	TM	Part %
Agravis Ergänzer Sauen Brand	880	20
Wheat	879	28.50
Spelt	880	50
Soy oil	999	0.5
Beer yeast	893	1.0

Table 18: Weender Analysis of ingredients of the pig feed

ingredient	unit	minimum	content	88% dry mass
Dry matter	%	88	88.04	88
Metabolizable energy (ME) pig (2010)	MJ	13	12.89	12.88
Starch	%		41.88	41.86
Crude fibre	%	5	7.01	7.01
Crude protein	%	16.5	15.59	15.58

The manure had a pH of 7.05 – 7.15 and a dry matter content of 0.70 – 8.06 %DM (Table 19). The manure was collected on a regular schedule every two weeks to ensure consistency in terms of its age profile.

Table 19: chemical analysis of pig manure used for emission trials

parameter	unit	
pH		7.05 – 7.15
DM	%	0.70 – 8.06
COD	mg/l	95140
NH ₄ -N	mg/l	208
NO ₃ -N	mg/l	3.03
Acid capacity	mmol/l	70.8
PO ₄	mg/l	1820

3.13.2. Gas emission experiment set-up

The emission experiments were run in triplicate, with one set of triplicates collected in a biogas bag (Restek, USA) (Figure 11). Each experiment was run at room temperature (20 – 22 °C). And the manure was mixed before being poured into the glass bottles to ensure homogeneity. The biochars were then applied to the manure and the setup was left without stirring for 72 hours in a sealed flask. This flask was attached to a biogas bag used to extract treated gas emissions for analysis. Each biochar manure experiment was carried out with three different concentrations of biochar using 250 ml of manure mixture for each experiment. The biochars were applied in concentration values of 0.25, 0.5 and 1% w/v. These concentrations were chosen to simulate feasible concentrations in bigger tanks, while still having enough biochar present to generate a viable effect relevant for subsequent upscaling. A syringe was then used to insert the gas samples from the bags into the gas chromatograph (GC) (Shimadzu GC-2014 with packed

column (2.1 m, HayesepQ)). The gas was injected into the GC at a temperature of 110°C. The analysis was carried out using helium 5.0 with a flow of 27 mL min⁻¹ and a thermal conductivity detector (TCD).

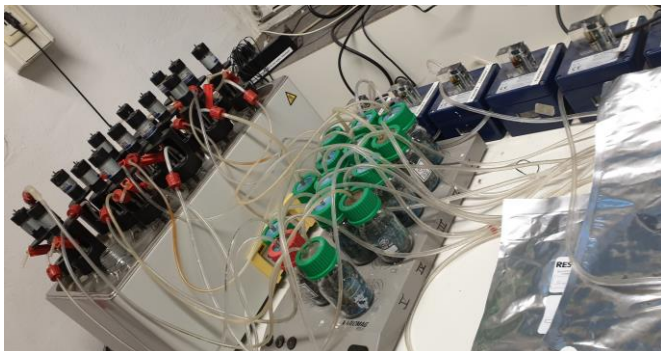


Figure 11: Experimental set-up of the emission trials run with swine manure and biochar

3.14. Dye adsorption experiments

3.14.1. Experimental arrangement

Cationic dye was chosen as the most suitable dye for adsorption analysis (Sewu, Boakye and Woo, 2017). As the biochars produced in this study were alkaline the use of a cationic dye should favour adsorption because of the negative surface charge. Malachite green was chosen as the cationic dye for this trial. Malachite green dye was mixed with de-ionised water to create solutions of various concentrations. The dilutions were prepared in the following mixtures 1:10, 1:20, 1:50 and 1:100 (Table 20). As a next step, 10 mg biochar was weighed into a centrifuge tube and 30 mL of the dye solution was added and the mixture was left for 48h to 60h to observe adsorption. In the end, 3 ml of the mixture was taken from the middle of the filled volume, to analyse the dilutions with a spectrophotometer (DR 6000, HACH). The dilutions were analysed by the spectrophotometer before and after the experimental run, to calculate the adsorption rate. The Langmuir and Freundlich models were employed to characterise adsorption. To be able to calculate the kinetics with pseudo first (PFO) and second order (PSO), biochar

was mixed at a rate of 0.5 % w/v. This means that 0.0125 g of biochar was mixed with 2.5 mL of the solution. The solution was analysed using a Cary 60 spectrophotometer (Agilent Technologies, Inc., USA).

Table 20: dilutions used in the adsorption experiments with the respective initial concentration of dye in mg L^{-1} (ppm)

dilution	C_0 (mg L^{-1})
1:10	10
1:20	5
1:50	2
1:100	1

3.14.2. Adsorption isotherm models

Two adsorption isotherm models were used in the adsorbate-adsorbent interaction analysis to identify the adsorption mechanism (Sewu, Boakye and Woo, 2017; Chen *et al.*, 2018). The effect of different biochar concentrations (0.1, 0.5 and 1.0%w/v) was investigated for the adsorption process. The dye adsorption process by biochar was described by the Langmuir and Freundlich isotherm.

The Langmuir model can be expressed as:

$$\frac{C_e}{Q_e} = \frac{C_e}{Q_m} + \frac{1}{Q_m K_L}$$

where C_e is the equilibrium concentration of dye (mg L^{-1}), which is the concentration of adsorbate solution (mg/L) after adsorption equilibrium. Q_e is the amount of dye adsorbed per mass of biochar (mg g^{-1}), which is the difference in adsorbance to the pure dye solution divided by the amount of biochar used. Q_m is the maximum adsorption capacity of biochar (mg g^{-1}), which is 1 divided by the slope of the function. And K_L is the

Langmuir constant ($L \text{ mg}^{-1}$), which can be expressed by dividing the intercept with the y-axis of the function by Q_m . The Langmuir adsorption isotherm is used to describe the equilibrium between adsorbate and adsorbent, meaning that it shows how much one adsorbate can be adsorbed of a certain adsorbent.

The Freundlich model is described as:

$$\log Q_e = \log K_F + \frac{1}{n} \log C_e$$

where K_F is the Freundlich adsorbent capacity, where the log of K_F is the intercept of the function with the y-axis and n_F is the heterogeneity factor (Chen *et al.*, 2018). The model shows the relationship between the concentration of a solute (dye) adsorbed onto the surface of a solid (biochar) and the concentration given in the liquid phase.

3.14.3. Adsorption kinetics – Pseudo-First Order and Pseudo-Second Order

The linearized PFO and PSO models are given in the equations below where q_e is the calculated equilibrium adsorption capacity (mg g^{-1}) and q_t (mg g^{-1}) is the adsorption capacity at time t (min); and, k_1 (min^{-1}) and k_2 ($\text{g mg}^{-1} \text{ min}^{-1}$) are the PFO and PSO rate constants, respectively (Sumalinog, Capareda and de Luna, 2018).

PFO:

$$q_t = q_e (1 - e^{-k_1 t})$$

or

$$\ln(q_e - q_t) = \ln(q_e) - k_1 * t$$

PSO:

$$\frac{t}{q_t} = \frac{1}{k_2 q_e^2} + \frac{1}{q_e} t$$

3.15. Statistical analysis

The statistical analysis was carried out using Excel and Prism Software. Both programs were used to calculate means, standard deviations and significances between the samples using ANOVA tests ($p < 0.0001$, $p < 0.001$, $p < 0.01$, $p < 0.05$).

4. Results

4.1. Biochar yield

Depending on the biochar used, the yield of the biochar produced varies between 11.72 – 36.94 %FM (Table 21) and between 27.65 – 60.58 %DM (Table 23). Table 21 shows the biochar yield for all materials produced from fresh matter (FM) calculated in %FM, whereas Table 22 presents the yield of fresh materials calculated on a DM basis. The yield of the peat materials is in the middle of the overall range. Biochars produced from brewery grains have the highest yield, reflected by their high dry matter content. The biochar yield for peat decreases from 21.26 to 14.09 %FM. Peat fibre has a similar yield whereas the brewery grain yield varies between 36.94 and 25.84 %FM for the two materials.

Table 21: Biochar yield (%FM) calculated for different production temperatures as described in section 3.3

	450 °C	550 °C	650 °C	750 °C
Raw peat	21.26±1.55	16.98±0.19	15.23±0.26	14.09±0.17
Peat fibre	23.67±0.99	20.38±1.50	18.56±0.31	16.61±0.74
Fine urban green waste	17.59±0.18	14.18±0.01	12.89±0.37	11.72±0.50
Brewery grain black	36.94±0.33	33.97±0.01	31.62±0.12	30.44±0.05
Brewery grain white	30.86±0.64	29.10±0.38	26.96±0.59	25.84±0.15

Table 22: Biochar yield of fresh materials (%DM) calculated for different production temperatures as described in section 3.3

	450 °C	550 °C	650 °C	750 °C
Raw peat	53.18±3.88	42.47±0.48	38.09±0.65	35.24±0.43
Peat fibre	49.01±2.05	42.19±3.11	38.43±0.64	34.39±1.53
Fine urban green waste	62.78±0.64	50.61±0.04	46.00±1.32	41.83±1.78
Brewery grain black	39.06±0.35	35.92±0.01	33.43±0.13	32.18±0.05
Brewery grain white	33.39±0.69	31.49±0.41	29.17±0.64	27.96±0.16

Table 23: Biochar yield (%DM) calculated for different production temperatures as described in section 3.3

	450 °C	550 °C	650 °C	750 °C
Raw peat	51.43±0.98	45.20±0.23	41.37±0.16	35.89±0.13
Peat fibre	51.03±1.08	44.60±0.44	40.75±0.29	38.58±0.98
Fine urban green waste	62.16±0.20	57.72±0.24	53.64±0.58	52.64±0.25
Brewery grain black	39.01±0.19	35.80±0.05	33.86±0.09	33.39±0.08
Brewery grain white	34.13±0.38	31.12±0.28	31.14±2.57	27.87±0.17

A more even picture can be seen for all twenty biochars produced from dried material (Table 23). Biochars produced from dried fine urban green waste (fine ugw) have the highest yield across all the temperatures, whereas biochars from brewery grains have the lowest yield but still reach a yield of around 30 %DM across all the temperatures.

When comparing the yield loss of fresh materials with pre-dried materials it can be seen that the dried materials have a slightly smaller loss in yield. It was determined that the temperature has a significant influence on the production process of biochar from dried material ($p < 0.05$). While the peat samples have a yield of around 20 %FM, the

urban waste biochars show a slightly lower yield (17.59 – 11.72 %FM). The highest yield was observed by the brewery grain samples (36.94 %FM). Comparing these findings to the ones calculated from dried materials on a dry matter basis, the lowest yield was observed for the brewery grain samples (27.87 – 39.01 %DM), whereas fine ugw presented the highest yield (62.16 %DM).

As there is not much difference between the yield of fresh material calculated on a dry matter basis and the yield of the dried material, for the rest of this study, biochars produced from dried materials will be used. This will ensure the comparability of the results found here with the ones produced in the literature.

4.2. Feedstock analysis – dry matter & moisture content, pH

The results show a dry matter (DM) content of the peat materials between 39.98 and 48.30 % FM and a content of 28.02 %FM (fine ugw) to 94.58% FM (brewery black) for the other materials (Figure 12). It can be observed that similar materials (e.g. brewery grain black and white) have similar DM contents and therefore also similar moisture contents.

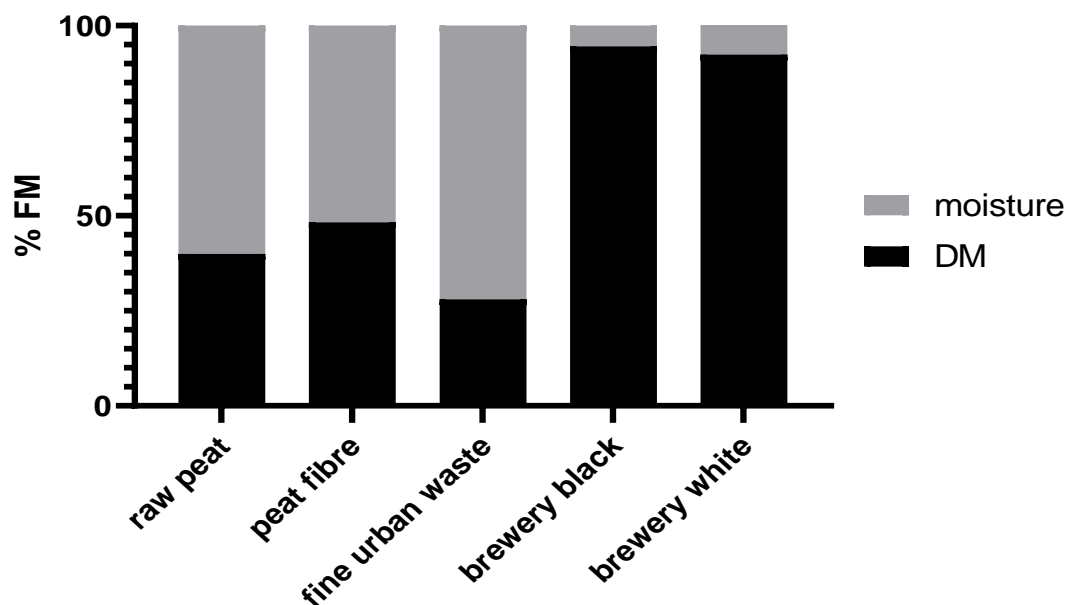


Figure 12: Dry matter (DM) and moisture content of feedstocks used for biochar production in %FM

The pH results of all feedstocks vary between 4.64 and 6.07 (Table 24). In comparison to that, the pH values of the biochars are higher at all temperatures than the untreated feedstock and keep increasing with higher treatment temperatures. The pH of raw peat biochars increases from 5.76 to 9.17 while the fresh material has a pH of 4.87 (Table 25). The rise of pH with increasing treatment temperatures varies depending on the material used.

Table 24: dry matter, moisture content and pH results obtained from feedstocks used for biochar production

	DM (%FM)	Moisture content (%FM)	pH
Raw peat	39.98±1.39	60.02±1.39	4.82±0.06
Peat fibre	48.30±2.06	51.70±2.06	4.64±0.11
Fine urban green waste	28.02±1.02	71.98±1.02	7.50±0.06
Brewery grain black	94.58±0.27	5.42±0.27	5.71±0.02
Brewery grain white	92.41±0.22	7.83±0.69	6.07±0.01

Table 25: pH values of feedstocks in comparison to biochars produced at 450 - 750 °C from fresh material

	pH				
	feedstock	450 °C	550 °C	650 °C	750 °C
Surface peat	4.87	5.76	7.47	8.46	9.17
Peat fibre	4.64	6.56	7.58	8.45	9.27
Brewery grain black	5.71	9.54	10.75	10.89	11.49
Brewery grain white	6.07	8.98	9.55	10.22	10.91
Fine urban green waste	7.50	9.17	10.33	10.12	11.20

The pH values of biochars produced from pre-dried materials are higher (Table 26). Here the pH values of biochars produced at 450 °C vary between 6.50 and 9.93, whereas the pH of biochars produced from fresh materials at the same temperature varies between 5.76 and 9.54 (Table 25).

Table 26: pH values of biochar produced from pre-dried material

	pH			
	450 °C	550 °C	650 °C	750 °C
Surface peat	6.55	7.78	8.74	9.63
Peat fibre	6.50	7.72	8.32	9.59
Brewery grain black	9.52	11.04	11.57	11.09
Brewery grain white	9.93	11.37	10.72	10.87
Fine urban green waste	8.65	10.41	10.50	10.54

4.3. TGA results

The results of the volatile matter (VM) content analysis range from 11.46 wt%, d.b. to 36.31 wt%, d.b. (Figure 13). The moisture content of biochars obtained by the TGA is not as linear as the VM content for all the materials. Most of the materials have a higher moisture content at 750 °C than at lower temperatures though the decrease of moisture for the temperatures of 450 to 650 °C is quite linear. The content ranges from 4.89 %DM to 2.66 %DM (Table 27). Overall biochars produced from brewery black grains have the lowest VM content and the highest FC content (Figure 14). Whereas biochars from peat have the highest VM contents and the lowest ash contents. Biochars from fine ugw contain more ash than FC (Table 27). One thing all materials and biochars have in common is that the VM content decreases with higher treatment temperature and most biochars contain more FC than ash (Figure 15). Though this is not true for biochars produced from fine ugw.

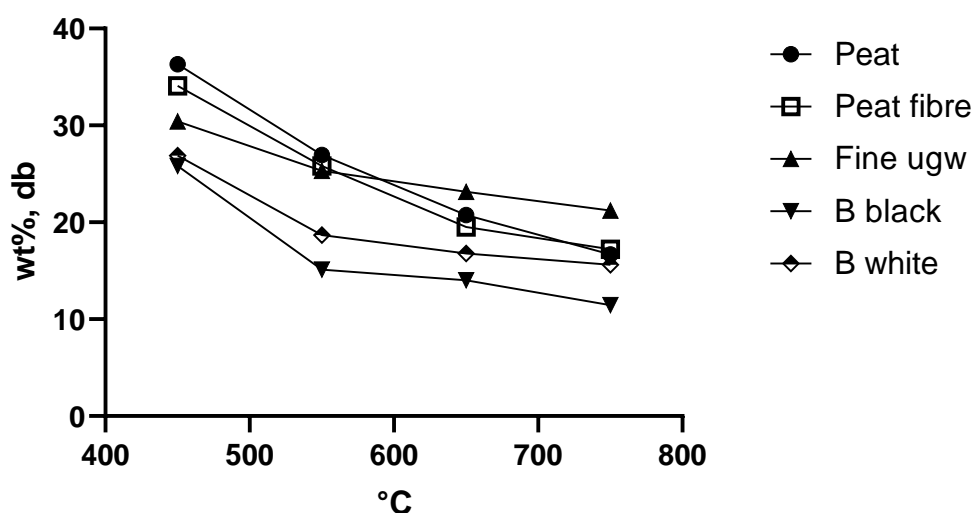


Figure 13: Volatile matter content of biochars produced from pre-dried materials obtained from samples heated up to 900°C under nitrogen flow

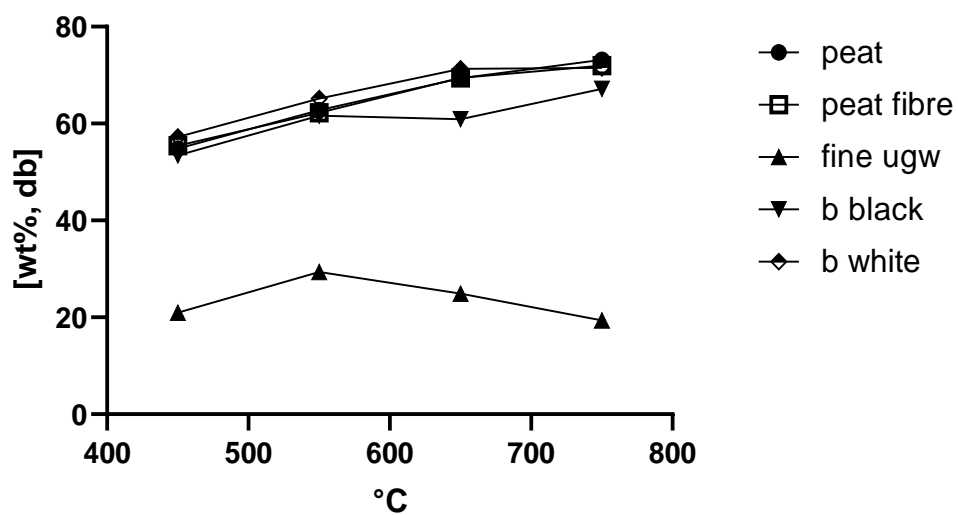


Figure 14: Fixed carbon content of biochars produced from pre-dried materials obtained at 900°C under nitrogen flow

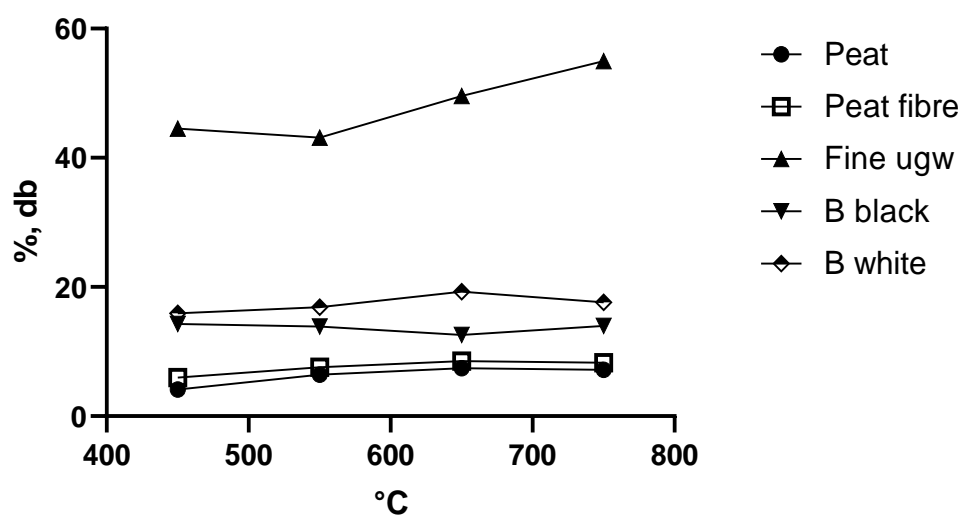


Figure 15: Ash content of biochars produced from pre-dried materials obtained at 900°C under airflow

Table 27: results obtained by thermo-gravimetric analysis of all five materials

Material	Temperature (°C)	Moisture (%)	VM (wt%, db)	FC (wt%, db)	Ash (% , db)
Peat	450	4.69±0.52	36.31±0.15	54.86±0.83	4.14±0.28
	550	3.76±0.14	26.96±0.63	62.74±0.92	6.40±0.09
	650	2.87±0.08	20.74±0.49	69.36±0.73	7.42±0.50
	750	3.60±0.5	16.69±0.80	73.16±0.55	7.18±0.71
P fibre	450	4.89±0.11	34.08±0.46	55.40±0.10	5.99±0.22
	550	4.08±0.07	25.81±0.48	62.21±0.64	7.59±0.63
	650	3.03±0.90	19.52±0.40	69.43±0.01	8.54±0.94
	750	2.73±0.81	17.22±0.12	71.99±0.61	8.25±0.92
Fine ugw	450	3.96±0.30	30.42±1.77	20.97±6.21	44.52±2.86
	550	3.21±0.36	25.31±1.61	29.36±3.14	43.14±0.84
	650	2.94±0.24	23.16±0.85	24.87±0.33	49.58±1.20
	750	3.35±0.36	21.21±1.63	19.35±5.53	54.97±4.68
B black	450	3.18±0.22	25.80±0.57	57.26±2.11	14.25±1.63
	550	2.66±0.34	15.11±4.63	65.17±1.29	13.89±0.76
	650	2.39±0.20	14.02±0.36	71.27±0.10	12.59±0.35
	750	3.14±0.36	11.46±0.28	71.53±0.55	13.96±0.54
B white	450	3.78±0.11	26.87±0.36	53.46±0.09	15.94±0.33
	550	2.98±0.12	18.68±0.36	61.64±0.35	16.86±0.21
	650	3.10±0.28	16.79±0.32	60.92±0.12	19.26±0.13
	750	4.36±1.65	15.62±5.16	67.16±0.44	17.65±0.74

Table 28: Fixed carbon content calculated on a dry ash-free basis using the formula published by (Riley, 2007)

Material	Temperature (°C)	Conversion factor	FC (% db, ash-free)
Peat	450	1.08	59.34
	550	1.11	69.87
	650	1.12	77.67
	750	1.11	81.12
P fibre	450	1.12	62.12
	550	1.14	70.85
	650	1.14	79.17
	750	1.13	81.31
Fine ugw	450	-0.89	-18.67
	550	-2.13	-62.56
	650	-1.01	-25.03
	750	-0.54	-10.51
B black	450	1.33	76.23
	550	1.27	82.83
	650	1.21	86.56
	750	1.24	88.88
B white	450	1.42	76.17
	550	1.38	84.85
	650	1.46	89.09
	750	1.36	91.10

Weight changes of one of the b black samples (Figure 16) analysed using TGA and for one of the fine ugw samples (Figure 17) are examples of the change of weight all

samples undertake during TGA analysis. It can be seen as well that each material is reacting differently during the analysis. At the different temperatures, the changes in weight leading to the results below can be clearly seen. In the first part of the graph up to 110 °C the biochar is losing its moisture. When the heat is rising to 900 °C the volatiles are driven off. The ash fraction of the samples was produced in a second run under O₂ conditions and can therefore not be presented in the same graph. The 20 biochars produced in this study contain 11.46 – 36.31 wt%, d.b. VM (Figure 13), 4.14 – 54.97 %, d.b. ash (Figure 15) and 19.35 – 73.16 wt%, d.b. of fixed carbon (Figure 14).

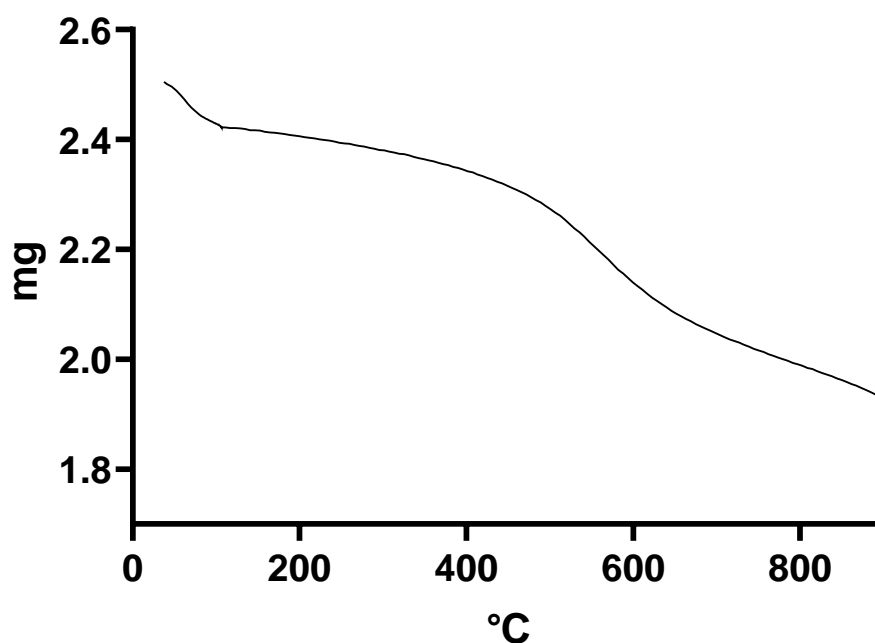


Figure 16: TGA plot of biochar produced from b black at 450°C; Graph goes till the end of N₂ run at the TGA

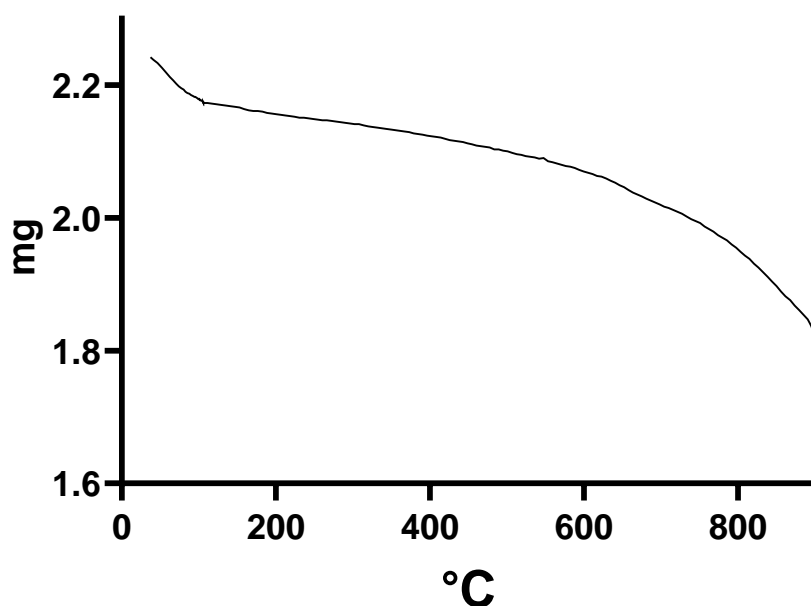


Figure 17: TGA plot of biochar produced from fine ugw at 750°C; Graph goes till the end of N₂ run at the TGA

4.4. BET results

The surface area ($\text{m}^2 \text{g}^{-1}$) of all biochars increased with higher treatment temperatures (Figure 18). The highest surface area of biochars produced from pre-dried materials was reported for peat biochar produced at 750 °C ($442.43 \text{ m}^2 \text{g}^{-1}$). The brewery white biochars have a surface area of only $8.50 - 94.91 \text{ m}^2 \text{g}^{-1}$. In general, the surface area of biochars produced in this study at 750 °C increased 7 – 119 times from those produced at 450 °C. The micropore area follows the same trend as the surface area (Figure 19). The peat biochar produced at 750 °C has the highest micropore area, whereas the brewery white biochar produced at the same temperature displays the lowest area of all biochars produced at 750 °C. For lower temperatures, fine ugw and brewery black present the lowest values. While the surface area, the micropore area as well as the total pore volume

increase with treatment temperatures up to 650 °C. A slight decrease can be observed for the numbers at 750 °C.

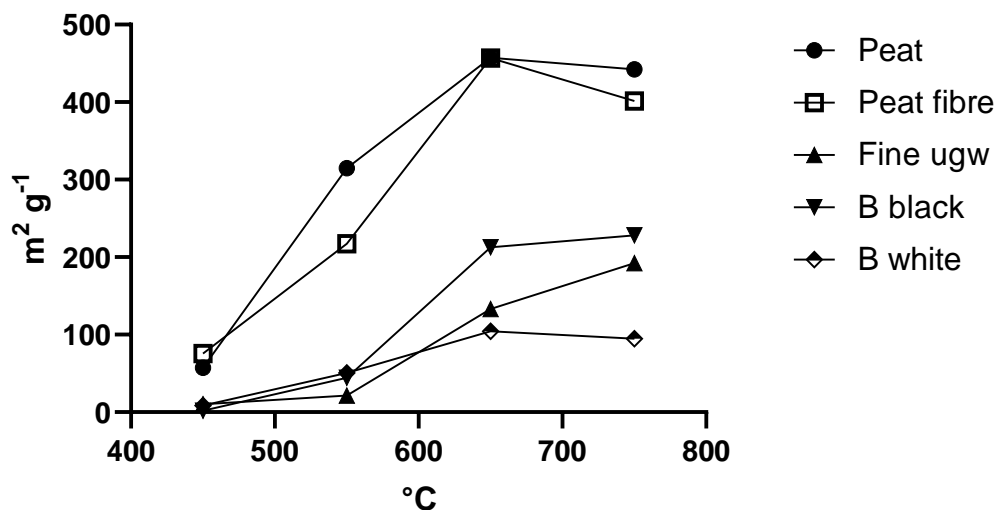


Figure 18: surface area of biochars produced from pre-dried materials

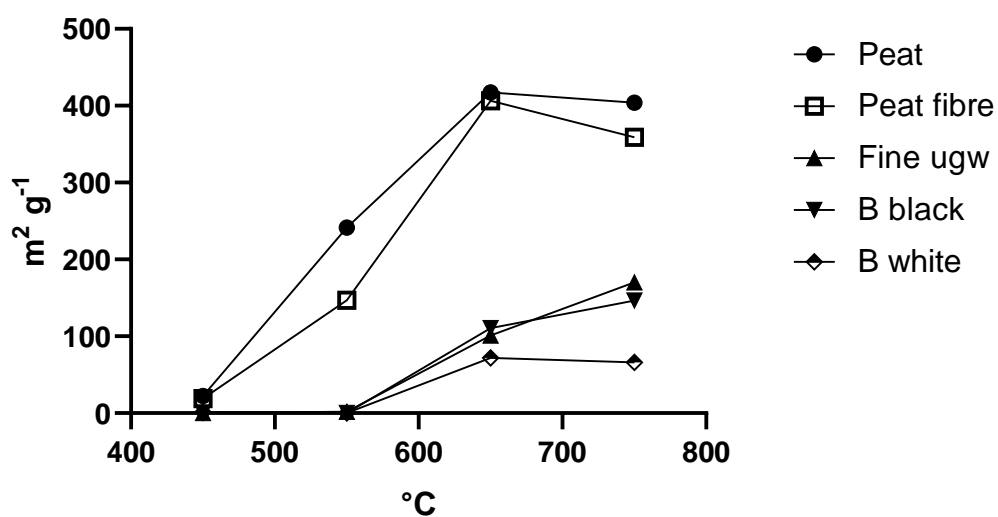


Figure 19: micropore area of biochars produced from pre-dried materials

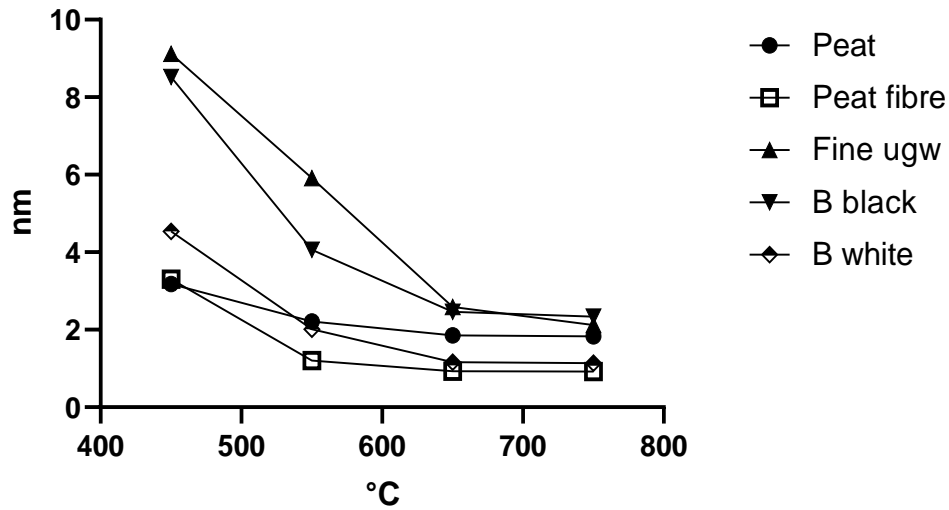


Figure 20: average pore size of biochars produced from pre-dried materials

The results of the BET analysis are presented as follows: the average pore size in nm and the total pore volume in $\text{cm}^3 \text{g}^{-1}$ of the biochars produced from dried materials (Figure 20, Figure 21). The pore size reduces with higher treatment temperature while the total pore volume slightly increases. The total pore volume ranges from 0.00 – 0.21 $\text{cm}^3 \text{g}^{-1}$ (Figure 21) and the average pore size from 0.92 – 9.12 nm (Figure 20).

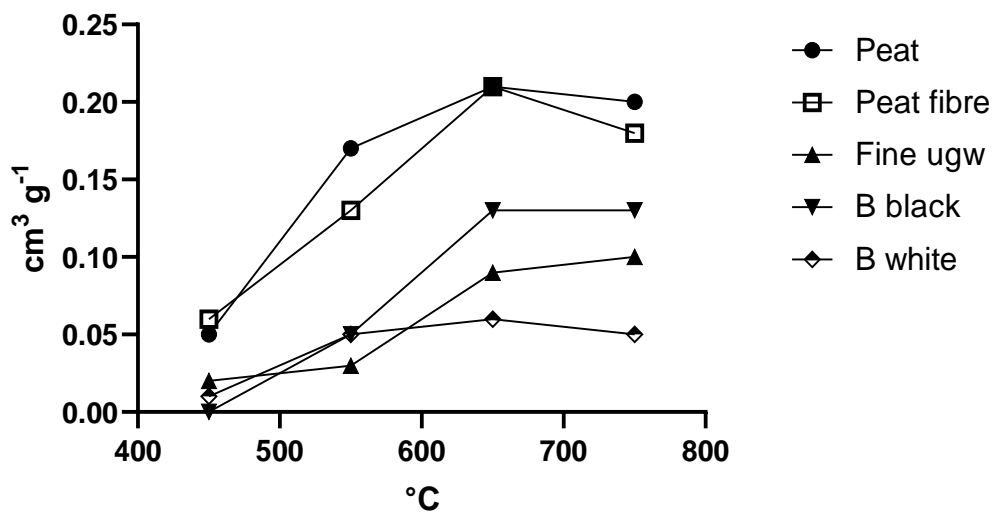


Figure 21: total pore volume of biochars produced from pre-dried materials

4.5. SEM results

SEM images taken from feedstocks and biochars show the impact pyrolysis has on the materials. It is shown that the material became more porous and the outline of the surface also changed (Figure 22, Figure 23). Biochars produced from peat at 600 °C for 2h exhibited a porous structure. Further comparison of feedstocks with the respective biochars showed that biochars produced at 450 – 750 °C produced porous profiles for most of the materials used (Figure 24 - Figure 27). Only biochars produced from fine ugw were comparatively less porous. The porosity of peat (Figure 23) can be visibly compared to brewery grain (Figure 25) and is a reasonable explanation for the high surface area (Figure 18).

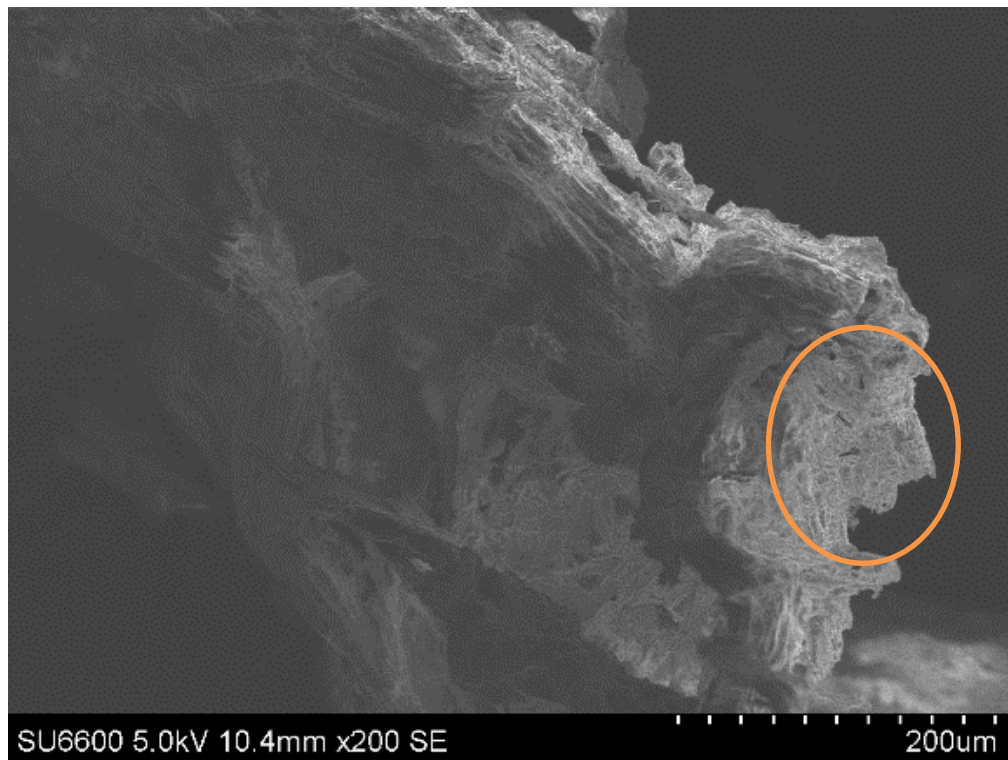


Figure 22: SEM picture of dried peat without treatment showing a smooth surface

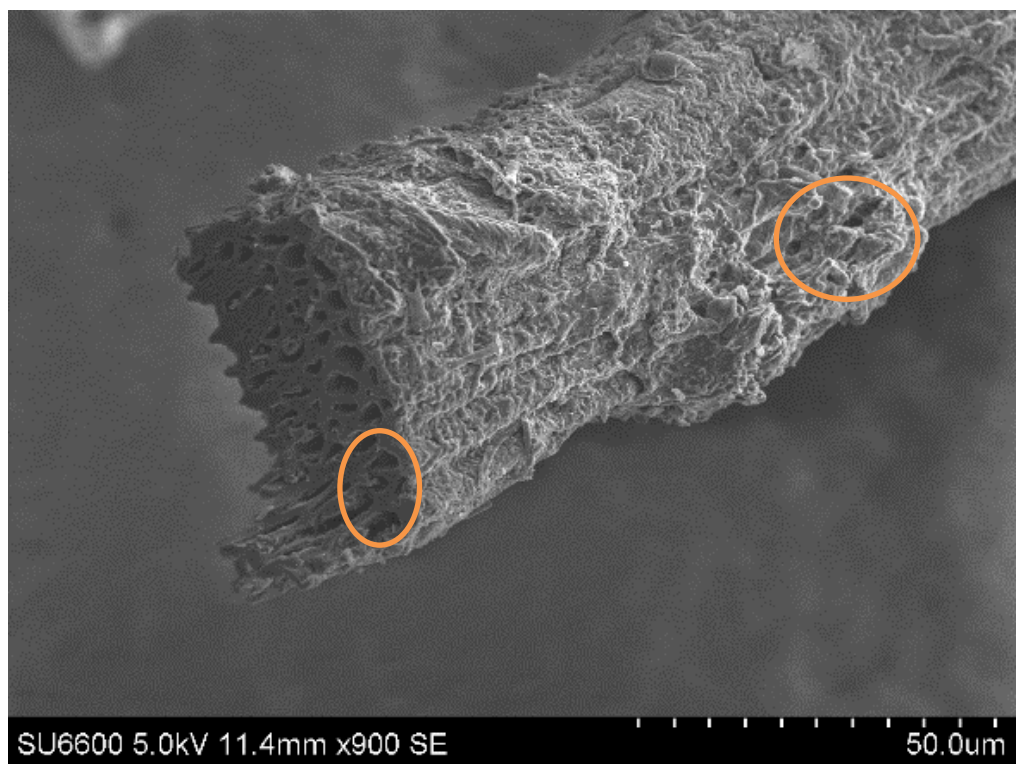


Figure 23: SEM picture of biochar produced from peat at 750 °C with the porous surface

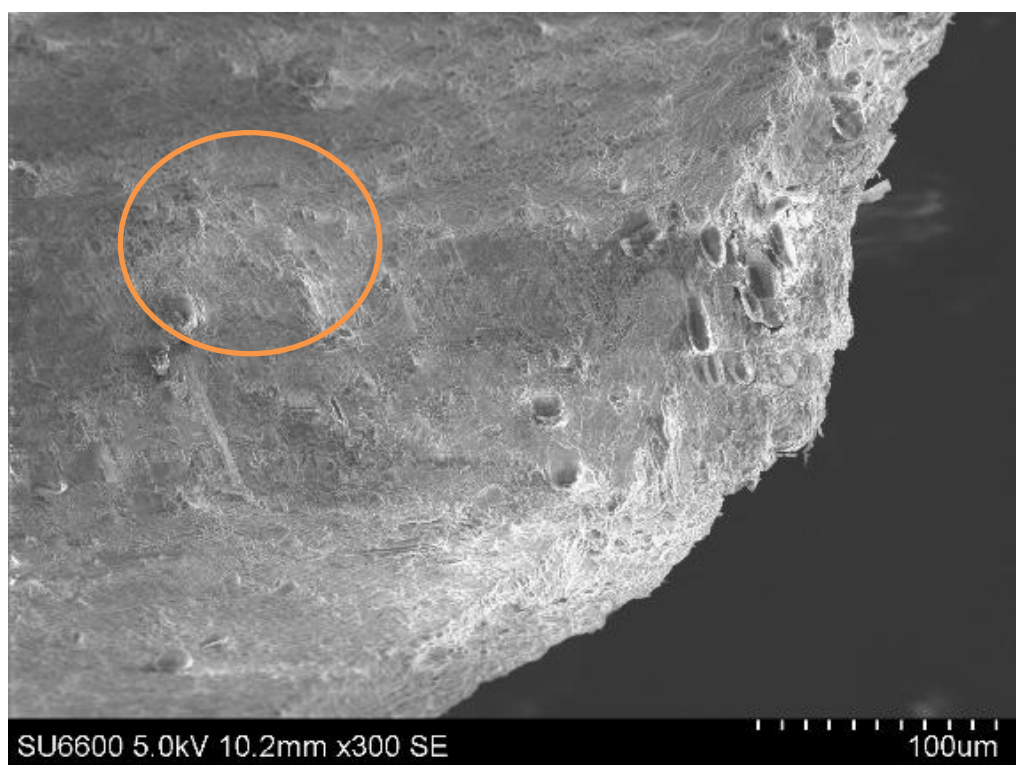


Figure 24: SEM image of dried brewery grain white showing a smooth surface before pyrolysis

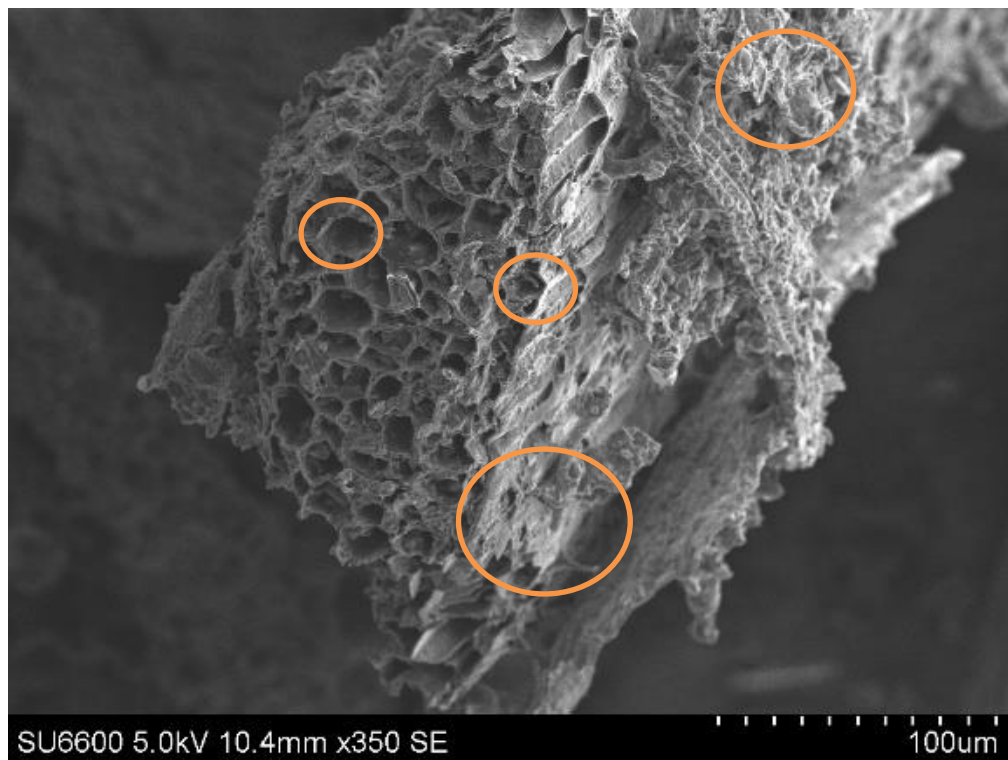


Figure 25: SEM image of biochar produced from brewery grain white at 550°C with the porous and irregular surface

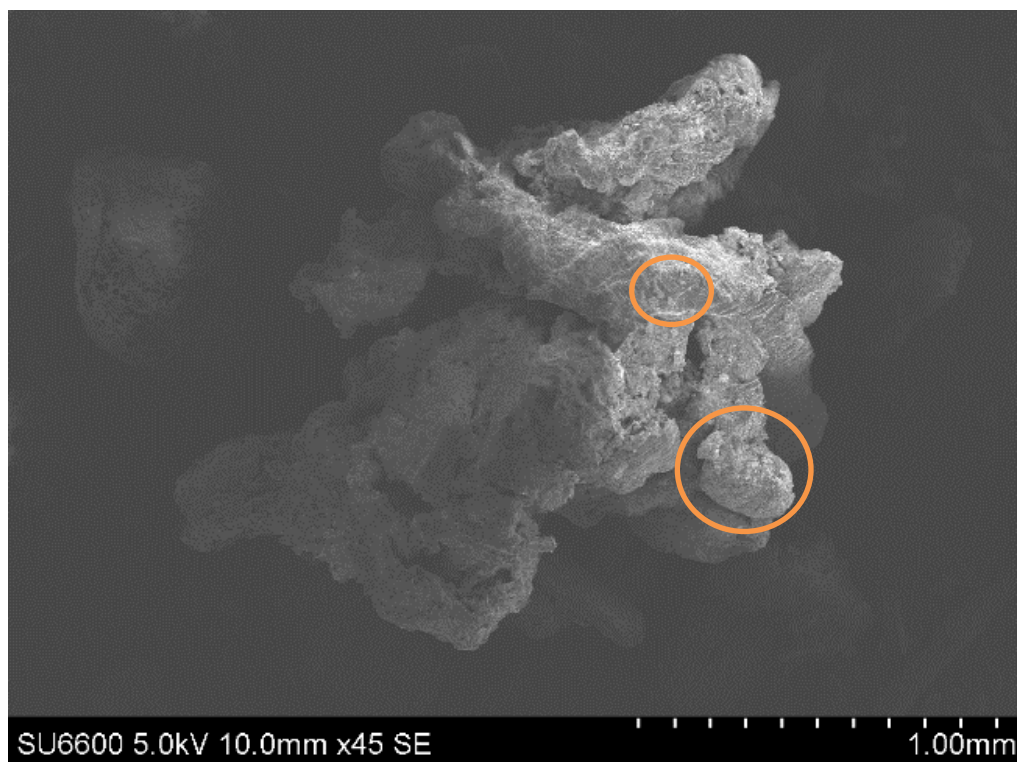


Figure 26: SEM image of dried fine urban green waste showing a smooth surface

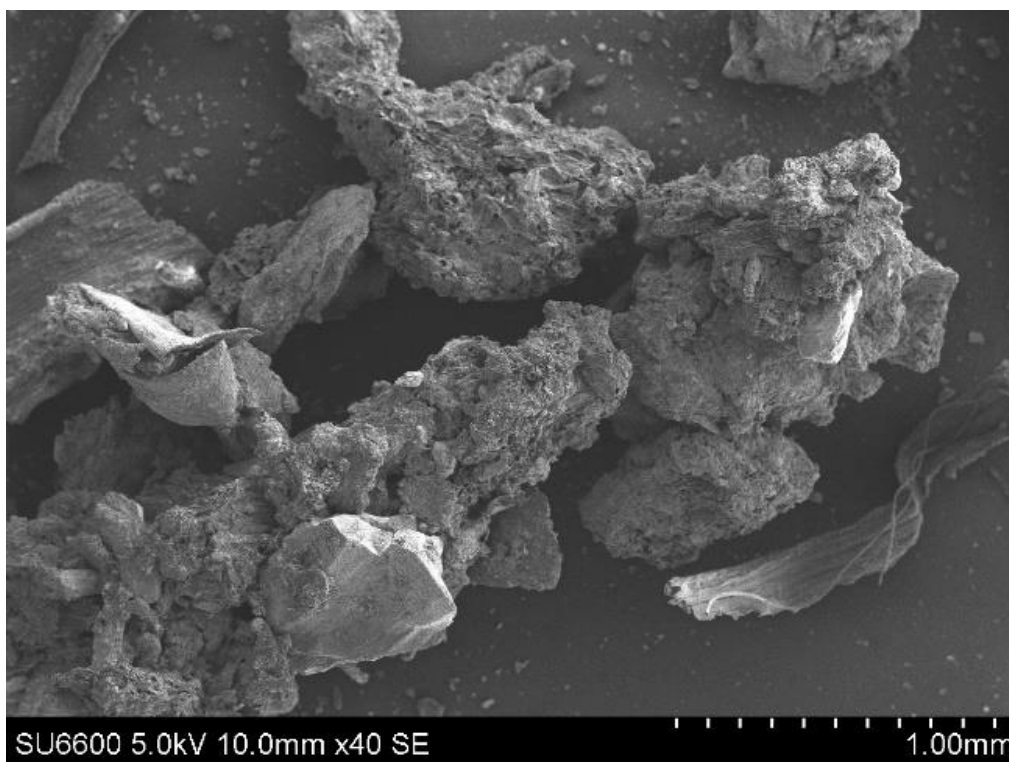


Figure 27: SEM image of biochar produced from fine urban green waste at 650°C

4.6. ATR / FT-IR results

An overview shows the results obtained through ATR analysis of biochars produced from brewery grain black and peat at four different temperatures (Figure 28, Figure 29,). Biochars produced from the other three materials at 750 °C did not contain functional groups at the surface. In general, with an increase in pyrolysis temperature, the number of functional groups on the surface decreases, and some peaks are detected with a lower intensity. Biochars produced at 450 °C showed peaks between 2200 and 770 cm^{-1} depending on the material used. At the same time, biochars produced at 550 °C and 650 °C showed peaks between 2200 – 740 cm^{-1} , and between 3200 – 1010 cm^{-1} depending on the material used, showing how the pyrolysis temperature influences the functional groups on the surface of the biochars. The functional groups at the surface of the biochars are carbonate, hydroxide (O-H) bendings, carbonyl (C=O), alcohol (C-O), C=C, C-C stretchings and aromatic hydrocarbons (C-H). In other settings peaks of between 3400 to

3410 cm^{-1} signify H-bonded O–H stretching vibrations of hydroxyl groups from alcohols, phenols, and organic acids. Peaks at 2850 to 2950 cm^{-1} show C–H stretching of alkyl structures at 1620–1650 cm^{-1} aromatic and olefinic C=C vibrations, C=O in amide (I), ketone, and quinone groups and at 1580 to 1590 cm^{-1} COO[–] asymmetric stretchings. Peaks at 1460 cm^{-1} show C–H deformation of the CH₃ group, while peaks at 1280–1270 cm^{-1} present O–H stretchings of phenolic compounds and three bands around 460, 800, and 1000–1100 cm^{-1} stand for bending of Si–O stretchings (Jindo *et al.*, 2014).

The figures below (Figure 28 and Figure 29) show how the peaks and therefore functional groups get removed from biochars with rising production temperatures. Figure 28 shows the removal of peaks A at around 2168 cm^{-1} correlating with C – H stretching, B at around 1570 cm^{-1} correlating with COO[–] asymmetric stretching, C at around 1370 cm^{-1} correlating with CH deformation modes in alkenes and D at around 1113 cm^{-1} correlating with bending of Si–O stretching. Figure 29 shows the removal of peaks E at around 1590 cm^{-1} correlating with COO[–] asymmetric stretching and F at around 1156 cm^{-1} correlating with bending of Si–O stretching.

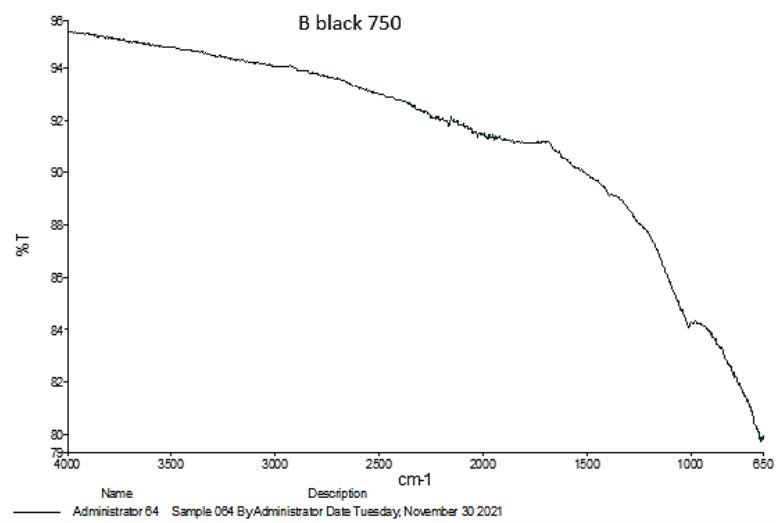
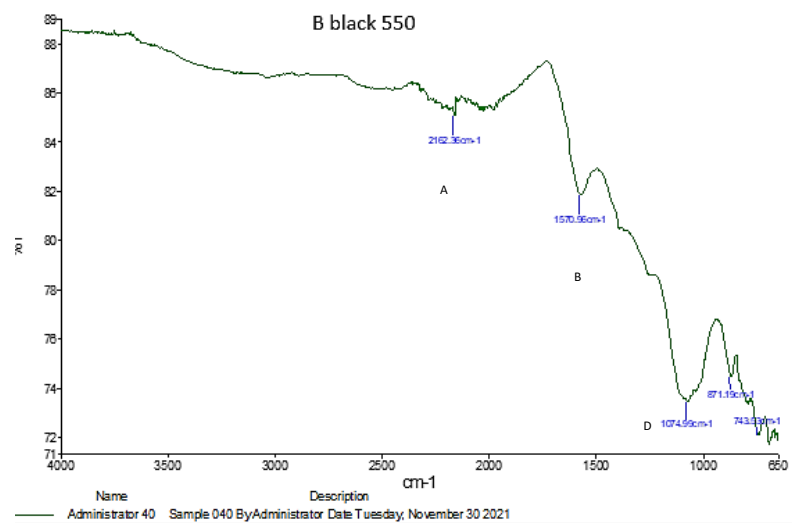
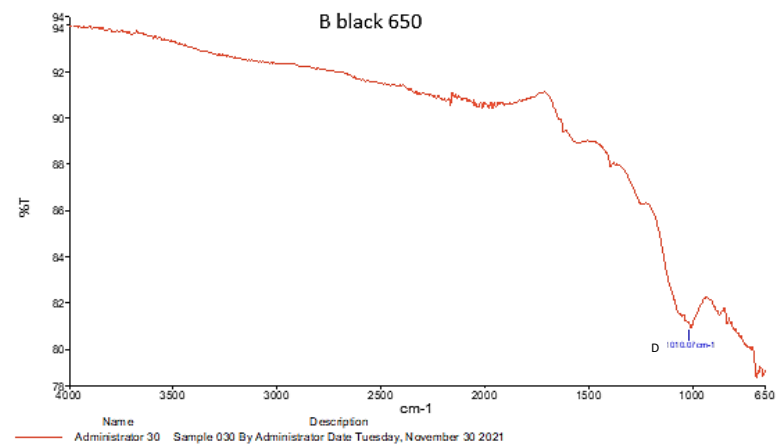
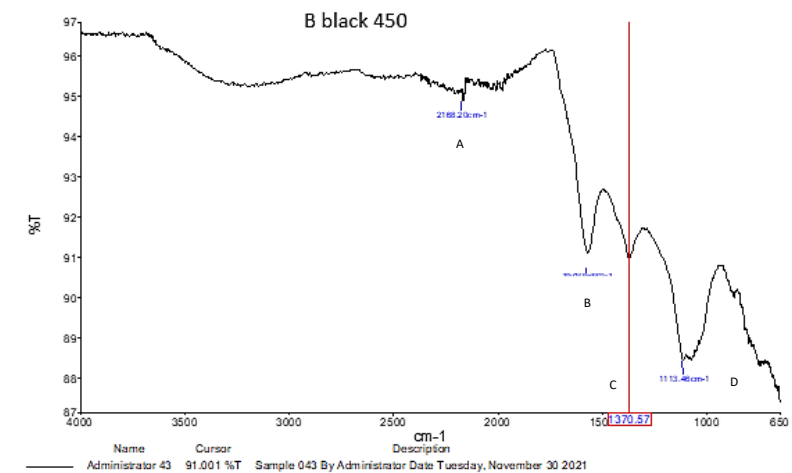


Figure 28: ATR results of biochars produced from b black at various temperatures

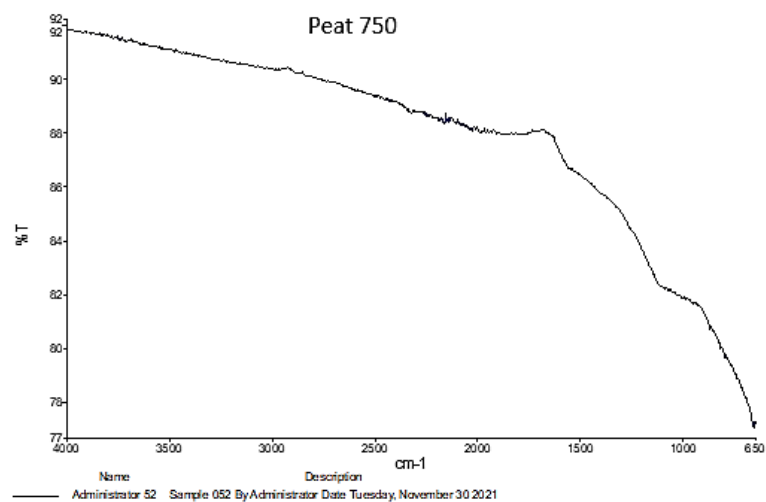
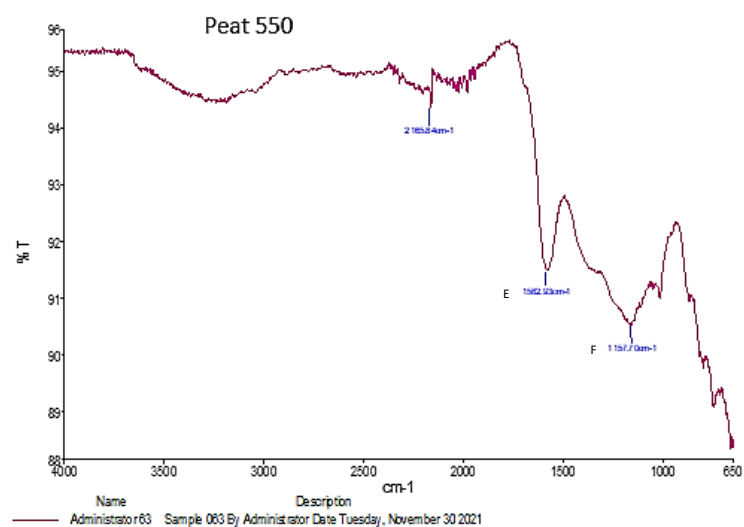
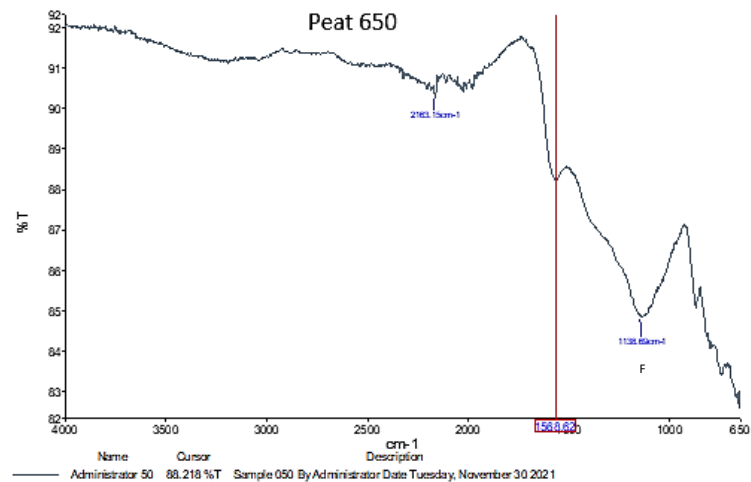
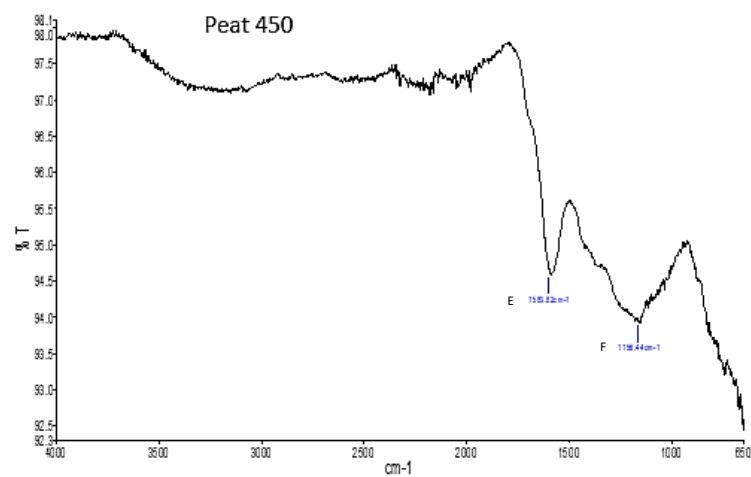


Figure 29: ATR results of biochars produced from peat at various temperatures

4.7. PAH results

The chromatograph obtained for the standard containing the 16 PAHs for which the biochars were tested as well is presented below (Figure 30). All 16 PAHs are visible, showing that the machine (Agilent 6890N gas chromatograph and Agilent 5975 mass spectrometer) can detect them (Figure 30). Exemplary results out of all biochars from this study do not contain any of the 16 PAHs (Figure 31). The peaks seen in the chromatograph can be attributed to products of the toluene extraction. The ten samples run in this study do not contain traceable amounts of PAHs.

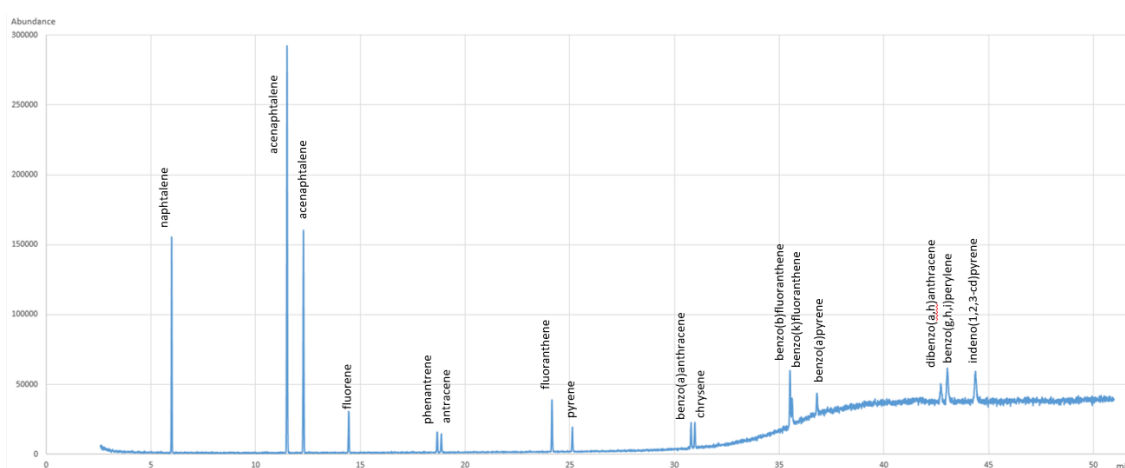


Figure 30: chromatograph of 16 PAHs reference with total ion count mass spectrometer detector

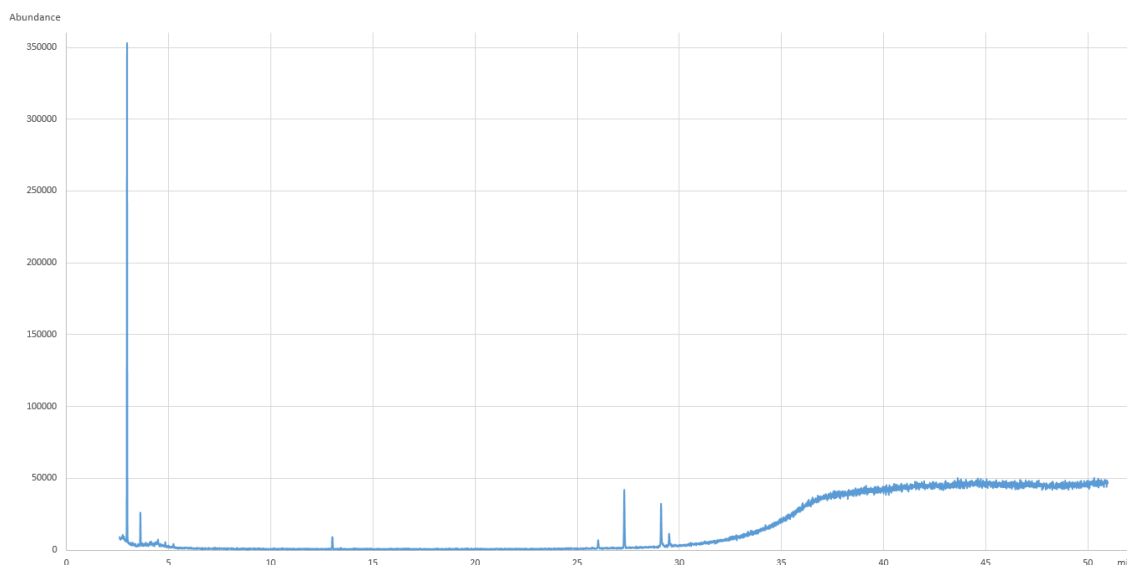


Figure 31: PAH results of GC chromatograph of peat 750 biochar sample

4.8. RAMAN spectroscopy results

The figure below (Figure 32) shows the maxima of the D- and G- bands obtained from the biochars prepared in this study. All twenty biochars exhibit clear D- and G- bands in the ranges reported in the literature (Figure 32). The FWHM (full-width half maximum) of the bands could not be determined as the peaks did not show a clear enough separation between them (Figure 32).

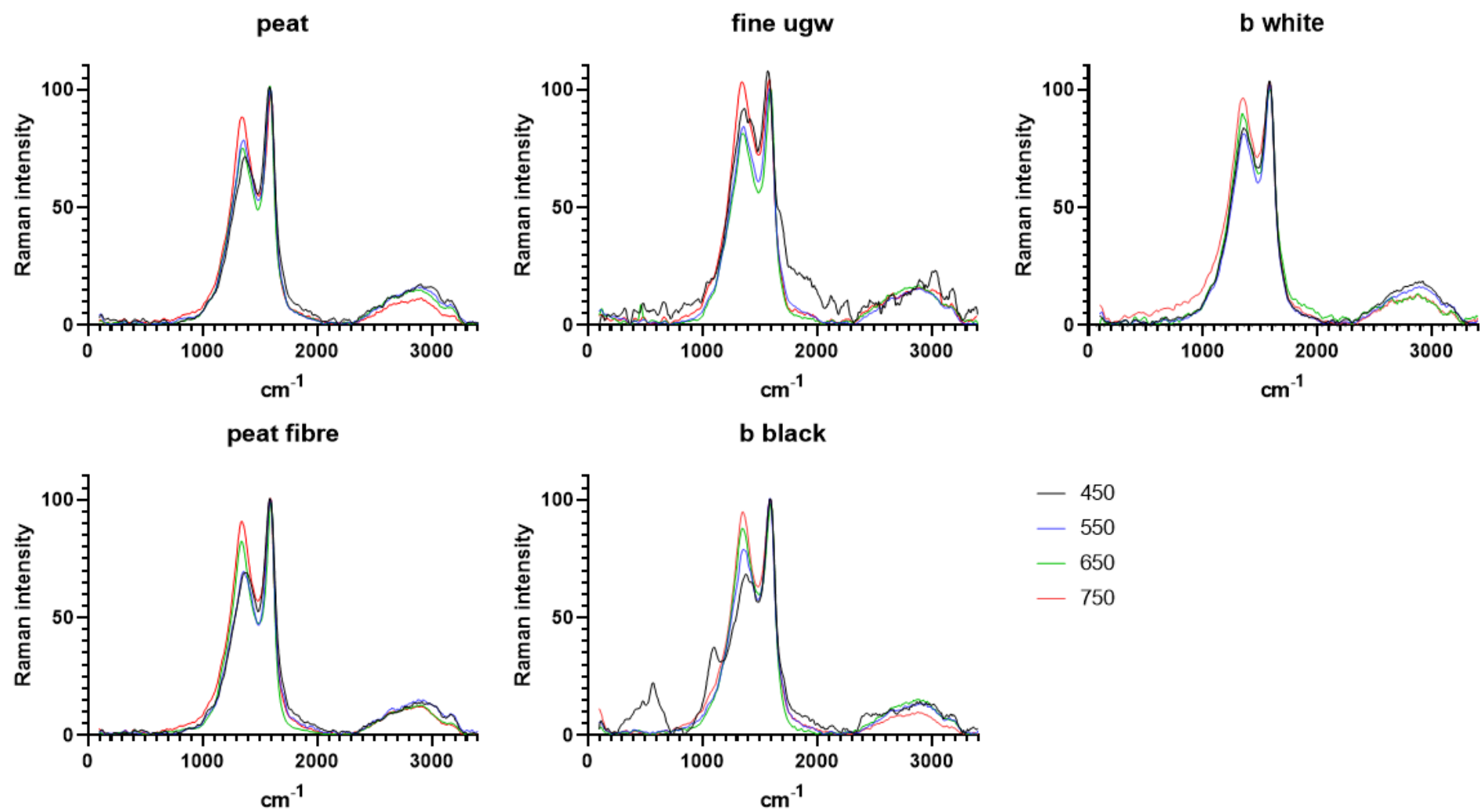


Figure 32: RAMAN results overview of all 20 biochars

To show the results obtained and presented above in more detail, the appendix includes figures which present the RAMAN data obtained for biochars produced from b black at four temperatures (see appendix). The higher the treatment temperatures the lower the intensity of the peak at wavenumbers in the ranges of $800 - 1100 \text{ cm}^{-1}$ and $1700 - 1900 \text{ cm}^{-1}$. The position of the D and G bands changes for all twenty samples (Figure 33). The D band slightly decreases with rising treatment temperature for all five materials. The G band on the other hand does not present those clear trends, leading to an increase in the ratio of the intensity of the D to G peak with increasing pyrolysis temperatures, indicating changes in the chemical structure of the pyrolysed feedstock (Figure 34 – Figure 37).

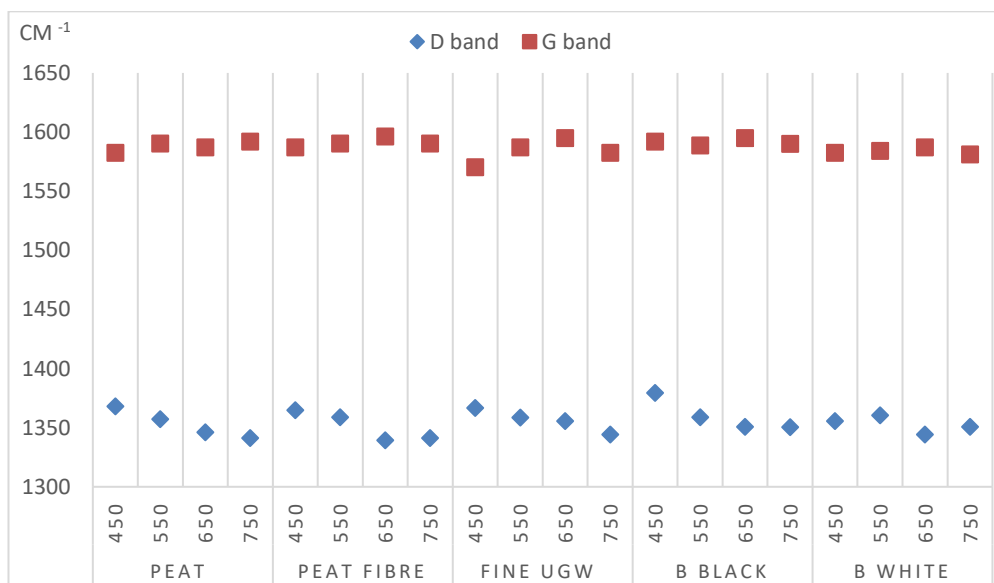


Figure 33: D and G band changes throughout the samples

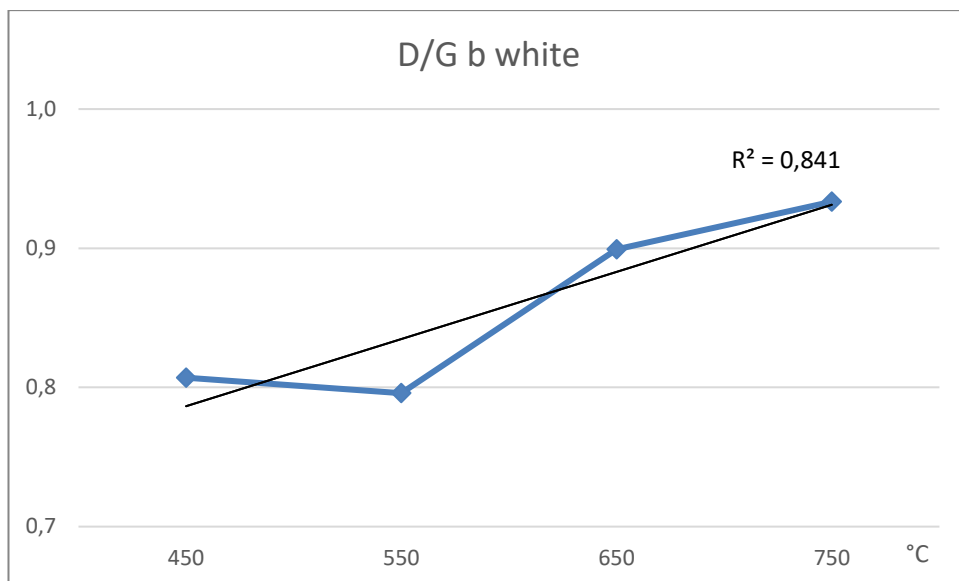


Figure 34: D/G intensity ratio in relation to production temperature for b white biochars

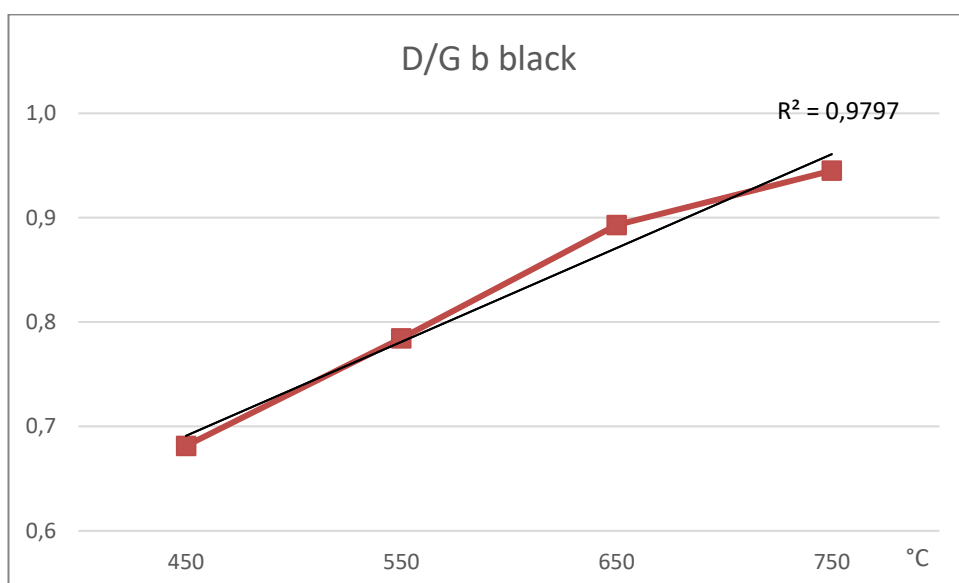


Figure 35: D/G intensity ratio in relation to production temperature for b black biochars

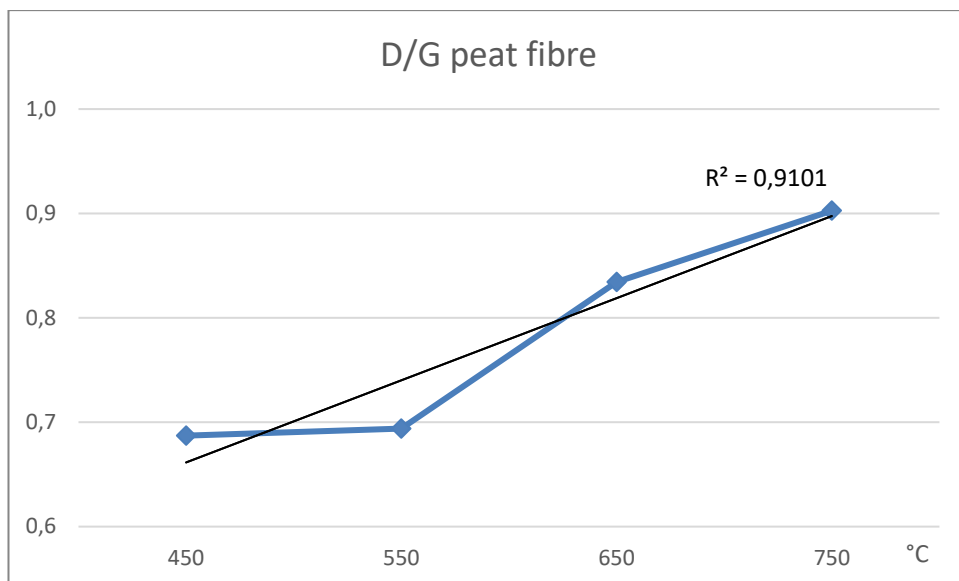


Figure 36: D/G intensity ratio in relation to production temperature for peat fibre biochars

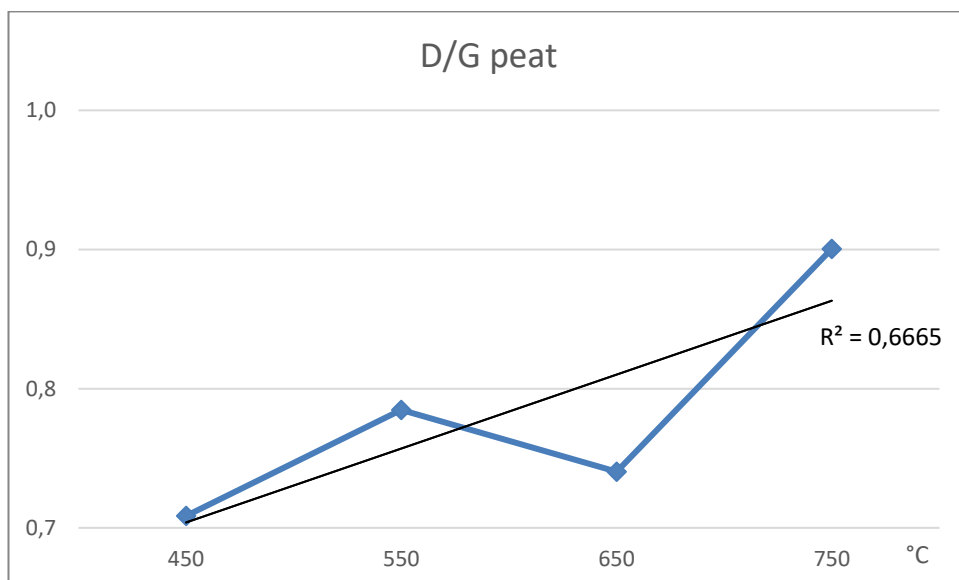


Figure 37: D/G intensity ratio in relation to production temperature for peat biochars

The results above show that it is worth considering Raman spectroscopy as a screening method for the surface chemistry of biochars as Raman can show the changes in the chemo-physical nature of biochars. Certainly, the correlation between the D/G intensity ratio and HTT is worth further investigation.

4.9. CHNS results

Figure 38 - Figure 41 and Table 29 present a summary of how the materials react to higher treatment temperatures concerning their elemental composition. The figures give a clearer picture of how temperature influences the elemental contents in the biochars. While the carbon and hydrogen contents show clear trends indicating a change in the chemical nature of the biomass used, the nitrogen and oxygen contents do not present clear trends throughout treatment temperatures. A possible reason for the findings is that sampling can lead to a more heterogeneous sample and therefore less probability to produce clear trends throughout the elements, which is supported by standard deviations of up to around 20.32 %. The carbon (C) content (Figure 38) presents the same trend as the fixed carbon content of the biochars. It is increasing with higher temperatures for every material except for the biochars produced from fine ugw, which can be explained by the high relatively high VM and ash content presented in section 4.3. Those biochars have a lower carbon content and higher oxygen (O) content (Figure 41) with rising treatment temperatures (Table 29). For the other materials, it can be said that the carbon content is increasing, while the hydrogen (H) (Figure 39), nitrogen (N) (Figure 40), sulphur (S) and oxygen content are decreasing with higher treatment temperatures.

Table 29: CHNS results from all twenty biochars

Biochar material	Production temperature (°C)	C (wt%)	H (wt%)	N (wt%)	S (wt%)	O (wt%)	Ash (% db)
Peat	450	62.89±8.24	3.22±0.15	1.19±0.54	0.05±0.07	24.27±3.00	3.90±0.06
	550	68.18±10.99	2.81±0.17	1.32±0.73	0.05±0.07	16.47±1.99	4.56±0.22
	650	70.09±12.48	2.08±0.16	2.46±1.84	0.04±0.05	14.00±3.42	5.07±0.03
	750	78.75±0.82	1.40±0.08	1.03±0.60	0.03±0.05	11.54±2.75	6.74±2.40
Peat fibre	450	65.63±7.85	3.17±0.11	1.08±0.67	0.03±0.04	21.39±1.36	3.27±0.17
	550	75.28±7.04	2.59±0.07	1.48±0.72	0.05±0.07	20.40±1.54	3.88±1.46
	650	71.26±14.36	1.96±0.15	1.25±0.88	0.10±0.07	10.69±4.02	4.33±0.38
	750	73.63±6.11	1.22±0.09	1.04±0.78	0.04±0.05	13.57±2.06	5.27±0.11
Fine ugw	450	47.75±5.20	2.20±0.22	2.72±0.29	0.05±0.07	1.25±0.36	43.64±0.77
	550	43.61±6.71	1.60±0.03	2.54±0.49	0.05±0.07	6.33±0.93	50.14±0.62
	650	38.65±5.79	1.15±0.11	1.84±0.21	0.06±0.08	11.85±3.5	51.53±1.49
	750	33.66±3.39	0.71±0.09	1.36±0.82	0.07±0.07	6.06±2.54	61.74±1.71
B black	450	52.32±4.62	2.93±0.19	1.59±0.43	0.00±0.00	30.60±3.01	10.23±0.88
	550	54.56±20.23	2.29±0.16	1.21±0.41	0.00±0.00	18.24±1.90	9.53±0.66
	650	54.22±11.29	1.54±0.21	0.83±0.48	0.00±0.00	23.65±0.44	11.91±0.41
	750	54.90±3.70	1.01±0.10	0.66±0.47	0.01±0.02	28.23±2.89	12.79±1.24
B white	450	58.24±8.63	2.93±0.10	3.16±0.85	0.18±0.26	18.10±1.96	17.80±9.82
	550	56.50±8.09	2.28±0.20	2.94±0.74	0.09±0.12	18.27±4.42	14.68±0.64
	650	56.43±3.21	1.78±0.08	2.20±0.36	0.09±0.09	26.02±3.18	15.04±1.23
	750	60.96±5.47	1.09±0.05	2.07±0.59	0.00±0.00	17.47±6.14	17.62±0.33

Figure 38 - Figure 41 also present insights into how significantly different the elemental content of each biochar is from another one produced from the same material at a different temperature. The results were obtained using ANOVA. The symbols in the figures are used as follows: The nitrogen contents (Figure 40) of all the samples do not present any significant differences which can be because of the small overall values, whereas the hydrogen contents (Figure 39) present significance for nearly every sample. The carbon

contents presented significant differences for biochars produced from fine ugw and b black (Figure 38). A significance was found for the relation of biochars produced at 450 °C to higher temperatures and the significance varied between $p<0.05$ and $p<0.001$. Comparing the carbon and fixed carbon content, it can be seen that the values for peat, peat fibre and partially for fine ugw align with the trends of the fixed carbon content (Table 27). The oxygen content presented significant differences ($p<0.05$) between peat 450 and 750 as well as b black 450 and 550 (Figure 41). Though it has to be kept in mind that the actual values might differ slightly as the oxygen content is calculated by difference so it might contain some error and should not be taken as absolute. Even though the results of the analysed biochars present standard deviations of up to 20.32 %, significant differences between some of the samples could be found.

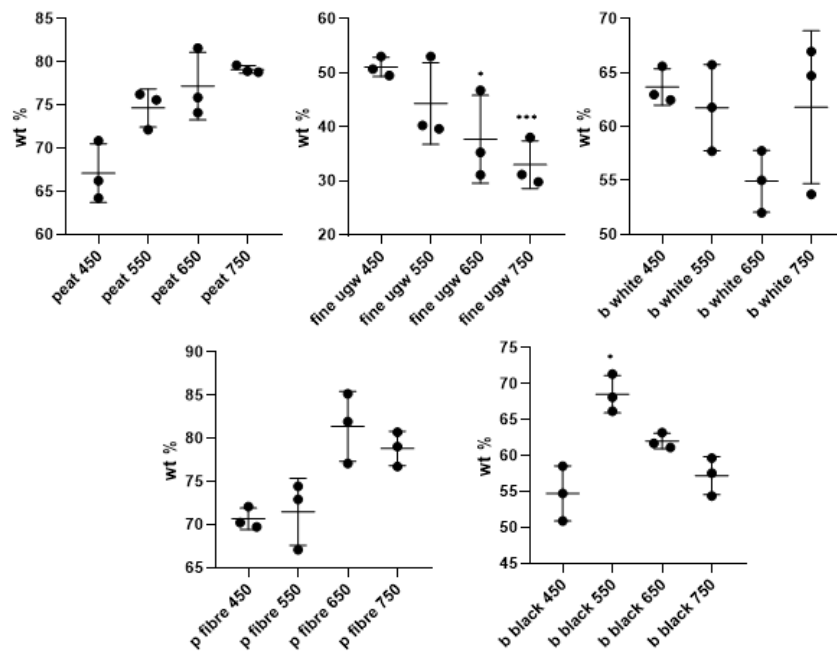


Figure 38: Carbon content of biochars produced at four different temperatures from five different materials (**** $p<0.0001$, *** $p<0.001$, ** $p<0.01$, * $p<0.05$ for samples which are significantly different from the biochar produced at 450 °C; +++++ $p<0.0001$, +++ $p<0.001$, ++ $p<0.01$, + $p<0.05$ for samples which are significantly different from the biochar produced at 550 °C; and ---- $p<0.0001$, --- $p<0.001$, -- $p<0.01$, - $p<0.05$ for samples which are significantly different from the biochar produced at 650 °C)

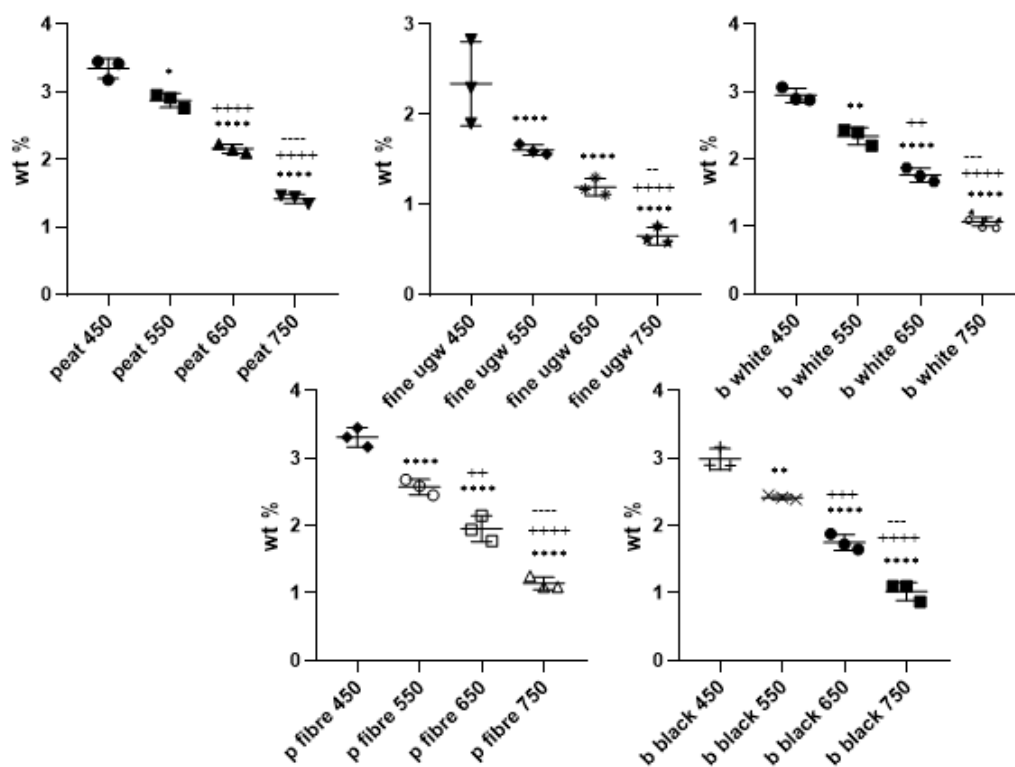


Figure 39: hydrogen content of biochars produced at four different temperatures from five different materials (**** $p < 0.0001$, *** $p < 0.001$, ** $p < 0.01$, * $p < 0.05$ for samples which are significantly different from the biochar produced at 450 °C; +++++ $p < 0.0001$, +++ $p < 0.001$, ++ $p < 0.01$, + $p < 0.05$ for samples which are significantly different from the biochar produced at 550 °C; and ---- $p < 0.0001$, --- $p < 0.001$, -- $p < 0.01$, - $p < 0.05$ for samples which are significantly different from the biochar produced at 650 °C)

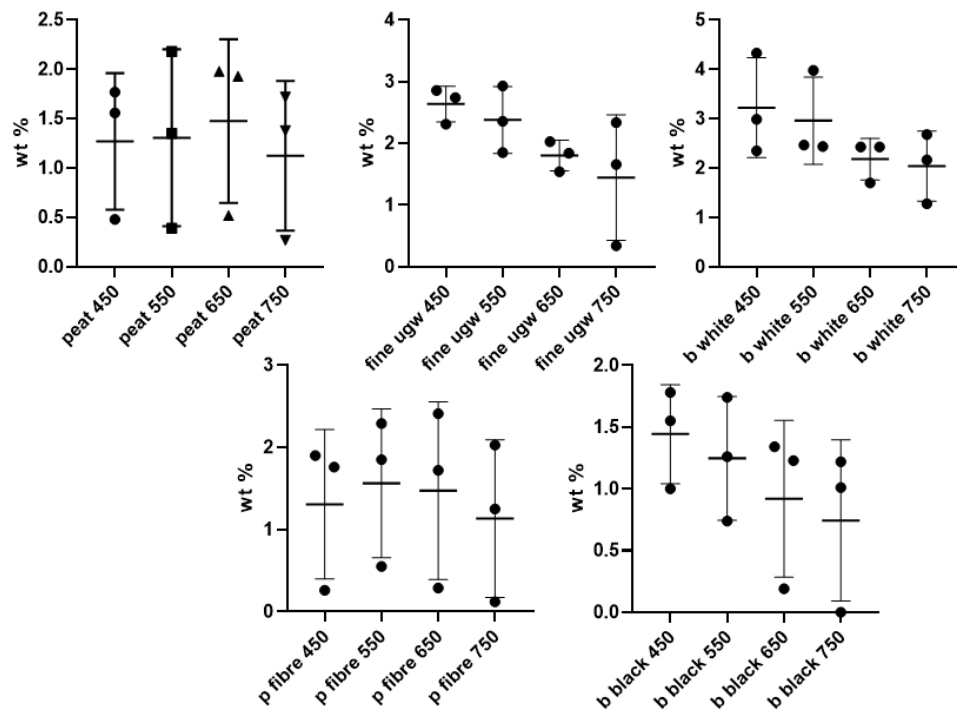


Figure 40: nitrogen content of biochars produced at four different temperatures from five different materials (**** $p < 0.0001$, *** $p < 0.001$, ** $p < 0.01$, * $p < 0.05$ for samples which are significantly different from the biochar produced at 450 °C; +++++ $p < 0.0001$, +++ $p < 0.001$, ++ $p < 0.01$, + $p < 0.05$ for samples which are significantly different from the biochar produced at 550 °C; and ---- $p < 0.0001$, --- $p < 0.001$, -- $p < 0.01$, - $p < 0.05$ for samples which are significantly different from the biochar produced at 650 °C)

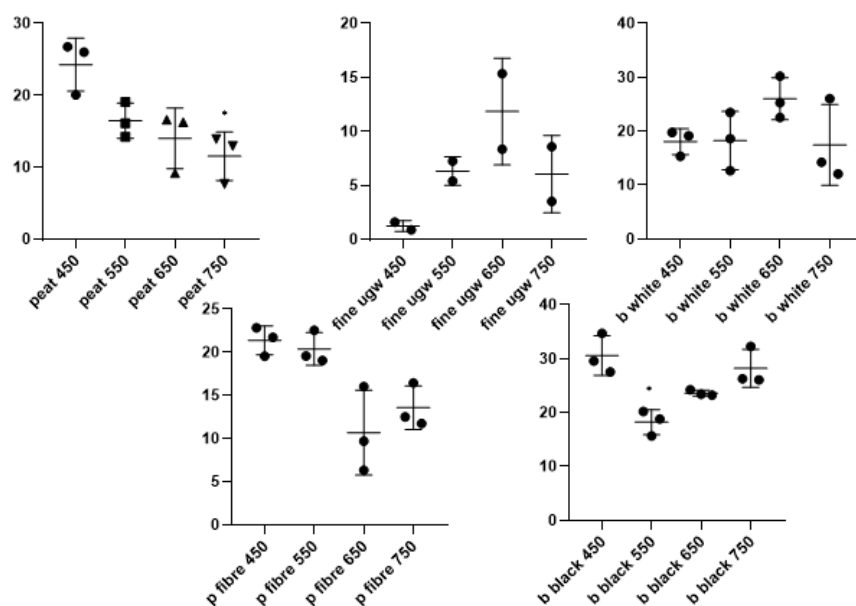


Figure 41: oxygen content of biochars produced at four different temperatures from five different materials (**** $p < 0.0001$, *** $p < 0.001$, ** $p < 0.01$, * $p < 0.05$ for samples which are significantly different from the biochar produced at 450 °C; +++++ $p < 0.0001$, +++ $p < 0.001$, ++ $p < 0.01$, + $p < 0.05$ for samples which are significantly different from the biochar produced at 550 °C; and ---- $p < 0.0001$, --- $p < 0.001$, -- $p < 0.01$, - $p < 0.05$ for samples which are significantly different from the biochar produced at 650 °C)

The biochars produced in this study exhibit H/C ratios up to 0.67 and O/C ratios of 0.18 – 1.45 (Table 30). The Van Krevelen diagrams are presented to determine the degree of aromaticity and maturation in the biochar structure (Figure 42 - Figure 43). One of the diagrams shows the trends throughout all materials tested in this study (Figure 43), whereas the other figure presents the general trend of all 20 biochars (Figure 42). Three out of five materials show a clear trend, whereas biochars produced from b white and fine ugw do not present a clear trend (Figure 43). A decrease in H/C ratios can be observed with rising treatment temperatures for all five materials (Table 30). Most of the biochars produced showed a slight decrease in O/C ratios with higher production temperatures.

Only biochars produced from fine ugw did not follow that trend. Their O/C ratios increase with higher treatment temperatures.

Table 30: H/C and O/C ratios of biochars produced between 450-750°C from five different materials

Biochar material	Production temperature (°C)	H/C	O/C
Peat	450	0.60±0.03	0.27±0.04
	550	0.46±0.00	0.17±0.02
	650	0.34±0.01	0.14±0.04
	750	0.22±0.03	0.11±0.03
Peat fibre	450	0.56±0.02	0.23±0.02
	550	0.43±0.02	0.22±0.03
	650	0.29±0.03	0.10±0.04
	750	0.17±0.02	0.13±0.02
Fine ugw	450	0.55±0.09	0.00±0.02
	550	0.44±0.06	0.04±0.11
	650	0.39±0.05	0.18±0.16
	750	0.24±0.00	0.09±0.06
B black	450	0.66±0.02	0.42±0.07
	550	0.42±0.02	0.20±0.03
	650	0.34±0.02	0.29±0.01
	750	0.21±0.02	0.37±0.05
B white	450	0.56±0.02	0.21±0.02
	550	0.46±0.03	0.23±0.07
	650	0.39±0.00	0.36±0.06
	750	0.21±0.03	0.22±0.10

* One of the results, which was produced in triplicates, showed very different amounts from the other two. Therefore, the results presented here are just duplicates, not triplicates.

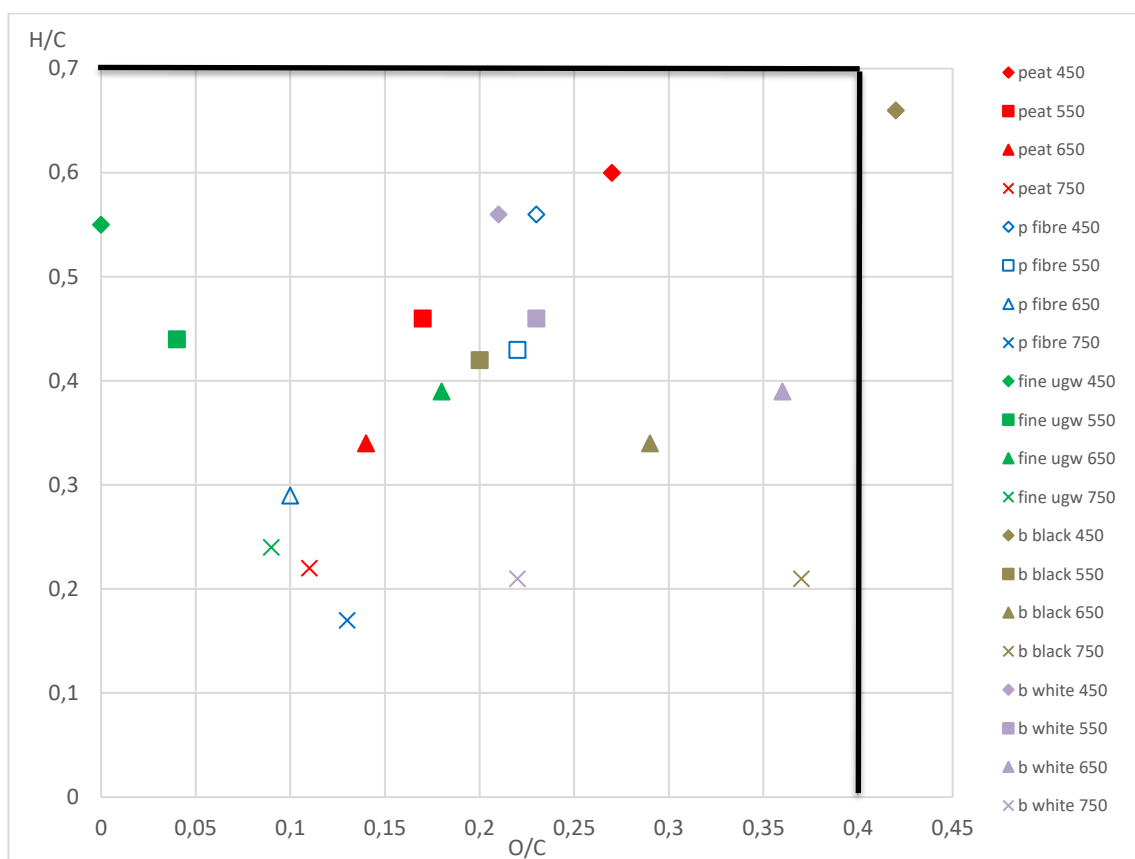


Figure 42: Van Krevelen diagram of all twenty biochars produced from five materials at four temperatures with EBC and IBI limits for H/C and O/C molar ratios (International Biochar Initiative, 2015; EBC (2012-2022), 2022)

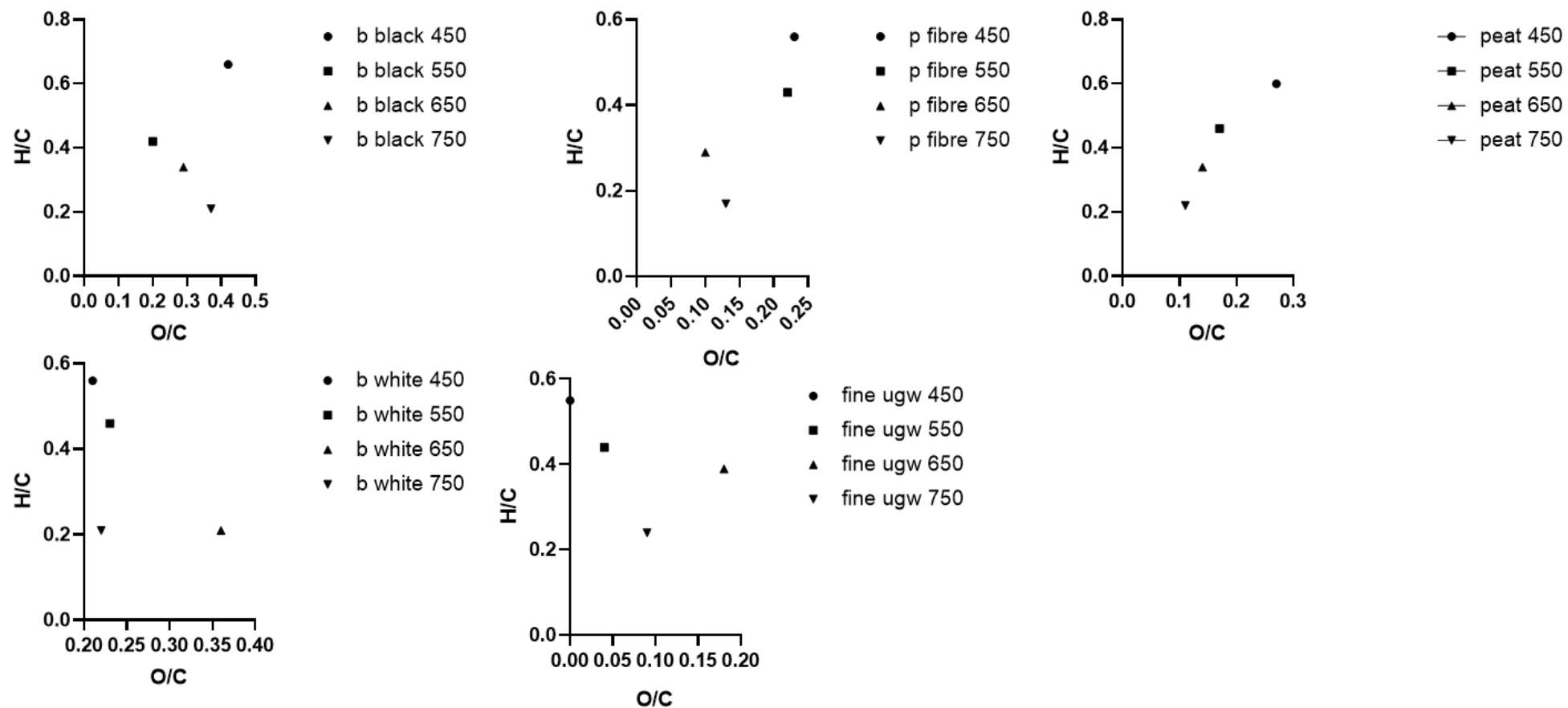


Figure 43: Van Krevelen Diagram trends throughout the materials for biochars produced at four temperatures

4.10. ICP-MS results

The results by ICP-MS are presented in the following tables (Table 31, Table 32) and figures (Figure 44-Figure 48). The results vary between the materials used for biochar production as well as between the production temperatures. The contents of the tested elements vary between <0.00 and 21952.79 mg kg⁻¹ (21.95 g kg⁻¹). While elements like Co, As and Cd are barely or not at all traceable, other elements like P, Mg and K are there at quite elevated levels.

Table 31: ICP-MS results of all biochars analysed in a 1:1000 dilution, part 1

sample	B mg/kg	Co mg/kg	Ni mg/kg	Cu mg/kg	As mg/kg	Cd mg/kg	Pb mg/kg
peat 450	89.16	0.41	15.52	17.58	0.05	0.32	3.07
peat 550	5.19	0.52	<0.00	<0.00	0.40	0.56	1.43
peat 650	<0.00	0.05	<0.00	<0.00	<0.00	0.10	0.29
peat 750	22.77	0.583	6.55	8.55	<0.00	0.19	3.92
p fibre 450	87.38	0.521	<0.00	22.04	<0.00	0.56	3.57
p fibre 550	<0.00	0.44	<0.00	<0.00	0.14	0.22	1.67
p fibre 650	2.00	0.51	<0.00	0.863	<0.00	0.34	3.70
p fibre 750	14.63	0.99	68.61	79.88	1.16	0.90	3.80
fine ugw 450	63.92	5.07	9.82	69.28	3.34	0.37	44.20
fine ugw 550	14.05	3.21	<0.00	16.99	3.82	0.58	46.12
fine ugw 650	39.36	3.44	0.52	18.47	4.13	0.53	58.10
fine ugw 750	31.29	4.09	38.73	73.27	5.64	2.48	45.47
b black 450	29.35	0.25	<0.00	25.55	0.09	0.86	2.88
b black 550	<0.00	<0.00	<0.00	<0.00	<0.00	0.28	<0.00
b black 650	<0.00	0.07	<0.00	<0.00	<0.00	0.17	<0.00
b black 750	23.70	0.507	51.42	61.30	0.02	0.52	7.31
b white 450	31.90	0.377	<0.00	8.40	<0.00	0.38	<0.00
b white 550	<0.00	0.137	<0.00	<0.00	0.34	0.19	<0.00
b white 650	<0.00	0.17	<0.00	<0.00	<0.00	0.25	<0.00
b white 750	3.39	0.537	18.69	27.70	0.23	0.97	2.68

Table 32: ICP-MS results of all biochars analysed in a 1:1000 dilution, part 2

sample	P mg/kg	Ca mg/kg	Mn mg/kg	Fe mg/kg	Zn mg/kg	Na mg/kg	Mg mg/kg	K mg/kg
peat 450	353.02	5199.79	15.05	530.90	424.48	259.93	1673.31	394.97
peat 550	271.39	2158.14	15.11	1033.07	<0.00	<0.00	2547.82	<0.00
peat 650	182.26	707.84	8.17	469.92	<0.00	<0.00	1378.63	<0.00
peat 750	245.79	7046.35	11.74	1131.25	14.40	496.10	2181.05	1203.20
p fibre 450	1023.29	2443.69	32.71	780.10	<0.00	<0.00	2086.45	390.09
p fibre 550	372.86	1577.21	28.28	1192.75	<0.00	<0.00	1907.59	39.12
p fibre 650	586.68	1602.87	32.66	1246.16	<0.00	<0.00	2110.32	288.18
p fibre 750	504.66	8612.96	38.09	1162.45	810.61	4695.62	2493.03	9174.11
fine ugw 450	6573.89	15271.89	505.18	8623.07	40.83	404.78	5799.49	11795.24
fine ugw 550	5639.78	13077.64	526.82	10257.83	<0.00	<0.00	4408.37	9289.69
fine ugw 650	7232.01	15452.38	459.24	7806.05	<0.00	<0.00	4563.72	9120.06
fine ugw 750	5190.17	17502.21	404.83	6950.06	599.45	1369.88	4545.04	10809.53
b black 450	3977.15	<0.00	41.80	253.55	131.81	31.12	1299.31	16480.54
b black 550	6029.21	<0.00	62.84	22.73	<0.00	<0.00	1830.50	19970.7
b black 650	5207.34	<0.00	43.35	<0.00	<0.00	<0.00	1702.48	21952.79
b black 750	6718.85	1952.90	83.95	448.46	2630.75	510.39	1781.07	20285.25
b white 450	7448.69	1016.30	68.89	238.97	<0.00	<0.00	2442.78	18351.52
b white 550	8816.82	716.26	84.55	372.10	<0.00	<0.00	2912.92	20545.38
b white 650	7174.75	2051.00	57.40	269.33	<0.00	<0.00	1983.83	15474.64
b white 750	6531.89	5093.92	62.57	385.91	1305.09	3038.29	2204.73	15784.72

Germany's Federal Soil Protection Act (Bundes-Bodenschutzverordnung or BBodSchV, 2020) (BMUV, 2020), and Switzerland's Chemical Risk Reduction Act (Schweizerische Chemikalien-Risikoreduktions-Verordnung or ChemRRV, 2005) are used as the reference guidelines when it comes to the maximum values for heavy metals in biochars (EBC, 2012). The respective thresholds refer to the biochar's total dry mass (DM). The European Biochar Initiative distinguishes between basic grade biochars with limits for heavy metals of Pb < 150 mg kg⁻¹ DM; Cd < 1,5 mg kg⁻¹ DM; Cu < 100 mg kg⁻¹ DM; Ni < 50 mg kg⁻¹ DM; Zn < 400 mg kg⁻¹ DM and premium grade with thresholds of Pb < 120 mg kg⁻¹ DM; Cd < 1 mg kg⁻¹ DM; Cu < 100 mg kg⁻¹ DM; Ni < 30 mg kg⁻¹ DM; Zn < 400 mg kg⁻¹ DM (EBC, 2012). The biochars produced in this study were within range of the premium grade biochar for most of the elements stated, only Ni and Zn values were higher than the threshold in some biochars (Table 31, Table 32). Though it can be seen in the figures below, that some materials produce biochars with fewer trace metals than others (Figure 44 – 50). Especially biochars produced from fine ugw contain more trace metals in comparison to the others irrespective of the pyrolysis temperature linking into the composition of the feedstock. This shows that for example heavy metals are present in urban green waste during composting and their percentage after pyrolysis will be higher in comparison to the percentage of organic matter. The trends are normally to be expected, if the metal is not volatile, the trend should be proportional to the temperature because the metals are being concentrated in a smaller mass of char at higher temperatures used in pyrolysis. The exception is when the metals start to become volatile at higher pyrolysis temperatures, then a lower than proportional increase in concentration as the temperature in pyrolysis increases is visible. With these biochars, those clear trends throughout the temperatures are not clearly visible. It could be that a too small amount of the sample is analysed to get a representative picture of the whole material. Likely the difficulty in having representative subsamples for analysis may have caused a certain error in the

obtained results as already mentioned in the bulk elemental analysis (4.9.) Figure 48 supports earlier results (Figure 44), that there are appreciable levels of Cu and Pb in biochars produced from fine ugw. It also can be seen that there are minimal levels of Cu, As, Cd, Ni and Pb in either the peat or the grain biochars (Figure 48).

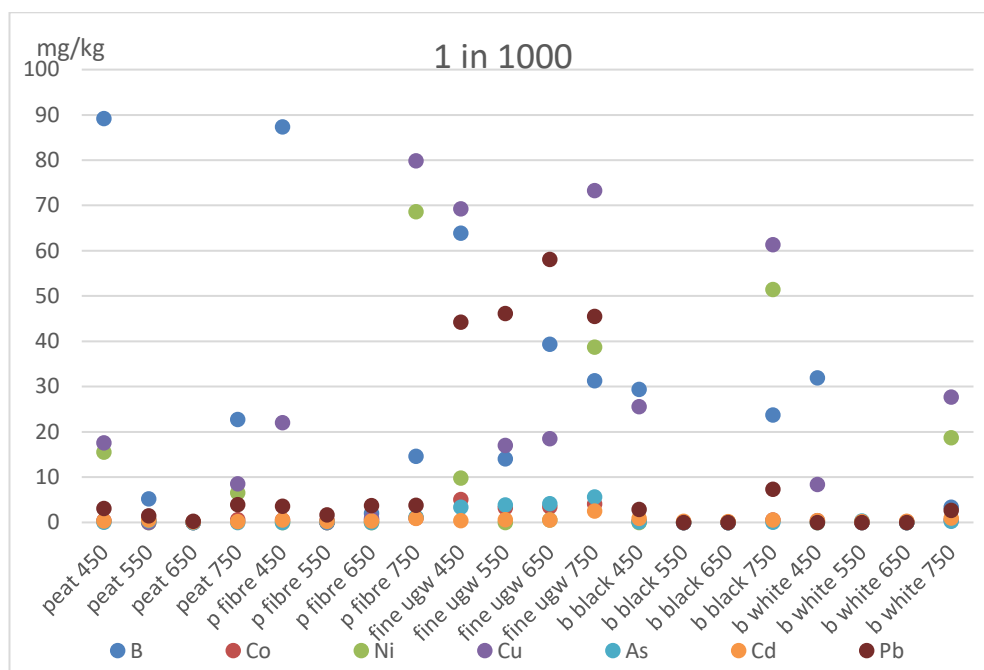


Figure 44: ICP-MS results for 1:1000 dilution of low concentrations elements in mg kg^{-1}

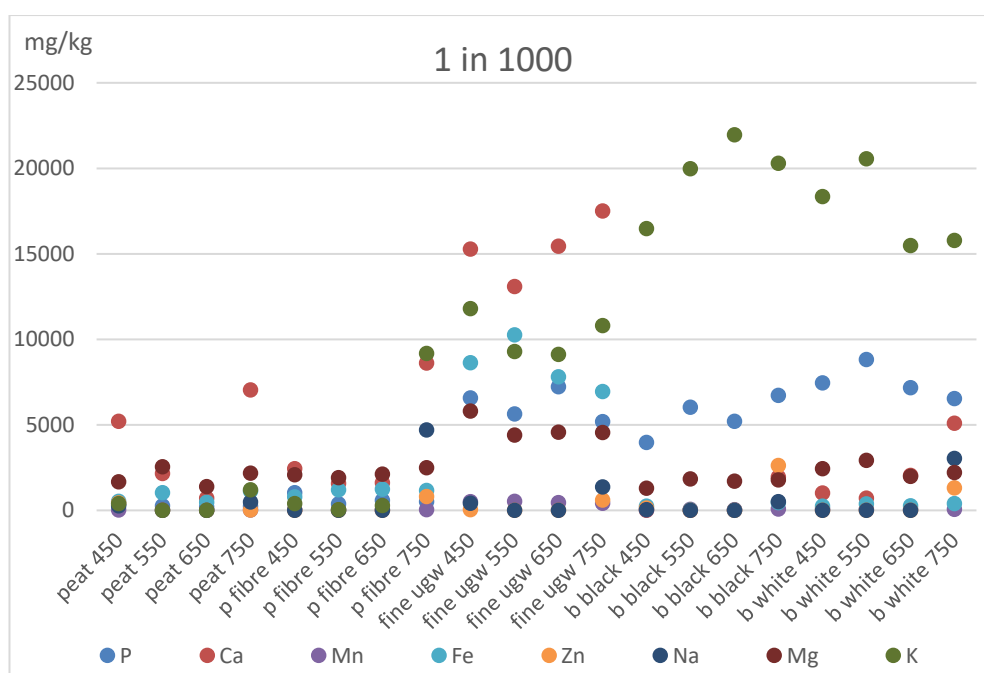


Figure 45: ICP-MS results for 1:1000 dilution of high concentration elements in mg kg^{-1}

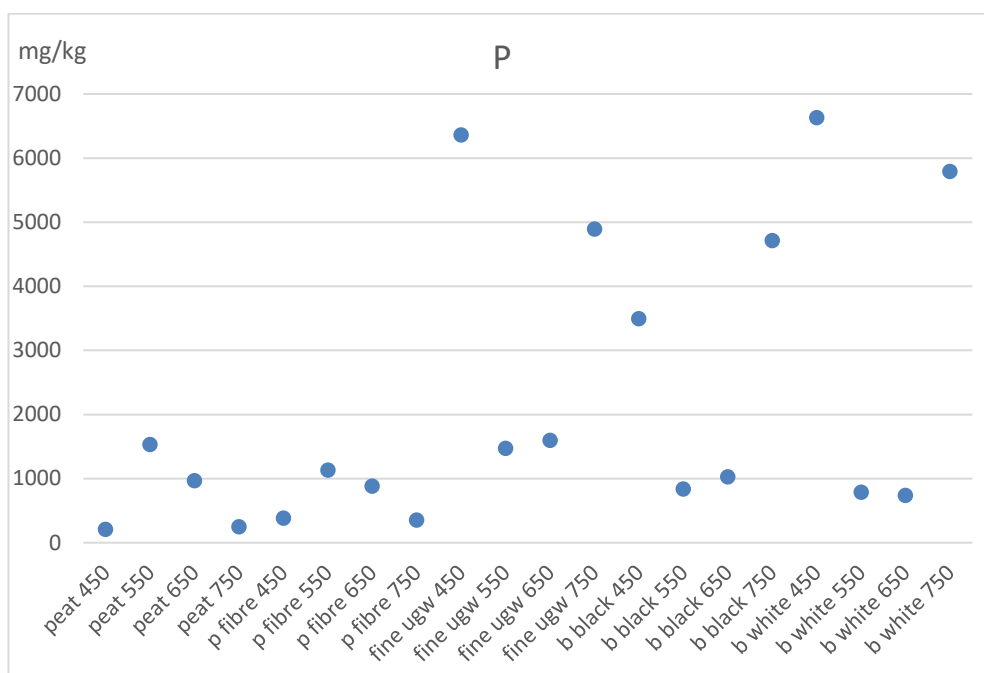


Figure 46: ICP-MS results of the 1:10 dilution for P in mg kg^{-1}

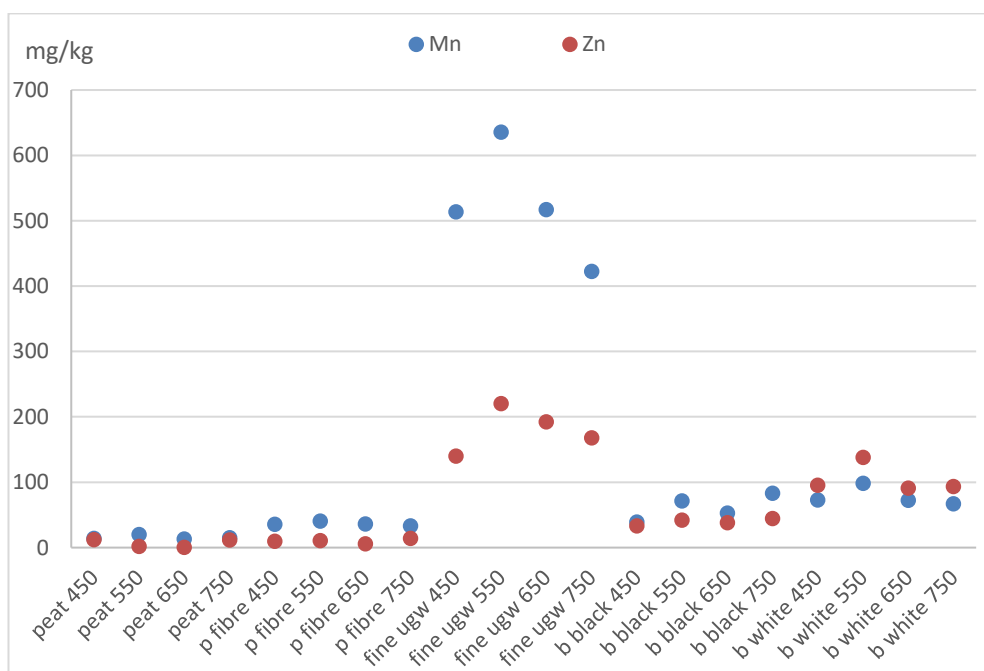


Figure 47: ICP-MS results of the 1:10 dilution for Mn and Zn in mg kg^{-1}

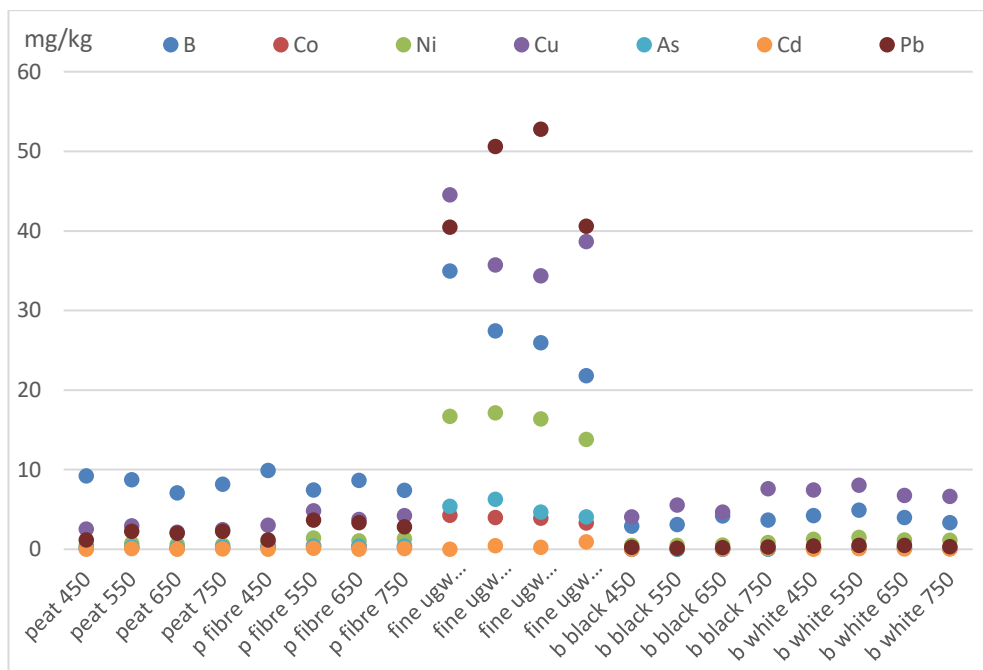


Figure 48: ICP-MS results of the 1:10 dilution

4.11. Gas emission experiment results

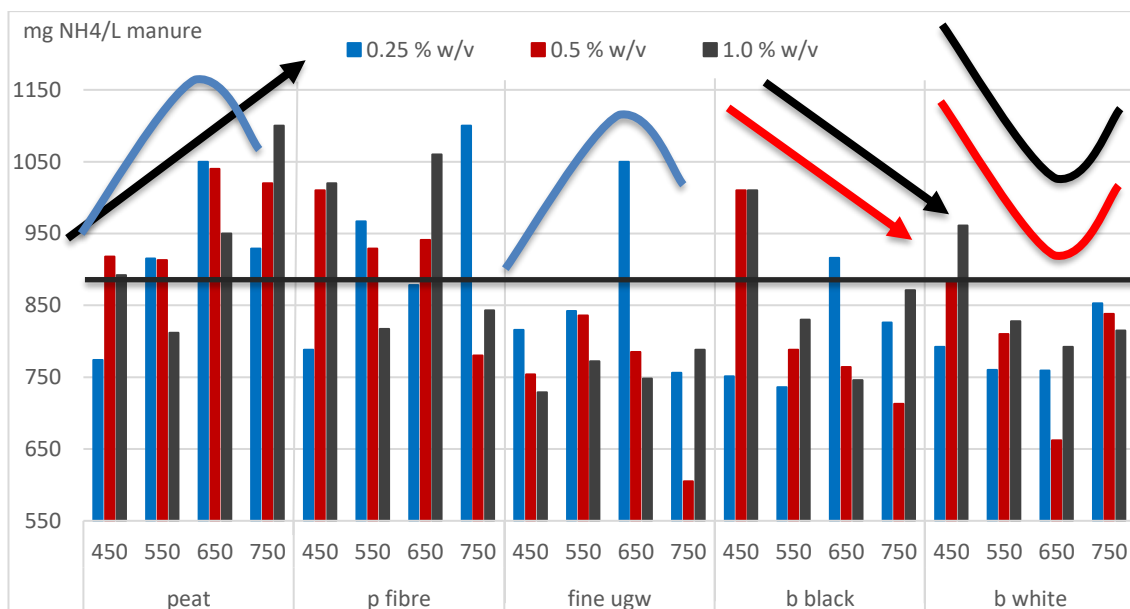


Figure 49: NH₄ remaining in the filtered manure/biochar including the amount of NH₄ remaining in the control (black line); tested with cuvette test

NH₃ emission was detected by evaluating the NH₄⁺ remaining in the manure with or without biochar (Figure 49). The black line in the figure above (Figure 49) represents the amount of NH₄-N remaining in the manure after the emission trials without biochar. The amount of NH₄ left in manure without biochar addition was calculated over 14 samples. The amounts ranged from 693 – 1120 mg L⁻¹ with an average value of 890 mg L⁻¹. Only a few biochars (e.g. peat 650 or 750) were able to retain NH₄-N in the manure, whereas most manures contained less NH₄-N being exposed to biochar after the experiment than without biochar addition. Biochars produced from peat or peat fibre were able to retain more NH₄-N than biochars produced from the other three materials (fine ugw, b. black, b white). In the cases of peat or peat fibre application to manure, the 0.5 %w/v shows the best retention results (Figure 49). A trend which is not that clearly visible for the other materials. As within the other materials, eight out of twelve times the 0.25 %w/v application rate presents the best results. Another trend, which is reflected by the characterization is that biochars from peat and peat fibre produced at 650°C seem to be able to retain the most NH₄ in the manure.

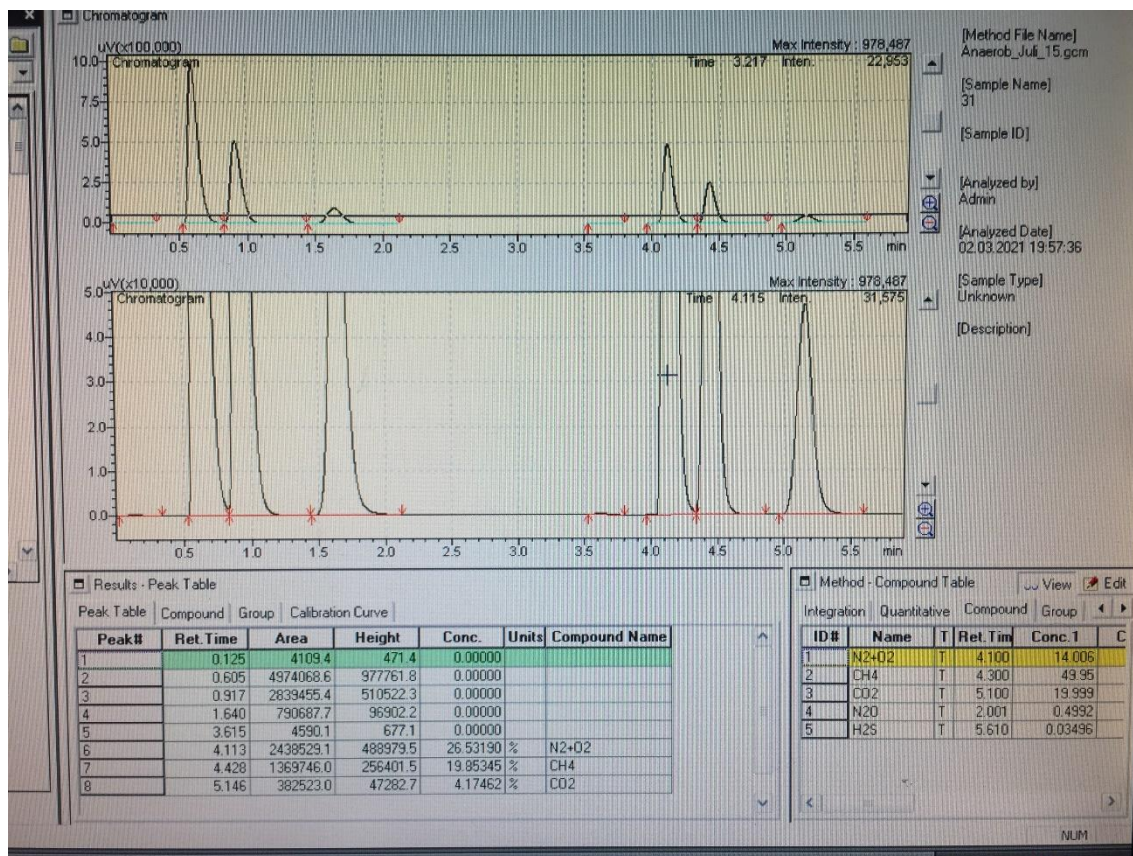


Figure 50: A screenshot of one of the chromatographs taken during GC analysis of the gas emission samples; 1st peak air (N₂ and O₂), 2nd peak CH₄, 3rd peak CO₂ (two repetitions)

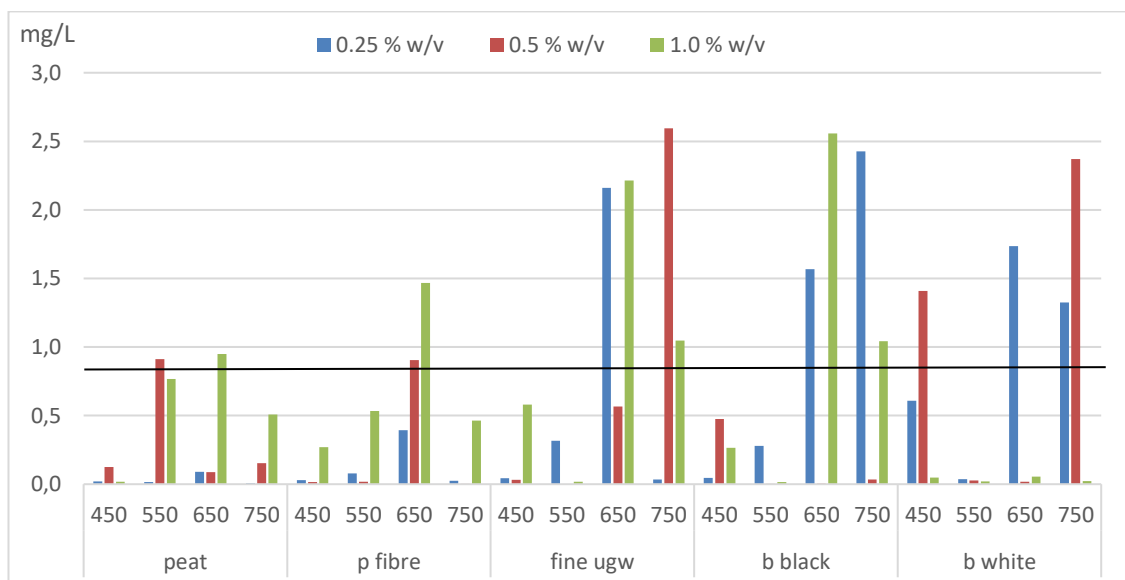


Figure 51: GC results for the CH₄ content of gases released from biochar manure mixtures after three days in mg/L

The gases collected in the bags were analysed using GC (Figure 50). It is noticeable that the emissions associated with biochar application to the manure show a wide range of response patterns (Figure 51 and Figure 52). The addition of biochar reduces the amount of CH₄ released from pig manure in many cases if compared to the amount of CH₄ released by the manure itself, which is 0.87 mg L⁻¹ (black line). It can be seen that especially lower amounts of biochar added to manure (0.25 %w/v) can reduce the amount of CH₄ emissions released when the focus is on biochars produced from peat or peat fibre. Biochars from fine ugw or any brewery grain present a less homogeneous picture as no clear trend is visible. An overall trend regarding production temperatures is not visible throughout all the samples. Though biochars produced from peat (fibre) at low temperatures which are then added to manure in low concentrations show the best results for the reduction of CH₄ emissions in these experiments.

The average amount of CO₂ produced without biochar addition was 0.13 mg L⁻¹ (Figure 52). This value is above two-thirds of the results obtained (Figure 52). Results obtained show that most of the biochar–manure mixtures containing 0.25 %w/v release less than the average amount of 0.13 mg L⁻¹ CO₂ (Figure 52). However, the relationship between biochar addition to manure and the emission of CO₂ is potentially complex and is highly dependent on the feedstock source and the production temperatures but it is also dependent on the intended end use as the composition of the manure itself is a factor in this dynamic (Figure 52).

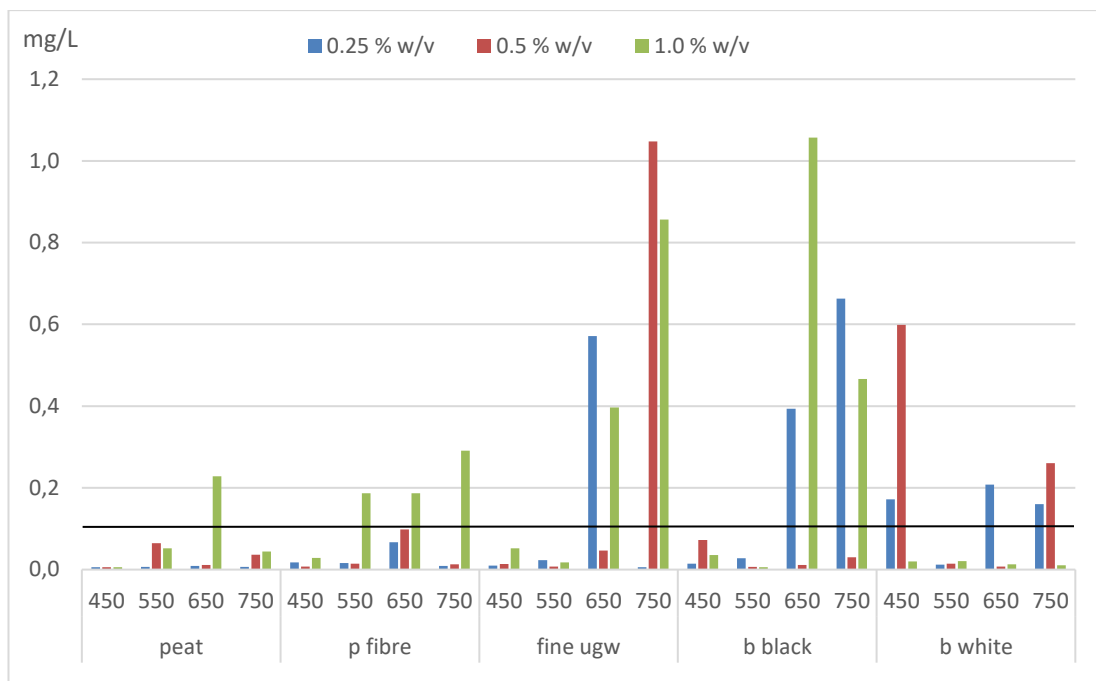


Figure 52: GC results for the CO₂ content of gases released from biochar manure mixtures after three days in mg/L

4.12. Adsorption results of dye onto biochars

Biochars adsorbed malachite green dye in different concentrations. The figure below shows various biochars subjected to different kinds of concentrations of dye. The figure (Figure 53) shows that for most biochars the adsorption increases with higher MG concentrations.

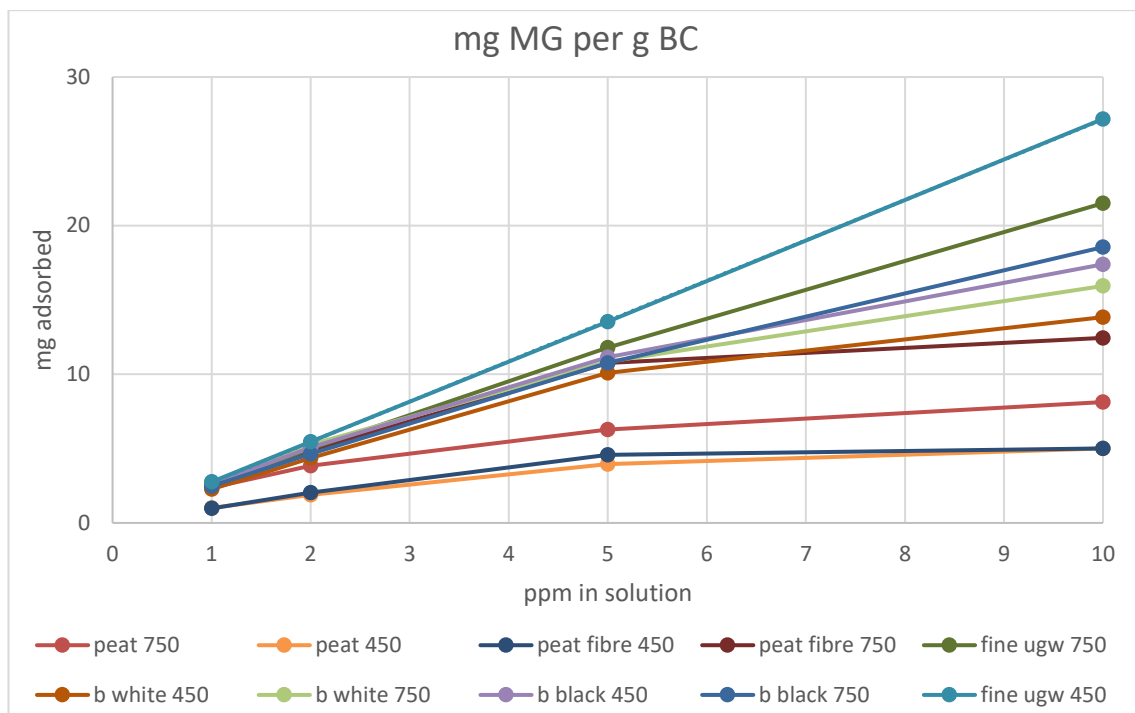


Figure 53: Milligram of malachite green adsorbed onto one gram of biochar

Here, the Langmuir isotherm seems to be a better fit than the Freundlich isotherm (Table 33, Figure 54, Figure 55). In the experiments run, the Q_M obtained varies around 7.13 – 47.39 mg g⁻¹. The experiments show that biochars with a low surface area were able to adsorb the most dye. These results are supported by the high R^2 numbers.

Table 33: Adsorption of malachite green onto biochars at different dilutions

Material	Temperature (°C)	Langmuir			Freundlich		
		Q_M (mg g ⁻¹)	K_L (L mg ⁻¹)	R^2	n_F	K_F (mg g ⁻¹) (L mg ⁻¹) ^{1/n}	R^2
Peat	450	7.5930	0.0702	0.9843	1.546	1.444	0.9649
	550	9.6712	0.0134	0.93	3.068	4.154	0.9646
	650	11.522±2.26	0.009±0.00	0.977±0.00	2.414±0.05	4.765±1.06	0.931±0.00
	750	8.9526	0.0110	0.9924	1.931±1.32	3.598±0.84	0.998±0.00
Peat fibre	450	7.126±0.77	0.064±0.01	0.974±0.02	1.824±0.28	1.708±0.38	0.921±0.00
	550	9.6339	0.0069	0.9844	2.709	4.612	0.9613
	650	12.192±5.68	0.020±0.02	0.910±0.04	2.216±0.03	4.327±2.53	0.968±0.04
	750	13.6612	0.0029	0.9979	2.081	5.715	0.9944
Fine ugw	450	37.7358	0.0008	0.9503	1.282±0.28	21.544±8.37	0.993±0.01
	550	47.3934	0.0012	0.8739	1.180±0.13	10.631±2.31	0.982±0.02
	650	36.3636	0.0191	0.9933	1.361	9.253	0.9937
	750	35.760±9.10	0.001±0.00	0.941±0.06	1.610±0.45	13.109±3.84	0.944±0.06
B black	450	21.6920	0.0023	0.9973	1.812	8.696	0.9754
	550	40.000	0.0007	0.998	1.434±0.05	13.989±5.51	0.973±0.02
	650	42.1941	0.0010	0.9886	1.323	14.517	0.9812
	750	30.200±2.19	0.002±0.00	0.967±0.02	1.487±0.03	8.414±0.65	0.993±0.01
B white	450	18.1818	0.0049	0.9928	1.302±0.53	4.079±2.65	0.868±0.12
	550	18.1159	0.0027	0.9663	0.595	7.987	0.9562
	650	20.4918	0.0016	0.9522	2.340	9.979	0.9967
	750	17.9856	0.0021	0.9941	1.616±0.86	5.469±4.51	0.922±0.07

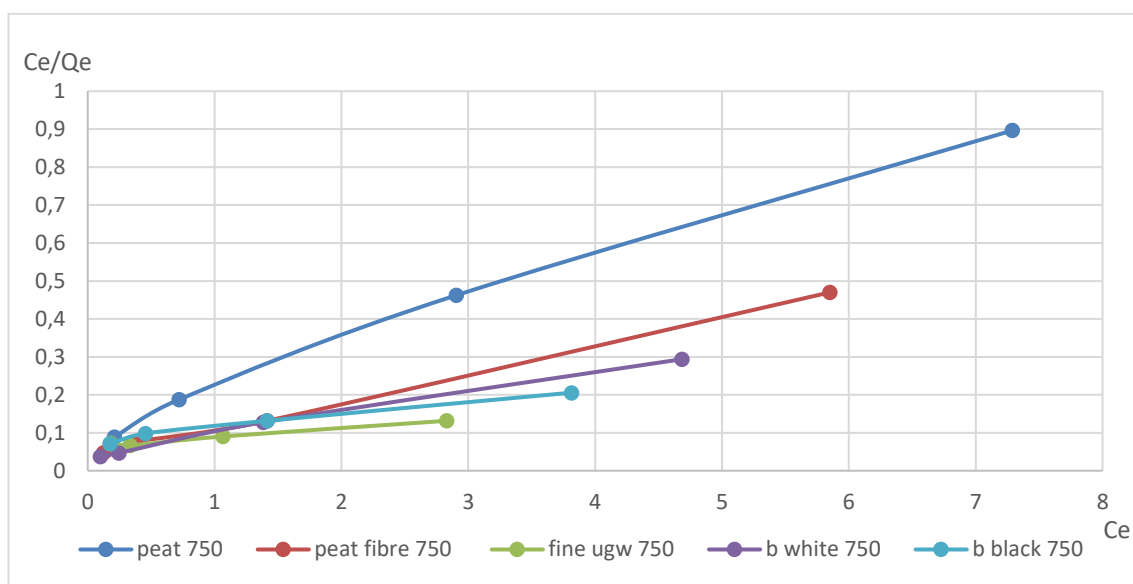


Figure 54: Langmuir plots of adsorption experiments conducted with biochars produced at 750 °C

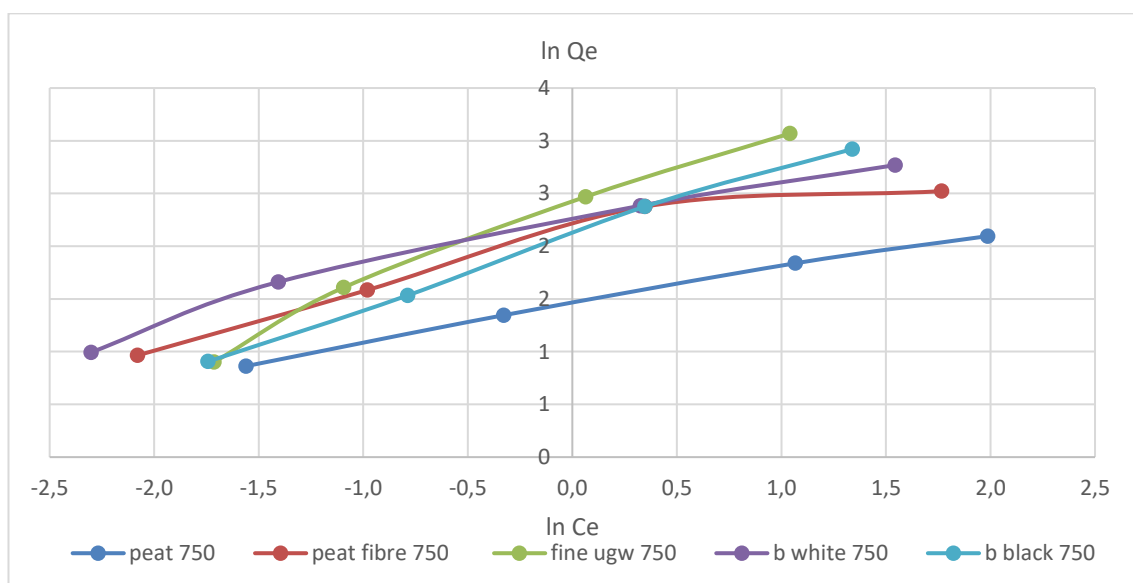


Figure 55: Freundlich plots of adsorption experiments with biochars produced at 750 °C

The table below (Table 34) shows the PFO and PSO results for the biochars analysed. Exemplary plots for the results obtained for PFO and PSO are presented below (Figure 56 and Figure 57). These plots show the kinetics calculated for biochar produced from fine ugw at 450 °C in a 1 – 10 dilution of malachite green to give an example of how the

data obtained in this study fit the PFO and PSO kinetic model. There is only a small variance between the results per sample for different dilutions. This applies mostly to the PFO results, while there are slightly bigger differences in the PSO results. Furthermore, PSO seems to be a better fit for the analysed samples as their R^2 values are higher and closer to 1.

Table 34: Adsorption kinetics of malachite green onto biochars at different dilutions

material	Temperature (°C)	dilution	PFO			PSO		
			q_e (mg g ⁻¹)	k_1 (min ⁻¹)	R^2	q_e (mg g ⁻¹)	k_2 (g mg ⁻¹ min ⁻¹)	R^2
peat	450	1 to 10	0.065	5.350	0.858	0.066	11.502	1.000
		1 to 20	0.061	3.064	0.977	0.062	3.636	1.000
		1 to 50	0.061	3.785	0.884	0.063	4.264	0.998
peat	650	1 to 20	0.094	3.231	0.992	0.097	1.044	0.999
		1 to 50	0.087	3.183	0.995	0.091	1.020	0.999
peat	750	1 to 10	0.084	3.336	0.902	0.087	1.222	0.999
		1 to 20	0.078	3.215	0.969	0.081	1.663	1.000
		1 to 50	0.031	3.493	0.963	0.033	5.109	0.995
		1 to 100	0.064	3.037	0.942	0.068	1.892	0.999
peat fibre	450	1 to 10	0.064	0.001	0.963	0.064	4.738	1.000
		1 to 20	0.069	0.035	0.898	0.070	5.488	1.000
peat fibre	650	1 to 10	0.088	3.248	0.904	0.090	1.413	0.998
		1 to 20	0.087	2.980	0.913	0.090	0.997	0.998
		1 to 50	0.050	3.125	0.968	0.055	1.576	0.994
		1 to 100	0.068	2.980	0.904	0.072	1.426	0.998
peat fibre	750	1 to 10	0.09±0.00	3.36±0.62	0.93±0.02	0.08±0.02	1.44±0.61	1.00±0.00
		1 to 20	0.09±0.01	2.98±0.55	0.95±0.00	0.09±0.00	1.72±1.88	1.00±0.00
		1 to 50	0.07±0.02	3.25±0.24	0.94±0.05	0.14±0.07	0.68±0.85	0.99±0.02
		1 to 100	0.03±0.03	2.73±0.38	0.98±0.01	0.064	0.832	0.985
fine ugw	450	1 to 10	0.09±0.01	2.65±0.42	0.97±0.02	0.10±0.01	0.60±0.42	0.98±0.02
		1 to 20	0.52±0.60	2.83±0.04	0.91±0.06	0.10±0.00	1.09±0.11	1.00±0.00
		1 to 50	0.08±0.01	2.76±1.19	0.93±0.02	0.21±0.19	0.61±0.84	1.00±0.00
		1 to 100	0.08±0.00	3.05±0.12	0.98±0.00	0.08±0.00	1.28±0.20	1.00±0.00
fine ugw	550	1 to 10	0.096	3.209	0.978	0.099	1.446	1.000
		1 to 20	0.088	3.004	0.949	0.092	1.539	0.999
		1 to 50	0.074	2.997	0.983	0.078	1.230	1.000
		1 to 100	0.051	3.456	0.975	0.054	2.518	0.997
b black	450	1 to 10	0.093	3.531	0.913	0.095	2.278	1.000
		1 to 20	0.092	0.031	0.936	0.093	3.259	0.999
		1 to 50	0.073	3.579	0.867	0.078	3.591	0.991
		1 to 100	0.029	3.640	0.906	0.034	2.189	0.952

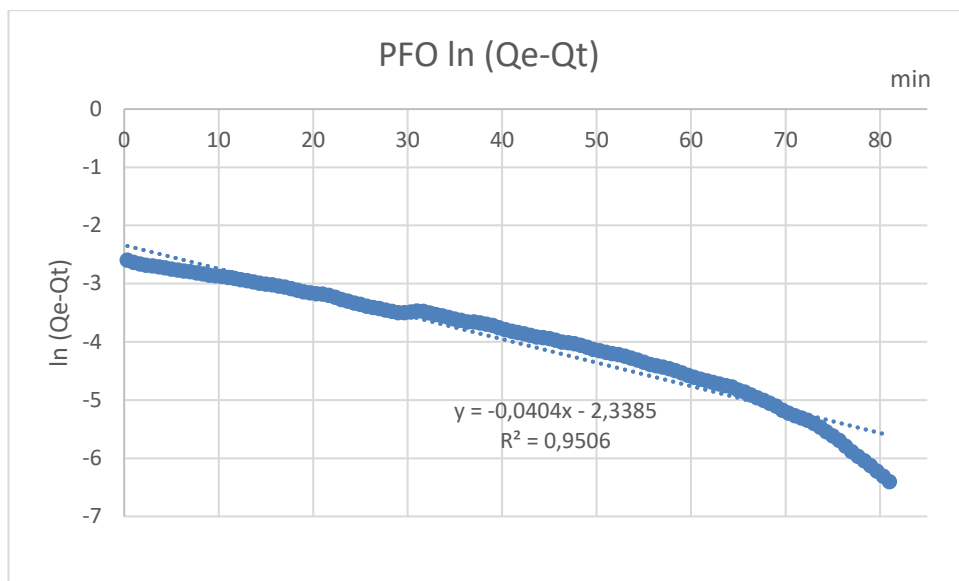


Figure 56: PFO kinetics calculated for fine ugw 450 in a 1-10 dilution of malachite green

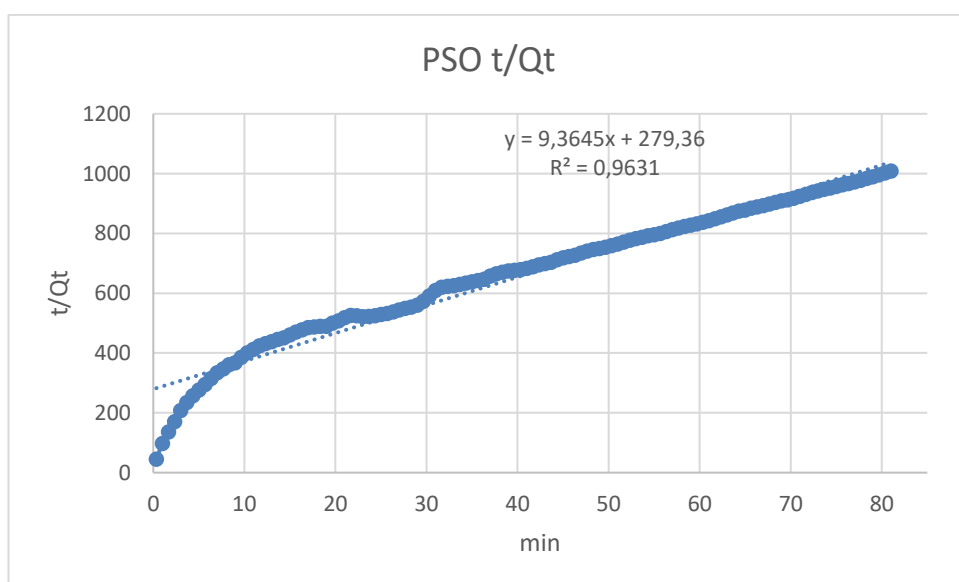


Figure 57: PSO kinetics calculated for fine ugw 450 in a 1-10 dilution of malachite green

5. Discussion

5.1. Chemo-physical analysis of biochar produced from waste materials in comparison to a peat-based feedstock from drained Irish ombrotrophic peatlands

Biochar yields from here are comparable with results obtained from the literature. In the literature values of between 51.44-36.19 %DM for peat-based biochar samples produced at 5 °C min⁻¹ (Sutcu, 2007) as well as values for two kinds of peat (horticultural and fuel peat) at temperatures of 450 – 650 °C analysed by the UKBRC (29 – 50 %d.b.) (Table 7) are presented- Those are mostly lower than the peat-based biochar yields obtained here (41.37 – 51.43 %DM), making the material used here more favourable for production in terms of yield. It has been reported that biochars produced at 450 °C vary between 63.00 – 28.4 %DM, depending on the heating rate and residence time (Ronsse *et al.*, 2013; Abrishamkesh *et al.*, 2015; Domingues *et al.*, 2017; Zhang *et al.*, 2017), but they also show that the yield obtained here is within the range reported in the literature. As already reported by others and seen here as well, the biochar yield (%) tends to decline with higher treatment temperatures (Sutcu, 2007; Ronsse *et al.*, 2013; Gai *et al.*, 2014; Suliman *et al.*, 2016; Zhang *et al.*, 2017).

Looking more at the chemo-physical changes made during pyrolysis, the pH is an important factor to look at. The change in pH becomes important when the biochar is applied to another medium such as soil as it will affect its pH (Xiaofeng *et al.*, 2017). Biochars from different materials exhibit pH between 3.18 and 10.85 with production temperatures of 200 to 650 °C (Stella Mary *et al.*, 2016; Feola Conz *et al.*, 2017; Huang *et al.*, 2018; Dejene and Tilahun, 2020). These values align with the results found here for biochars produced within the same temperature range. Furthermore, it is also shown that higher treatment temperatures produce biochars with higher pH values.

Pyrolysis increases the pH of all materials used, making the biochars more alkaline than the original feedstock. Higher pH can be explained by the temperature effect on the release of volatile matter consisting of acid functional groups and concentrated ash contents, therefore elevating the pH (Enders *et al.*, 2012). Furthermore, it was found that biochars produced at higher temperatures are more alkaline, because of a higher relative abundance of non-pyrolysed inorganic elements or aromatic basal planes (Novak *et al.*, 2009) (Table 25, Table 26). Li *et al.* also found that the increase in pH was predominantly due to the splitting and breakage of weaker bonds, like hydroxyl bonds, within the biochar structure at a high pyrolysis temperature (Li *et al.*, 2018). This also aligns with the findings of Enders *et al.* (2012) regarding the effect of the release of volatile matter from biochars at higher treatment temperatures.

Looking at the thermochemical side it was found that when comparing the findings made here with results in the literature depending on which material the biochars were produced from, the results vary quite a bit. Biochars examined using the same method as here have ash contents of 1.4 – 55.1 wt%, d.b., FC contents of 3.1 – 83.4 wt%, d.b. or 73.67 -85.05 %daf and VM contents of 11.8 – 52.9 wt%, d.b. or 7.47 – 85.33 %daf, respectively (Buss and Mašek, 2014; Mašek *et al.*, 2018; Rathnayake *et al.*, 2020). Volatiles found in biochars, reported by the literature, can be benzene, toluene, ethylbenzene, PAHs or phenols (Rathnayake *et al.*, 2020). All of which can be present in different ratios at different production temperatures.

Biochars reported in the literature have moisture contents of 2.6 – 3.4 %d.b., ash contents of 72.7 – 76.8 %d.b., VM 11.9 – 6.3 %d.b. and FC of 12.6 – 14.3 %d.b. (Taherymoosavi *et al.*, 2017) for municipal solid waste. Rapeseed stem biochars produced between 200 – 700 °C present moisture contents of 0.66 – 1.88 %, VM contents 81.81 – 9.28 %, FC 13.30 – 75.18 % and ash contents of 3.02 – 14.10 % (Zhao *et al.*, 2018). Other biochars

produced from 300 – 600 °C present volatile matter, ash and FC contents of 76.87 – 86.09 %,d.b., 6.42 – 13.07 %, 7.49 – 10.17 %, d.b. (He *et al.*, 2018).

The proximate analysis conducted here shows that four out of five materials can produce biochars with high FC contents. Even more so when calculated on an ash-free basis (Table 28). These contents can be used as a stability indicator as FC is closely related to stable C content (Leng *et al.*, 2019), indicating that biochars with high FC contents are more stable than those with lower FC contents. Furthermore, a higher FC yield can present a higher potential as a climate change mitigation tool (Brassard, Godbout and Raghavan, 2016). Biomass converted to biochars with high FC contents can help to sequester C from the atmosphere for a longer time than if those biomasses would be brought to a landfill or burned and produced CO₂ and CH₄ during this process. It is also reported that as VM and FC are values as a percentage of the total biochar and the ash content varies dramatically between different feedstocks used for biochar production, therefore a comparison between FC or VM values of biochars from different materials would probably not be accurate in providing precise stability information (Leng *et al.*, 2019), This is making it harder to compare and evaluate the results found and to give precise overall information on the longevity of biochars in general. Though a comparison on a dry-and ash-free basis could help to eliminate that bias. Giving a better indication of the biochar's stability.

Another important factor to discuss is the surface area. The surface area, the micropore area as well as the total pore volume increase with treatment temperatures up to 650 °C for biochars produced in this study. A slight decrease can be observed for the numbers at 750 °C (Figure 18, Figure 19). The resulting “peak” at 650°C has already been reported in the literature (Y. Chen *et al.*, 2017; Dieguez-Alonso *et al.*, 2018; Ji *et al.*, 2019). However, there is some uncertainty attached to this outcome as it may be an

artefact of N₂ measurements, as the peak could not be confirmed by CO₂ analysis (Maziarka *et al.*, 2021).

The total pore volume has been commonly reported as ranging between 0.016 – 0.083 cm³ g⁻¹ and when a fitting precursor and suitable pyrolysis parameters are chosen (Leng *et al.*, 2021), the volume can be increased to 0.25 cm³ g⁻¹ (Yang *et al.*, 2016; Leng *et al.*, 2021) (Figure 21). These results show that most of the biochars produced in this study must have been prepared under suitable pyrolysis conditions, as even the surface area of half of the samples produced was found to be higher than the range of 8 – 132 m² g⁻¹ (Leng *et al.*, 2021). Biochars with a similar surface area as those produced in this study were produced from corn straw, poplar leaves, bamboo waste, coconut shells, sugarcane bagasse, or others at 250 – 950 °C. They exhibit surface areas of 0.65 – 465.02 m² g⁻¹ (Yang *et al.*, 2016; Xiaofeng *et al.*, 2017; Batista *et al.*, 2018; Cabriga *et al.*, 2021), setting the biochars produced in this study and the conditions of the production in a fitting context.

The surface area of biochars has been widely reported as ranging between 2.57 – 590.00 m² g⁻¹ and the micropore areas vary between 9.46 – 53.6 m² g⁻¹, while the micropore volumes have been reported with values ranging from 0.012 – 0.231 cm³ g⁻¹, with production temperatures of between 300 – 900 °C (Angin and Şensöz, 2014; Chowdhury *et al.*, 2016; Hung *et al.*, 2017; Mendonça *et al.*, 2017; Batista *et al.*, 2018; Leng *et al.*, 2021). In terms of biochars produced from peat feedstock, the reported surface areas vary from 2.5 m² g⁻¹ to 346 m² g⁻¹ where production temperatures ranged between 300 and 700 °C (Wang *et al.*, 2017; Kim, Lee and Khim, 2019). These results suggest that the surface area results produced in this study for peat biochars (Figure 18) can not only be found in other production settings but that the materials used in this study result in higher surface area values (442.43 m² g⁻¹). The total pore volumes were detected within

the range of $4.1 \times 10^{-8} - 0.083 \text{ cm}^3 \text{ g}^{-1}$ (Angin and Şensöz, 2014; Hung *et al.*, 2017; Batista *et al.*, 2018; Leng *et al.*, 2021).

These overall reported values from the literature align with the results obtained in this study, showing that the feedstocks used here are suitable for biochar production and present valuable results. This is likely to be a consequence of an increase in pyrolysis temperature as this can enhance the aromaticity and the calcination of main minerals like calcite as more micro- and mesopores are generated, aiding the development of a higher surface area (Hung *et al.*, 2017). Furthermore, the observed increase in surface area can also be explained by the decomposition of amorphous organic content within carbon structure inducing the formation of pores where the walls are based on broken aromatic structures (Mendonça *et al.*, 2017).

SEM images taken from feedstocks and biochars show the impact pyrolysis has on the materials. It is shown that the material became more porous and the outline of the surface also changed (Figure 22 - Figure 27). Biochars produced from peat at 600 °C for 2h exhibited a porous structure which could indicate a large specific area and high porosity (Wang *et al.*, 2017). Results found by Wang *et al.* align with results found here, showing that peat as a biochars feedstock is producing biochars with a high surface area.

Further comparison of feedstocks with the respective biochars showed that biochars produced at 450 – 750 °C produced porous profiles for most of the materials used (Figure 23 - Figure 27). Only biochars produced from fine ugw were comparatively less porous. A less porous structure is probably associated with devolatilization which occurs during pyrolysis and is supported by low values of volatile matter (Tasim *et al.*, 2019), a fact which is contradicted by the results in this study (see 4.3). This might suggest low volatile matter contents do not necessarily lead to less porous structures (Figure 25). The porosity

of biochar from peat (Figure 23) can be visibly compared to the biochar from brewery grain (Figure 25) and is a reasonable explanation for the high surface area (Figure 18).

An overview of ATR results (Figure 28, Figure 29) shows that biochars produced from the other three materials at 750 °C did not contain functional groups at the surface. In general, with an increase in pyrolysis temperature, the number of functional groups on the surface decreases, and some peaks are detected with a lower intensity. It was also found that increasing treatment temperatures lead to a reduction in the intensity of peaks and a reduction of functional groups on the surface in general (Nair, Mondal and Weichgrebe, 2020). It has been widely reported that with biochars produced at 750 °C most of the organic functional groups present in the biochar structure were lost (Domingues *et al.*, 2017), an outcome that is consistent with the findings in this study.

Focussing on other groups which can be present in biochars, the group of PAHs is important to look at. The United States Environmental Protection Agency (USEPA) lists 16 polycyclic aromatic hydrocarbons (PAHs) as priority pollutants based on their high concentrations in the environment and their mutagenic and carcinogenic properties (Patel *et al.*, 2020; Han *et al.*, 2022) (Table 35). Because of their inherent properties, PAHs are persistent pollutants that have a wide range of biological toxicity and the remediation of PAHs from the environment has been a global concern for some time (Patel *et al.*, 2020). PAHs are toxic to humans, other wildlife, and soil (Honda and Suzuki, 2020; Patel *et al.*, 2020). Contaminants such as PAHs can be formed during biochar production and remain in the biochar (Kamali *et al.*, 2021). The concentration of PAHs is greatly influenced by feedstock type, production temperature and residence time (Dissanayake *et al.*, 2020).

Table 35: sixteen PAHs which have been designated High Priority Pollutants by the Environmental Protection Agency (EPA); in no specific order

1.	naphthalene (NAP)
2.	acenaphthylene (ACY)
3.	acenaphthene (ACE)
4.	fluorene (FLU)
5.	phenanthrene (PHEN)
6.	anthracene (ANTH)
7.	fluoranthene (FLTH)
8.	pyrene (PYR)
9.	benzo[a]anthracene (B[a]A)
10.	chrysene (CHRY)
11.	benzo[b]fluoranthene (B[b]F)
12.	benzo[k]fluoranthene (B[k]F)
13.	benzo[a]pyrene (B[a]P)
14.	benzo[g,h,i]perylene (B[ghi]P)
15.	indeno[1,2,3-c,d]pyrene (IND)
16.	dibenz[a,h]anthracene (D[ah]A)

Furthermore, it was found that biochars produced by slow pyrolysis contain fewer PAHs compared to those produced through fast pyrolysis. A probable reason could be the longer residence time during slow pyrolysis as compared to fast pyrolysis (Hilber *et al.*, 2017; Dissanayake *et al.*, 2020). Exemplary results out of all biochars from this study do not contain any of the 16 PAHs (Figure 31). The peaks seen in the chromatograph can be attributed to products of the toluene extraction. The ten samples run in this study do not contain traceable amounts of PAHs, whereas other biochars analysed in the literature

contain collective amounts of the 16 commonly tested priority PAHs of 0.82 to 355.295 $\mu\text{g g}_{\text{biochar}}^{-1}$ (Hilber *et al.*, 2012; Stefaniuk, Oleszczuk and Bartmiński, 2016; Frišták, Pipiška and Soja, 2018; Weidemann *et al.*, 2018).

When moving on to RAMAN spectroscopy, it has been reported elsewhere that biochars show two reoccurring bands, which depending on the material or production temperature are clearly distinguishable (Mohanty *et al.*, 2013; Smith *et al.*, 2016; Mendonça *et al.*, 2017). Raman spectra of biochars show two characteristic bands that are located at about 1350 – 1370 cm^{-1} (D band) and 1580 – 1600 cm^{-1} (G band) (Chia *et al.*, 2012; Zhao *et al.*, 2013; Stefaniuk and Oleszczuk, 2015; Guizani *et al.*, 2017). These two bands correlate correspondingly to the in-plane vibrations of sp^2 -bonded carbon structures with structural defects (D band) and the in-plane vibrations of the sp^2 -bonded graphitic carbon structures (G band) (Zhao *et al.*, 2013; Stefaniuk and Oleszczuk, 2015; Guizani *et al.*, 2017). And when there is a material with a high proportion of amorphous carbon structures, like in the case of biochars, these two bands can overlap. This overlap is due to the contribution of the amorphous carbon structures to the Raman signal in the region between 1400 and 1550 cm^{-1} called the valley region “V” (Guizani *et al.*, 2017).

All twenty biochars produced here exhibit clear D- and G- bands in the ranges reported in the literature (Figure 32). The FWHM (full-width half maximum) of the bands could not be determined as the peaks did not show a clear enough separation between them (Figure 32). Nevertheless, there is no large background signal and therefore no fluorescence is visible in the spectra (Figure 32). This can indicate that no PAHs are present on the surface of the biochars and this supports the results presented in section 4.7.

To show the results obtained and presented above in more detail, the appendix includes figures which present the RAMAN data obtained for biochars produced from b black at

four temperatures (see appendix). The higher the treatment temperatures the lower the intensity of the peak at wavenumbers in the ranges of $800 - 1100 \text{ cm}^{-1}$ and $1700 - 1900 \text{ cm}^{-1}$, this is related to the change in chemical structure (Guizani *et al.*, 2017; Mendonça *et al.*, 2017). It has been reported that a decrease in the D band position, is corresponding to an increase in the G band position in the Raman spectrum of carbon materials. This could reflect an increase in the order degree of carbon structure (Potgieter-Vermaak *et al.*, 2011; Wang *et al.*, 2018; Yu *et al.*, 2018; Xu *et al.*, 2020). Raman spectroscopy has the potential to evaluate the properties of biochars rapidly (Xu *et al.*, 2020). As shown here, an increase in the ratio of the intensity of the D to G peak with increasing pyrolysis temperatures is indicating changes in the chemical structure of the pyrolysed feedstock (Figure 34 – Figure 37). Thus, RAMAN may be an easy non-destructive method to test the influence of production methods on biochars. Raman can be used as a probe for the chemical composition at a surface. It is simple and fibre optic spectrometers are becoming popular. The results above show that it is worth considering Raman spectroscopy as a screening method for the surface chemistry of biochars as Raman can show the changes in the chemo-physical nature of biochars. Certainly, the correlation between the D/G intensity ratio and HTT is worth further investigation.

Another important factor to consider is the change in the elemental composition of the biochars during pyrolysis. Here, the carbon (C) content (Figure 38) presents the same trend as the fixed carbon content of the biochars. It is highly increasing with higher temperatures for peat and peat fibre and a bit for grains. For biochars produced from fine ugw, it is not increasing, which can be explained by the high relatively high VM and ash content presented in section 4.3. Those biochars have a lower carbon content and higher oxygen (O) content (Figure 41) with rising treatment temperatures (Table 29). For the other materials, it can be said that the carbon content is increasing, while the hydrogen

(H) (Figure 39), nitrogen (N) (Figure 40), sulphur (S) and oxygen content are decreasing with higher treatment temperatures. This trend has been reported for biochars produced under various temperatures, showing how pyrolysis is influencing the chemical formula of the biomass (Feola Konz *et al.*, 2017; Li *et al.*, 2019). Though not every study cited above tested for all the elements determined in this study.

Biochars produced from cellulose, corn stover and hardwood at temperatures ranging from 300 to 600°C using slow pyrolysis were analysed for their elemental content. Their elemental analysis results show C contents of 52 – 96 %, H contents of 2 – 3.82% and N contents of 0.18 -1.65% (Fidel *et al.*, 2017). The results of this study for the C, H and N values are broadly consistent with that reported by (Fidel *et al.*, 2017), though some biochars generated in this study have a higher N content. It was stated that as hydrogen and oxygen contents decrease in biochars produced from rising temperatures, carbonisation, and aromatisation of carbon structures during pyrolysis reaction are indicated (Feola Konz *et al.*, 2017). This is reflected in the lower reactivity of biochars as temperature increases (Chan and Xu, 2009), which could influence the ability to absorb CH₄, CO₂ or dye.

The H/C and O/C ratios are important factors as well. Biochars are expected to help sequester carbon if the O/C is below 0.2 and the H/C ratios are lower than 0.7 (Brassard *et al.*, 2017). Based on values, some of the biochars produced in this study would be usable for the mentioned purposes. Generally, it can be said that all biochars produced in this study are within proposed IBI and EBC limits (≤ 0.7 H/C and ≤ 0.4 O/C) and therefore classify as stable biochars (International Biochar Initiative, 2015; EBC (2012-2022), 2022). The Van Krevelen diagrams are presented to determine the degree of aromaticity and maturation in the biochar structure (Figure 42, Figure 43). Three out of five materials show a clear trend, whereas biochars produced from b white and fine

ugw do not present a clear trend (Figure 43). An explanation for this could be the heterogeneity of the elemental analysis results, which in turn could be explained by the heterogeneity of the feedstocks and the amount of sample used for analysis. A decrease in H/C ratios, indicating an increase in aromaticity (Windeatt *et al.*, 2014), can be observed with rising treatment temperatures for all five materials (Table 30). Most of the biochars produced showed a slight decrease in O/C ratios, indicating a reduction in polarity (Windeatt *et al.*, 2014), with higher production temperatures. Only biochars produced from fine ugw did not follow that trend. Their O/C ratios increase with higher treatment temperatures, which can suggest an increased polarity of those biochars. Generally, the molecular ratio of H/C decreased faster than the O/C ratio with increasing treatment temperatures, indicating that H is more easily lost at lower pyrolysis temperatures than oxygen (Rodriguez *et al.*, 2020). The results generated in this study are largely consistent with values presented in the literature (Enders *et al.*, 2012; Pariyar *et al.*, 2020; Rodriguez *et al.*, 2020) this gives new insights into the elemental composition, aromaticity, and polarity of biochars produced from those materials (Table 12).

ICP-MS is another analysis focussing on the elemental composition of biochars. Biochars from different types of cow manure, which were analysed using similar methods (US EPA Method 3052 and US EPA Method 3051A), have generated values of 4137 – 5963 mg kg⁻¹ for P, 7251 – 15415 mg kg⁻¹ for K, < 0.1 mg kg⁻¹ for Cd, <10 mg kg⁻¹ for Pb, 43 – 152 mg kg⁻¹ for Cu, 109.3 – 166.9 mg kg⁻¹ for Mn and 3.61 – 7.42 mg kg⁻¹ for Ni (Guo *et al.*, 2021). While biochars produced from food waste and sewage sludge and different mixtures of those materials at temperatures of 300 – 500 °C have exhibited heavy metal contents of 1437.4 mg kg⁻¹ Zn, 738.5 mg kg⁻¹ Cu, 37.6 mg kg⁻¹ Cr, 22.1 mg kg⁻¹ Pb, 2.8 mg kg⁻¹ As, and 1.9 mg kg⁻¹ Cd (Jeong, Lee and Kim, 2020) when analysed with the same method as used in this study. The values obtained for K and Ca collected through ICP-

MS of 5.8 – 10.8 g kg⁻¹ Ca and 2.9 – 75.5 g kg⁻¹ K, which are partially higher (Mohanty *et al.*, 2013) than some of the ones captured here (e.g. peat 650). Others tested biochars using ICP-OES, collecting results of 3 – 880 mg kg⁻¹ for elements like Fe, Zn, Mn, Na, Cu and Ni (Onorevoli *et al.*, 2018).

The elemental composition and especially the content of toxic elements like heavy metals is important to consider when thinking about what to do with the biochars produced. Therefore, Germany's Federal Soil Protection Act (Bundes-Bodenschutzverordnung or BBodSchV, 2020) (BMUV, 2020), and Switzerland's Chemical Risk Reduction Act (Schweizerische Chemikalien-Risikoreduktions-Verordnung or ChemRRV, 2005) are used as the reference guidelines when it comes to the maximum values for heavy metals in biochars (EBC, 2012). The respective thresholds refer to the biochar's total dry mass (DM). The European Biochar Initiative distinguishes between basic grade biochars with limits for heavy metals of Pb < 150 mg kg⁻¹ DM; Cd < 1,5 mg kg⁻¹ DM; Cu < 100 mg kg⁻¹ DM; Ni < 50 mg kg⁻¹ DM; Zn < 400 mg kg⁻¹ DM and premium grade with thresholds of Pb < 120 mg kg⁻¹ DM; Cd < 1 mg kg⁻¹ DM; Cu < 100 mg kg⁻¹ DM; Ni < 30 mg kg⁻¹ DM; Zn < 400 mg kg⁻¹ DM (EBC, 2012). The biochars produced in this study were within range of the premium grade biochar for most of the elements stated, only Ni and Zn values were higher than the threshold in some biochars (Table 31, Table 32). Though it can be seen that some materials produce biochars with fewer trace metals than others. Especially biochars produced from fine ugw contain more trace metals in comparison to the others irrespective of the pyrolysis temperature linking into the composition of the feedstock. The trends are normally to be expected, if the metal is not volatile, the trend should be proportional to the temperature because the metals are being concentrated in a smaller mass of char at higher temperatures used in pyrolysis. The exception is when the metals start to become volatile at higher pyrolysis temperatures, then a lower than proportional

increase in concentration as the temperature in pyrolysis increases is visible. With these biochars, those clear trends throughout the temperatures are not clearly visible. It could be that a too small amount of the sample is analysed to get a representative picture of the whole material. Likely the difficulty in having representative subsamples for analysis may have caused a certain error in the obtained results as already mentioned in the bulk elemental analysis (4.9.)

To summarize, increasing pyrolysis temperature lead to a decrease in volatile matter content for all feedstocks used, whereas the surface area and the fixed carbon content of the resultant biochars were shown to increase (Table 36). This suggests that higher production temperatures are optimal to produce more stable biochars, which makes biochars an excellent material to sequester carbon, but this comes at a cost in energy demand and environmental terms. Furthermore, biochars produced here did not contain PAHs or heavy metals above the regulatory limits, making them a safe product for various applications.

Table 36: a schematic overview of the impact of rising production temperatures on the characteristics of biochar

Production temperature (°C)	yield	pH	VM	FC	ash	Surface area	Micropore area
↑	↓	↑	↓	↑	↑	↑	↑

5.2. Potential control of CO₂, CH₄ and NH₃ from swine manure

Adsorbing emissions or retaining them in the manure can help to improve the GHG impact of agriculture. In this study, only a few biochars (e.g. peat 650 or 750) were able to retain NH₄-N in the manure used in this study, whereas most manures contained less NH₄-N being exposed to biochar after the experiment than without biochar addition. Biochars produced from peat or peat fibre were able to retain more NH₄-N than biochars produced from the other three materials (fine ugw, b. black, b white). In the cases of peat

or peat fibre application to manure, the 0.5 %w/v shows the best retention results (Figure 49). A trend which is not that clearly visible for the other materials. As within the other materials, eight out of twelve times the 0.25 %w/v application rate presents the best results. Another trend, which is reflected by the characterization is that biochars from peat and peat fibre produced at 650°C seem to be able to retain the most NH_4 in the manure. This is consistent with a high surface area and micropore area. Biochars produced from black or white have a smaller surface area and micropore area and can retain less. Future work could include a possible way to confirm the results found here by increasing the dose of biochars added to the manure for all materials. The dominant process driving NH_4^+ adsorption onto biochars is likely their cation exchange capacity (CEC) (Clough *et al.*, 2013), which will be needed to be tested in the future.

However, the relationship between biochar addition to manure and the emission of CO_2 and CH_4 is potentially complex and is highly dependent on the feedstock source and the production temperatures but it is also dependent on the intended end use as the composition of the manure itself is a factor in this dynamic. It can be seen that especially lower amounts of biochar added to manure (0.25 %w/v) can reduce the amount of CO_2 and CH_4 emissions released when the focus is on biochars produced from peat or peat fibre (Figure 51, Figure 52). Biochars from fine ugw or any brewery grain present a less homogeneous picture as no clear trend is visible. An overall trend regarding production temperatures is not visible throughout all the samples. Though biochars produced from peat (fibre) at low temperatures which are then added to manure in low concentrations show the best results for the reduction of CO_2 and CH_4 emissions in these experiments. An explanation for these findings can be the structure of the feedstock as seen in Section 4.5. Peat and peat fibre have been decomposing for a long time before they were brought to use, whereas fine ugw and grain are a fresh material and therefore can contain a higher

content in labile components, which might influence the structure of the biochars, which can also explain the lower surface area found in section 4.4.

It has been reported that an increase in biochar addition to chicken manure compost decreased the detectable CH₄ emission (Jia *et al.*, 2016). This was explained by the high porosity of the biochar which enhanced the supply of oxygen and therefore restricted the activity of methanogenic organisms and enabled better adsorption or retention of CH₄ (Jia *et al.*, 2016). And finally, the addition of biochar to the compost changed the pH leading to a reduction in the activity of the methanogenic microorganisms, this is consistent with the response patterns and data emerging elsewhere (Vu *et al.*, 2015).

It was reported that the biochar addition to chicken manure compost increased the CO₂ emissions by 148% in comparison to the control (Jia *et al.*, 2016). It suggests that because of the high porosity of the biochar the oxygen supply was increased, which benefited aerobic microorganisms. This is a trend that could not be observed in this study, but this might also be the case for pig slurry which is typically produced and retained in a wetter environment than chicken manure. Clearly, swine manure which was the focus of this study differs from chicken manure, but the case highlights the potential for high variability in responses obtained and sets out the challenges in developing and tailoring biochars for defined end uses.

In a similar study, biochars were able to adsorb CO₂ but not CH₄ which may have been a consequence of the competition between the two gases and the pore size of the biochars (Sethupathi *et al.*, 2017). This explanation, together with the reasons given elsewhere, like high porosity and high pH of biochars restricting the activity of methanogenic microorganisms (Jia *et al.*, 2016) may explain the finding in this study. This would mean that if biochars have a certain pore size (0.33 to 0.40 nm) to capture the CH₄ (Adinata, Wan Daud and Aroua, 2007) but also have a large surface area (Figure 18) to bind CO₂

through physisorption and are added to manure which does not allow for a high O₂ intake, CO₂, as well as CH₄ emissions, could be reduced. This model fits with the findings in this study as biochars produced from peat or peat fibre exhibit the highest surface area and the smallest amounts of CO₂ emitted.

As seen in the result sections above the biochars produced in this study react differently to the adsorption of gas onto their surfaces. Peat and peat fibre biochars performed well in the reduction of GHG emissions. These results can be explained by the physicochemical structure of the biochars. Biochars need a certain pore size to capture the CH₄ (Adinata, Wan Daud and Aroua, 2007) as well as large surface areas to bind CO₂ through physisorption. It was noted the biochars produced from peat and peat fibre exhibited this pore size and surface area character.

The focus of this part was to find out if biochars have the potential to reduce emissions from this specific manure. And the results found in this study show that from a technical point of view, biochars can adsorb emissions from this specific manure (Figure 58). Though the economical side has to be evaluated more.

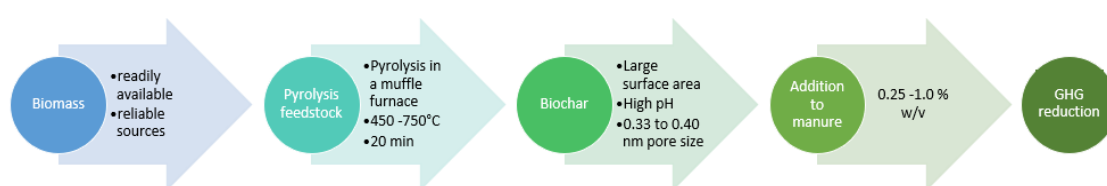


Figure 58: Schematic showing what is needed to reduce GHG emissions through biochar application

5.3. Potential adsorption of organics like dye and therefore potentially other contaminants from water

The data in the literature has shown that both Langmuir and Freundlich can be an analytical fit for dye adsorption onto biochars. In this case, the Langmuir isotherm seems to be a better fit than the Freundlich isotherm (Table 33, Figure 54, Figure 55). The

maximum adsorption capacity (Q_M) for adsorption isotherms of malachite green found in the literature range from 15 to 4117.7 mg g⁻¹ for the Langmuir isotherm (Hameed and El-Khaiary, 2008; Leng et al., 2015; Beakou et al., 2017; Chen et al., 2018; Rawat and Singh, 2018; Yang et al., 2019). The initial concentrations (C_0) vary around 20 - 500 mg L⁻¹ and 0.005 – 2.0 g biochar was used for the experiments reported. The variations in the concentration of dye and the amount and type of biochar used, show again how wide the range of biochar application is and how important it is to add results using less biochar to the knowledge already present. This can help to provide a better understanding of how biochars can be used in the field of adsorption of pollutants.

In the experiments run, the Q_M obtained varies around 7.13 – 47.39 mg g⁻¹. Biochars which have the highest surface area and were therefore thought to be able to adsorb the most dye, do not necessarily have that highest adsorption capacity. The experiments show that biochars with a low surface area were able to adsorb the most dye. These results are supported by the high R^2 numbers. A possible explanation for this is that the biochars with a high surface area have many micropores through which the water solution is not able to enter and therefore the dye is not able to be adsorbed. This shows that biochars produced from fine ugw or b black, which did not perform well at the GHG emission test are better suited to adsorb dye and possibly other pollutants from aqueous solutions, widening the field of application for biochars produced in this study. To adsorb the dye a lower surface area with fewer micropores is considered favourable.

The exemplary plots of the kinetics calculated for biochar produced from fine ugw at 450 °C in a 1 – 10 dilution of malachite green show that there is only a small variance between the results per sample for different dilutions. This applies mostly to the PFO results, while there are slightly bigger differences in the PSO results. Furthermore, PSO seems to be a better fit for the analysed samples as their R^2 values are higher and closer to 1. Something

which also can be observed in the literature (Beakou *et al.*, 2017; Park *et al.*, 2019). Published values for the q_e parameter for PFO and PSO tend to be higher than the ones obtained in this study (Rajgopal *et al.*, 2006; Leng *et al.*, 2015; Beakou *et al.*, 2017; Park *et al.*, 2019). And values for k_1 of 0.006 - 0.35 min^{-1} and for k_2 of 1.144×10^{-6} - 0.27 $\text{g mg}^{-1} \text{min}^{-1}$ for malachite green adsorption have been reported (Leng *et al.*, 2015; Beakou *et al.*, 2017; Chen *et al.*, 2018; Yang *et al.*, 2019), which are lower than the ones calculated in this study. Though the values of q_e obtained here for PFO and PSO are smaller, the R^2 values especially those obtained from PFO are higher which means the PFO and PSO calculated from the kinetics in this study are a better fit for the first and second-order equations than some reported in the literature as the linear relationship is stronger (Leng *et al.*, 2015; Sewu, Boakye and Woo, 2017; Yang *et al.*, 2019).

5.4. Future work

In the future, emission experiments using higher concentrations of biochars could be undertaken to compare and evaluate the results generated in this study and establish an equilibrium point beyond which further addition of biochars would have little effect on the reduction of emissions from swine manure. Additionally, it may be possible to evaluate if the swine manure reacts differently to the biochars throughout the year. Looking at the dye adsorption and the different influences which affect it, a hydrophobicity test could be run to give more insights into how the dye is adsorbed onto the biochars and as well how well they would perform in the water. This could help to explain why some biochars perform better or worse than others. Furthermore, a higher concentration of MG could be used to see how much dye can be adsorbed under different conditions.

6. Conclusion

At the start of this study, the following questions were asked. How does the chemo-physical nature of the Biomass-Biochar production system change when using conventional feedstocks in comparison to a peat-based feedstock from drained Irish ombrotrophic peatlands? Do Peat-based Biochars and Biochar produced from other conventional biomass feedstocks have the potential to control the efflux of carbon dioxide (CO_2), methane (CH_4) and ammonia (NH_3) from swine manure and what are the processes controlling this interaction? And how and to what extent the generated biochars were able to adsorb organics like dye and therefore likely other contaminants from water. The methods and tests used in this work provide a new understanding of the relationship between manure GHG emission control using readily available biochars vs peat-based biochars. The results presented give a deeper insight into how pyrolysis affects the chemo-physical nature of different biomass materials used as feedstock (viz peat, brewery wastes and urban green waste). The biochars produced have been characterised by reference to production systems and their chemo-physical structure. It was shown that thermal treatment increased the pH of the tested materials irrespective of the type of feedstock and irrespective of whether the feedstock was pre-dried or used fresh, making the biochars more alkaline than the original materials. The purity of peat and grain was confirmed as no heavy metals or PAHs were found in the biochars. It was also noted that the biochar surface area increases with treatment temperature, and it was found to be much bigger for peat in comparison to other materials used. Additionally, it was shown that the D/G intensity ratio increases with the treatment temperature which can be used as a screening method for further applications. A reduction of volatile matter content and an increase of the fixed carbon content with rising treatment temperatures was noted to result in more stable biochars, which makes biochars an excellent material to sequester

carbon in comparison to untreated biomass due to their longevity. For biochar applications, stability is a particularly important factor, so higher pyrolysis temperatures for the feedstocks selected are more likely to lead to the production of a more stable product.

Adding to the existing knowledge about biochars, this study suggests that using these feedstock sources with the given characteristics can lead to the production of biochars that can help reduce GHG emissions in piggery manure management. These outcomes are associated with the high pH, surface area and amounts of fixed carbon as well as the low amounts of volatile matter of the biochars which are all favourable characteristics when it comes to GHG emission reduction.

The second question concerned the issue of whether Peat-based Biochars and Biochar produced from other conventional biomass feedstocks have the potential to control the efflux of GHG emissions from swine manure. The results of this study suggest that biochars do have the potential to influence GHG effluxes in piggery management. The emission tests regarding fluxes of CH₄ and CO₂ from this swine manure treated with the designed biochars showed that around 12 to 13 biochars reduced the amount of gases emitted. It was further demonstrated that biochars produced from peat were able to decrease the CH₄ and CO₂ emissions from the manure better than some of the other three materials used. Furthermore, it was noted that by adding biochars produced from peat or peat fibre to the manure system resulted in elevated values for the level of NH₄ remaining in manure after emission trials. In contrast, the biochars produced from the other three materials reduced the level of NH₄ remaining in the manure and therefore promoted NH₃ efflux. These results could be driven by the CEC of the biochars as reported elsewhere (Clough *et al.*, 2013). Though further testing will be required to confirm this proposed explanation.

Finally, this study also sought to examine to what extent the biochars produced for this study could adsorb organics from water. It was shown that the biochars produced in this study were indeed able to adsorb organics from water, giving these biochars a broader spectrum of applications. The detailed analysis of the biochars produced and used in this study helps to understand the way pyrolysis influences the physicochemical properties of biochars. These understandings, also raise the potential for new treatment procedures using biochars that can be developed to address pollutants commonly occurring in liquid manure or water treatment.

To conclude, it can be said that this research has shown that biochars produced from peat and waste materials can reduce GHG emissions from this specific piggery manure as well as adsorb organics like dye from aqueous solutions. This might have the potential for further agricultural applications or the adsorption of other organic contaminants from water. However, the results presented here only apply to this specific manure. To generalise the findings further testing with different manures needs to be done. As well as adsorption of other organics needs to be tested.

References

- Abrishamkesh, S. *et al.* (2015) 'Effects of rice husk biochar application on the properties of alkaline soil and lentil growth', *Plant, Soil and Environment*, 62(11), pp. 475–482. doi: 10.17221/117/2015-PSE.
- Adinata, D., Wan Daud, W. M. A. and Aroua, M. K. (2007) 'Production of carbon molecular sieves from palm shell based activated carbon by pore sizes modification with benzene for methane selective separation', *Fuel Processing Technology*, 88(6), pp. 599–605. doi: 10.1016/j.fuproc.2007.01.009.
- Aguirre-Villegas, H. A. and Larson, R. A. (2017) 'Evaluating greenhouse gas emissions from dairy manure management practices using survey data and lifecycle tools', *Journal of Cleaner Production*, 143, pp. 169–179. doi: 10.1016/j.jclepro.2016.12.133.
- Allen, M. R. *et al.* (2018) *Framing and Context, Global Warming of 1.5°C. An IPCC Special Report on the impacts of global warming of 1.5°C above pre-industrial levels and related global greenhouse gas emission pathways, in the context of strengthening the global response to the threat of climate change.*
- Amin, F. R. *et al.* (2016) 'Biochar applications and modern techniques for characterization', *Clean Technologies and Environmental Policy*, 18(5), pp. 1457–1473. doi: 10.1007/s10098-016-1218-8.
- Angin, D. and Şensöz, S. (2014) 'Effect of Pyrolysis Temperature on Chemical and Surface Properties of Biochar of Rapeseed (*Brassica napus* L.)', *International Journal of Phytoremediation*, 16(7–8), pp. 684–693. doi: 10.1080/15226514.2013.856842.
- Ayawei, N., Ebelegi, A. N. and Wankasi, D. (2017) 'Modelling and Interpretation of Adsorption Isotherms', *Journal of Chemistry*, 2017. doi: 10.1155/2017/3039817.
- Babinszki, B. *et al.* (2021) 'Effect of slow pyrolysis conditions on biocarbon yield and properties: Characterization of the volatiles', *Bioresource Technology*, 338, p. 125567. doi: 10.1016/j.biortech.2021.125567.
- Bahuguna, A., Sharma, S. and Dadarwal, B. K. (2021) 'Biochar as carbon sequestration potential', *Marumegh*, 6(2), pp. 12–14. Available at: <https://www.researchgate.net/publication/351915813>.

Bain, R. L. (2004) ‘An Introduction to Biomass Thermochemical Conversion’, in *(DOE/NASLUGC) Biomass and Solar Energy Workshops*, p. 77. doi: 10.1017/CBO9781107415324.004.

Batista, E. M. C. C. *et al.* (2018) ‘Effect of surface and porosity of biochar on water holding capacity aiming indirectly at preservation of the Amazon biome’, *Scientific Reports*, 8(1), pp. 1–9. doi: 10.1038/s41598-018-28794-z.

Beakou, B. H. *et al.* (2017) ‘A novel biochar from *Manihot esculenta* Crantz waste: Application for the removal of Malachite Green from wastewater and optimization of the adsorption process’, *Water Science and Technology*, 76(6), pp. 1447–1456. doi: 10.2166/wst.2017.332.

BMUV (2020) *Bundes-Bodenschutz- und Altlastenverordnung vom 12. Juli 1999 (BGBl. I S. 1554), die zuletzt durch Artikel 126 der Verordnung vom 19. Juni 2020 (BGBl. I S. 1328 geändert worden ist, Bundesgesetzblatt I.*

Brassard, P. *et al.* (2017) ‘The production of engineered biochars in a vertical auger pyrolysis reactor for carbon sequestration’, *Energies*, 10(288), pp. 8–22. doi: 10.3390/en10030288.

Brassard, P., Godbout, S. and Raghavan, V. (2016) ‘Soil biochar amendment as a climate change mitigation tool: Key parameters and mechanisms involved’, *Journal of Environmental Management*, 181, pp. 484–497. doi: 10.1016/j.jenvman.2016.06.063.

Brennan, R. B. *et al.* (2015) ‘The effect of chemical amendments used for phosphorus abatement on greenhouse gas and ammonia emissions from dairy cattle slurry: Synergies and pollution swapping’, *PLoS ONE*, 10(6), pp. 1–20. doi: 10.1371/journal.pone.0111965.

Bundesministerium für Ernährung und Landwirtschaft (2021) *Verordnung über die Anwendung von Kultursubstraten und Pflanzenhilfsmitteln nach den Grundsätzen der guten fachlichen Praxis beim Düngen (Düngeverordnung - DüV)*. Available at: https://www.gesetze-im-internet.de/bundesrecht/d_v/gesamt.pdf.

Buss, W. *et al.* (2016) ‘Strategies for producing biochars with minimum PAH contamination’, *Journal of Analytical and Applied Pyrolysis*, 119, pp. 24–30. doi: 10.1016/j.jaap.2016.04.001.

- Buss, W. and Mašek, O. (2014) 'Mobile organic compounds in biochar - A potential source of contamination - Phytotoxic effects on cress seed (*Lepidium sativum*) germination', *Journal of Environmental Management*, 137, pp. 111–119. doi: 10.1016/j.jenvman.2014.01.045.
- Cabriga, C. K. C. *et al.* (2021) 'Evaluation of biochar derived from the slow pyrolysis of rice straw as a potential adsorbent for carbon dioxide', *Biomass Conversion and Biorefinery*. doi: 10.1007/s13399-021-01719-z.
- Cai, J. *et al.* (2017) 'Review of physicochemical properties and analytical characterization of lignocellulosic biomass', *Renewable and Sustainable Energy Reviews*, 76(October), pp. 309–322. doi: 10.1016/j.rser.2017.03.072.
- Cancelliere, R. *et al.* (2019) 'Biochar from brewers' spent grain: A green and low-cost smart material to modify screen-printed electrodes', *Biosensors*, 9(4). doi: 10.3390/bios9040139.
- Cantrell, K. B. *et al.* (2012) 'Impact of pyrolysis temperature and manure source on physicochemical characteristics of biochar', *Bioresource Technology*, 107, pp. 419–428. doi: 10.1016/j.biortech.2011.11.084.
- Chan, K. Y. and Xu, Z. (2009) 'Biochar: Nutrient Properties and Their Enhancement', in *Biochar for environmental management: Science and Technology*, pp. 67–84.
- Chan, L. S. *et al.* (2012) 'Error analysis of adsorption isotherm models for acid dyes onto bamboo derived activated carbon', *Chinese Journal of Chemical Engineering*, 20(3), pp. 535–542. doi: 10.1016/S1004-9541(11)60216-4.
- Chen, W. *et al.* (2017) 'Effects of different types of biochar on methane and ammonia mitigation during layer manure composting', *Waste Management*, 61, pp. 506–515. doi: 10.1016/j.wasman.2017.01.014.
- Chen, Y. *et al.* (2017) 'The structure evolution of biochar from biomass pyrolysis and its correlation with gas pollutant adsorption performance', *Bioresource Technology*, 246(August), pp. 101–109. doi: 10.1016/j.biortech.2017.08.138.
- Chen, Y. di *et al.* (2018) 'Highly efficient adsorption of dyes by biochar derived from pigments-extracted macroalgae pyrolyzed at different temperature', *Bioresource Technology*, 259, pp. 104–110. doi: 10.1016/j.biortech.2018.02.094.

- Chia, C. H. *et al.* (2012) 'Imaging of mineral-enriched biochar by FTIR, Raman and SEM-EDX', *Vibrational Spectroscopy*, 62, pp. 248–257. doi: 10.1016/j.vibspec.2012.06.006.
- Chowdhury, Z. Z. *et al.* (2016) 'Influence of carbonization temperature on physicochemical properties of biochar derived from slow pyrolysis of durian wood (*Durio zibethinus*) sawdust', *BioResources*, 11(2), pp. 3356–3372. doi: 10.15376/biores.11.2.3356-3372.
- Clough, T. J. *et al.* (2013) 'A review of biochar and soil nitrogen dynamics', *Agronomy*, 3, pp. 275–293. doi: 10.3390/agronomy3020275.
- Cowie, A. *et al.* (2015) 'Biochar, carbon accounting and climate change', in *Biochar for environmental management: Science, Technology and Implementation*, pp. 763–794.
- Dejene, D. and Tilahun, E. (2020) 'Characterization of Biochar Produced from Different Feed Stocks', *Asian Journal of Environment & Ecology*, (March), pp. 1–6. doi: 10.9734/ajee/2020/v12i130147.
- Dennehy, C. *et al.* (2016) 'Synergism and effect of high initial volatile fatty acid concentrations during food waste and pig manure anaerobic co-digestion', *Waste Management*, 56, pp. 173–180. doi: 10.1016/j.wasman.2016.06.032.
- Department of Agriculture, F. and the M. (2018) *Nitrates explanatory handbook for Good Agricultural Practice for the Protection of Waters Regulations 2018*.
- Dieguez-Alonso, A. *et al.* (2018) 'Towards biochar and hydrochar engineering-influence of process conditions on surface physical and chemical properties, thermal stability, nutrient availability, toxicity and wettability', *Energies*, 11(496). doi: 10.3390/en11030496.
- Dissanayake, P. D. *et al.* (2020) 'Biochar-based adsorbents for carbon dioxide capture: A critical review', *Renewable and Sustainable Energy Reviews*, 119, p. 109582. doi: 10.1016/j.rser.2019.109582.
- Domingues, R. R. *et al.* (2017) 'Properties of biochar derived from wood and high-nutrient biomasses with the aim of agronomic and environmental benefits', *PLoS ONE*, 12(5), pp. 1–19. doi: 10.1371/journal.pone.0176884.

Duffy, P. *et al.* (2021) *Ireland National Inventory Report 2021- GREENHOUSE GAS EMISSIONS 1990 - 2019 REPORTED TO THE UNITED NATIONS FRAMEWORK CONVENTION ON CLIMATE CHANGE*.

EBC (2012) *European Biochar Certificate - Guidelines for a Sustainable Production of Biochar*, European Biochar Foundation (EBC), Arbaz, Switzerland. doi: 10.13140/RG.2.1.4658.7043.

EBC (2012-2022) (2022) 'European Biochar Certificate - Guidelines for a Sustainable Production of Biochar', 10.1(January).

Enders, A. *et al.* (2012) 'Characterization of biochars to evaluate recalcitrance and agronomic performance', *Bioresource Technology*, 114, pp. 644–653. doi: 10.1016/j.biortech.2012.03.022.

European Parliament (2022) *Circular economy: definition, importance and benefits*. Available at: <https://www.europarl.europa.eu/news/en/headlines/economy/20151201STO05603/circular-economy-definition-importance-and-benefits#:~:text=The circular economy is a model of production,way%2C the life cycle of products is extended.>

Eurostat (2020) *Agriculture, forestry and fishery statistics: 2020 edition*, Publications Office of the European Union.

Eyring, V. *et al.* (2021) 'Human Influence on the Climate System', in *Climate Change 2021: The Physical Science Basis. Contribution of Working Group I to the Sixth Assessment Report of the Intergovernmental Panel on Climate Change [Masson-Delmotte, V., P. Zhai, A. Pirani, S.L. Connors, C. Péan, S. Berger, N. Caud, Y. Chen, . Cambridge University Press, Cambridge, United Kingdom and New York, NY, USA, pp. 423–552. doi: 10.1017/9781009157896.005.423.*

Feola Conz, R. *et al.* (2017) 'Effect of Pyrolysis Temperature and Feedstock Type on Agricultural Properties and Stability of Biochars', *Agricultural Sciences*, 08(09), pp. 914–933. doi: 10.4236/as.2017.89067.

Fidel, R. B. *et al.* (2017) 'Characterization and quantification of biochar alkalinity', *Chemosphere*, 167, pp. 367–373. doi: 10.1016/j.chemosphere.2016.09.151.

Frišták, V., Pipiška, M. and Soja, G. (2018) 'Pyrolysis treatment of sewage sludge: A

promising way to produce phosphorus fertilizer', *Journal of Cleaner Production*, 172, pp. 1772–1778. doi: 10.1016/j.jclepro.2017.12.015.

Gai, X. *et al.* (2014) 'Effects of feedstock and pyrolysis temperature on biochar adsorption of ammonium and nitrate', *PLoS ONE*, 9(12). doi: 10.1371/journal.pone.0113888.

Girardello, F. *et al.* (2013) 'Characterization of Brazilian peat samples by applying a multimethod approach', *Spectroscopy Letters*, 46(3), pp. 201–210. doi: 10.1080/00387010.2012.702184.

Greco, G. *et al.* (2020) 'Effects of slow-pyrolysis conditions on the products yields and properties and on exergy efficiency: A comprehensive assessment for wheat straw', *Applied Energy*, 279, p. 115842. doi: 10.1016/j.apenergy.2020.115842.

Gronwald, M. *et al.* (2018) 'Application of hydrochar and pyrochar to manure is not effective for mitigation of ammonia emissions from cattle slurry and poultry manure', *Biology and Fertility of Soils*, 54(4), pp. 451–465. doi: 10.1007/s00374-018-1273-x.

Guizani, C. *et al.* (2017) 'New insights on the structural evolution of biomass char upon pyrolysis as revealed by the Raman spectroscopy and elemental analysis', *Carbon*, 119, pp. 519–521. doi: 10.1016/j.carbon.2017.04.078.

Guo, J. *et al.* (2021) 'Effects of various pyrolysis conditions and feedstock compositions on the physicochemical characteristics of cow manure-derived biochar', *Journal of Cleaner Production*, 311, p. 127458. doi: 10.1016/j.jclepro.2021.127458.

Hameed, B. H. and El-Khaiary, M. I. (2008) 'Kinetics and equilibrium studies of malachite green adsorption on rice straw-derived char', *Journal of Hazardous Materials*, 153, pp. 701–708. doi: 10.1016/j.jhazmat.2007.09.019.

Han, H. *et al.* (2022) 'Contaminants in biochar and suggested mitigation measures – a review', *Chemical Engineering Journal*, 429(132287). doi: 10.1016/j.cej.2021.132287.

Hani, C. *et al.* (2012) 'Amendment of biochar to slurry: A possibility to mitigate ammonia emissions?', *Emission of Gas and Dust from Livestock – Saint-Malo, France – June 10-13, 2012*, 24, p. 4pp. Available at:

https://www.hafl.bfh.ch/fileadmin/docs/Forschung_Dienstleistungen/Agrarwissenschaften/Nachhaltigkeitsbeurteilung/DUE_Art_EMILI_fulltextC.Haeni.pdf.

- He, X. *et al.* (2018) 'Effects of pyrolysis temperature on the physicochemical properties of gas and biochar obtained from pyrolysis of crop residues', *Energy*, 143, pp. 746–756. doi: 10.1016/j.energy.2017.11.062.
- Hernandez-Soriano, M. C. *et al.* (2016) 'Biochar affects carbon composition and stability in soil: A combined spectroscopy-microscopy study', *Scientific Reports*, 6(October 2015), pp. 1–13. doi: 10.1038/srep25127.
- Hilber, I. *et al.* (2012) 'Quantitative determination of PAHs in biochar: A prerequisite to ensure its quality and safe application', *Journal of Agricultural and Food Chemistry*, 60(12), pp. 3042–3050. doi: 10.1021/jf205278v.
- Hilber, I. *et al.* (2017) 'Bioavailability and bioaccessibility of polycyclic aromatic hydrocarbons from (post-pyrolytically treated) biochars', *Chemosphere*, 174, pp. 700–707. doi: 10.1016/j.chemosphere.2017.02.014.
- Holly, M. A. *et al.* (2017) 'Greenhouse gas and ammonia emissions from digested and separated dairy manure during storage and after land application', *Agriculture, Ecosystems and Environment*, 239, pp. 410–419. doi: 10.1016/j.agee.2017.02.007.
- Honda, M. and Suzuki, N. (2020) 'Toxicities of polycyclic aromatic hydrocarbons for aquatic animals', *International Journal of Environmental Research and Public Health*, 17(4). doi: 10.3390/ijerph17041363.
- Hu, X. *et al.* (2019) 'Pyrolysis of different wood species: Impacts of C/H ratio in feedstock on distribution of pyrolysis products', *Biomass and Bioenergy*, 120(November 2018), pp. 28–39. doi: 10.1016/j.biombioe.2018.10.021.
- Huang, Y. *et al.* (2018) 'Lignin Content of Agro-forestry Biomass Negatively Affects the Resultant Biochar pH', *BioResources*, 13(3), pp. 5153–5163. Available at: http://stargate.cnr.ncsu.edu/index.php/BioRes/article/view/BioRes_13_3_5153_Huang_Lignin_Content_Agro_Forestry_Biomass.
- Hung, C. Y. *et al.* (2017) 'Characterization of biochar prepared from biogas digestate', *Waste Management*, 66, pp. 53–60. doi: 10.1016/j.wasman.2017.04.034.
- International Biochar Initiative (2015) 'Standardized Product Definition and Product Testing Guidelines for Biochar That Is Used in Soil', *International Biochar Initiative*, (November), p. 23. doi: 10.1016/j.zefq.2013.07.002.

International Biochar Initiative (2018) *No Title*.

IPCC (2019) *2019 Refinement to the 2006 IPCC Guidelines for National Greenhouse Gas Inventories, Volume 4: Agriculture, Forestry and Other Land Use: Emissions From Livestock and Manure Management*. Available at: <http://www.ipcc-nggip.iges.or.jp/public/2006gl/index.html>.

Ippolito, J. A. *et al.* (2016) 'Hardwood biochar and manure co-application to a calcareous soil', *Chemosphere*, 142, pp. 84–91. doi: 10.1016/j.chemosphere.2015.05.039.

Janczak, D. *et al.* (2017) 'Biochar to reduce ammonia emissions in gaseous and liquid phase during composting of poultry manure with wheat straw', *Waste Management*, 66, pp. 36–45. doi: 10.1016/j.wasman.2017.04.033.

Jeong, Y., Lee, Y. E. and Kim, I. T. (2020) 'Characterization of sewage sludge and food waste-based biochar for co-firing in a coal-fired power plant: A case study in Korea', *Sustainability*, 12, p. 9411. doi: 10.3390/su12229411.

Ji, B. *et al.* (2019) 'Adsorption of Methylene Blue onto Novel Biochars Prepared from *Magnolia grandiflora* Linn Fallen Leaves at Three Pyrolysis Temperatures', *Water, Air, and Soil Pollution*, 230(12), p. 2022. doi: 10.1007/s11270-019-4330-7.

Jia, X. *et al.* (2016) 'The Influence of Biochar Addition on Chicken Manure Composting and Associated Methane and Carbon Dioxide Emissions', *BioResources*, 11(2), pp. 5255–5264. doi: 10.1177/107110079601701211.

Jia, X., Yuan, W. and Ju, X. (2015) 'Short Report: Effects of Biochar Addition on Manure Composting and Associated N₂O Emissions', *Journal of Sustainable Bioenergy Systems*, 05(June), pp. 56–61. doi: 10.4236/jsbs.2015.52005.

Jindo, K. *et al.* (2014) 'Physical and chemical characterization of biochars derived from different agricultural residues', *Biogeosciences*, 11(23), pp. 6613–6621. doi: 10.5194/bg-11-6613-2014.

Jirka, S. and Tomlinson, T. (2014) '2013 State of the Biochar Industry: A Survey of Commercial Activity in the Biochar Field - A report by the International Biochar Initiative (IBI)', (March). doi: 10.13140/2.1.3807.1369.

- Kamali, M. *et al.* (2021) 'Biochar in water and wastewater treatment - a sustainability assessment', *Chemical Engineering Journal*, 420(P1), p. 129946. doi: 10.1016/j.cej.2021.129946.
- Kammann, C. *et al.* (2017) 'Biochar as a tool to reduce the agricultural greenhouse-gas burden – knowns, unknowns and future research needs', *Journal of Environmental Engineering and Landscape Management*, 25(2), pp. 114–139. doi: 10.3846/16486897.2017.1319375.
- Kamran, M. A. *et al.* (2018) 'Amelioration of soil acidity, Olsen-P, and phosphatase activity by manure- and peat-derived biochars in different acidic soils', *Arabian Journal of Geosciences*, 11(11). doi: 10.1007/s12517-018-3616-1.
- Kern, J. *et al.* (2017) 'Synergistic use of peat and charred material in growing media – an option to reduce the pressure on peatlands?', *Journal of Environmental Engineering and Landscape Management*, 25(2), pp. 160–174. doi: 10.3846/16486897.2017.1284665.
- Kim, J., Lee, S. S. and Khim, J. (2019) 'Peat moss-derived biochars as effective sorbents for VOCs' removal in groundwater', *Environmental Geochemistry and Health*, 41(4), pp. 1637–1646. doi: 10.1007/s10653-017-0012-9.
- Lee, J. *et al.* (2017) 'Effects of carbon dioxide on pyrolysis of peat', *Energy*, 120, pp. 929–936. doi: 10.1016/j.energy.2016.11.143.
- Lehmann, J. (2007) 'A handful of carbon', *Nature*, 447(7141), pp. 143–144. doi: 10.1038/447143a.
- Lehmann, J. *et al.* (2009) 'Stability of biochar in soil', in *Biochar for Environmental Management: Science and Technology*, pp. 183–206.
- Lehmann, Johannes and Joseph, S. (2009) *Biochar for Environmental Management: Science and Technology*, *Biochar for Environmental Management: Science and Technology*. doi: 10.4324/9781849770552.
- Lehmann, J. and Joseph, S. (2009) 'Biochar systems', in *Biochar for Environmental Management: Science and Technology*, pp. 147–168.
- Lehmann, J. and Joseph, S. (2015) 'Biochar for environmental management: An

introduction’, in *Biochar for Environmental Management: Science and Technology*, pp. 1–13. doi: 10.4324/9781849770552.

Leng, L. *et al.* (2015) ‘Surface characterization of rice husk bio-char produced by liquefaction and application for cationic dye (Malachite green) adsorption’, *Fuel*, 155, pp. 77–85. doi: 10.1016/j.fuel.2015.04.019.

Leng, L. *et al.* (2019) ‘Biochar stability assessment methods: A review’, *Science of the Total Environment*, 647, pp. 210–222. doi: 10.1016/j.scitotenv.2018.07.402.

Leng, L. *et al.* (2021) ‘An overview on engineering the surface area and porosity of biochar’, *Science of the Total Environment*, 763, p. 144204. doi: 10.1016/j.scitotenv.2020.144204.

Li, S. *et al.* (2018) ‘Nitrogen retention of biochar derived from different feedstocks at variable pyrolysis temperatures’, *Journal of Analytical and Applied Pyrolysis*, 133(March), pp. 136–146. doi: 10.1016/j.jaap.2018.04.010.

Li, S. *et al.* (2019) ‘Predicting biochar properties and functions based on feedstock and pyrolysis temperature: A review and data syntheses’, *Journal of Cleaner Production*, 215, pp. 890–902. doi: 10.1016/j.jclepro.2019.01.106.

Li, Y. *et al.* (2020) ‘A critical review of the production and advanced utilization of biochar via selective pyrolysis of lignocellulosic biomass’, *Bioresource Technology*, 312(March), p. 123614. doi: 10.1016/j.biortech.2020.123614.

Liu, L. *et al.* (2019) ‘Application of Nanotechnology in the Removal of Heavy Metal From Water’, in Luo, X. and Deng, F. (eds) *Micro and Nano Technologies, Nanomaterials for the Removal of Pollutants and Resource Reutilization*. Elsevier, pp. 83–147. doi: doi.org/10.1016/B978-0-12-814837-2.00004-4.

Luo, F. *et al.* (2014) ‘Characterization of contaminants and evaluation of the suitability for land application of maize and sludge biochars’, *Environmental Science and Pollution Research*, 21(14), pp. 8707–8717. doi: 10.1007/s11356-014-2797-8.

M.R. Yadav, R. K. Y. *et al.* (2017) ‘Role of Biochar in Mitigation of Climate Change through Carbon Sequestration’, *International Journal of Current Microbiology and Applied Sciences*, 6(4), pp. 859–866. doi: 10.20546/ijcmas.2017.604.107.

Malińska, K. *et al.* (2014) 'Effects of biochar amendment on ammonia emission during composting of sewage sludge', *Ecological Engineering*, 71, pp. 474–478. doi: 10.1016/j.ecoleng.2014.07.012.

Martin, S. L. *et al.* (2015) 'Biochar-mediated reductions in greenhouse gas emissions from soil amended with anaerobic digestates', *Biomass and Bioenergy*, 79, pp. 39–49. doi: 10.1016/j.biombioe.2015.04.030.

Mašek, O. *et al.* (2013) 'Influence of production conditions on the yield and environmental stability of biochar', *Fuel*, 103, pp. 151–155. doi: 10.1016/j.fuel.2011.08.044.

Mašek, O. *et al.* (2018) 'Consistency of biochar properties over time and production scales: A characterisation of standard materials', *Journal of Analytical and Applied Pyrolysis*, 132(February), pp. 200–210. doi: 10.1016/j.jaap.2018.02.020.

Maziarka, P. *et al.* (2021) 'Do you BET on routine? The reliability of N₂ physisorption for the quantitative assessment of biochar's surface area', *Chemical Engineering Journal*, 418(December 2020). doi: 10.1016/j.cej.2021.129234.

McCarl, B. A. *et al.* (2009) 'Economics of Biochar Production, Utilization and Greenhouse Gas Offsets', in *Biochar for environmental management: Science and Technology*, pp. 341–358.

McGeever, A. H. *et al.* (2018) 'Assessing the terrestrial capacity for Negative Emission Technologies at a small developed nation scale', *Carbon Management*, 0(0), pp. 1–20. doi: 10.1080/17583004.2018.1537516.

Mendonça, F. G. de *et al.* (2017) 'Tuning the surface properties of biochar by thermal treatment', *Bioresource Technology*, 246(July), pp. 28–33. doi: 10.1016/j.biortech.2017.07.099.

Mohanty, P. *et al.* (2013) 'Evaluation of the physiochemical development of biochars obtained from pyrolysis of wheat straw, timothy grass and pinewood: Effects of heating rate', *Journal of Analytical and Applied Pyrolysis*, 104, pp. 485–493. doi: 10.1016/j.jaap.2013.05.022.

Nair, R. R., Mondal, M. M. and Weichgrebe, D. (2020) 'Biochar from co-pyrolysis of urban organic wastes—investigation of carbon sink potential using ATR-FTIR and

TGA', *Biomass Conversion and Biorefinery*. doi: 10.1007/s13399-020-01000-9.

Novak, J. M. *et al.* (2009) 'Impact of biochar amendment on fertility of a southeastern coastal plain soil', *Soil Science*, 174(2), pp. 105–112. doi: 10.1097/SS.0b013e3181981d9a.

Oliveira, F. R. *et al.* (2017) 'Environmental application of biochar: Current status and perspectives', *Bioresource Technology*, 246(July), pp. 110–122. doi: 10.1016/j.biortech.2017.08.122.

Olszewski, M. P. *et al.* (2019) 'Pyrolysis kinetics of hydrochars produced from brewer's spent grains', *Catalysts*, 9(625). doi: 10.3390/catal9070625.

Onorevoli, B. *et al.* (2018) 'Characterization of feedstock and biochar from energetic tobacco seed waste pyrolysis and potential application of biochar as an adsorbent', *Journal of Environmental Chemical Engineering*, 6(1), pp. 1279–1287. doi: 10.1016/j.jece.2018.01.039.

Panwar, N. L., Pawar, A. and Salvi, B. L. (2019) 'Comprehensive review on production and utilization of biochar', *SN Applied Sciences*, 1(2). doi: 10.1007/s42452-019-0172-6.

Pariyar, P. *et al.* (2020) 'Evaluation of change in biochar properties derived from different feedstock and pyrolysis temperature for environmental and agricultural application', *Science of the Total Environment*, 713, p. 136433. doi: 10.1016/j.scitotenv.2019.136433.

Park, J. H. *et al.* (2019) 'Adsorption/desorption behavior of cationic and anionic dyes by biochars prepared at normal and high pyrolysis temperatures', *Colloids and Surfaces A: Physicochemical and Engineering Aspects*, 572, pp. 274–282. doi: 10.1016/j.colsurfa.2019.04.029.

Patel, A. B. *et al.* (2020) 'Polycyclic Aromatic Hydrocarbons: Sources, Toxicity, and Remediation Approaches', *Frontiers in Microbiology*, 11(562813). doi: 10.3389/fmicb.2020.562813.

Potgieter-Vermaak, S. *et al.* (2011) 'Raman spectroscopy for the analysis of coal: A review', *Journal of Raman Spectroscopy*, 42(2), pp. 123–129. doi: 10.1002/jrs.2636.

Qadeer, S. *et al.* (2017) 'A Dialogue on Perspectives of Biochar Applications and Its

Environmental Risks', *Water, Air, and Soil Pollution*, 228(8). doi: 10.1007/s11270-017-3428-z.

Qambrani, N. A. *et al.* (2017) 'Biochar properties and eco-friendly applications for climate change mitigation, waste management, and wastewater treatment: A review', *Renewable and Sustainable Energy Reviews*, 79(May), pp. 255–273. doi: 10.1016/j.rser.2017.05.057.

Rajgopal, S. *et al.* (2006) 'Utilization of fluidized bed reactor for the production of adsorbents in removal of malachite green', *Chemical Engineering Journal*, 116, pp. 211–217. doi: 10.1016/j.cej.2005.09.026.

Rathnayake, D. *et al.* (2020) 'How to trace back an unknown production temperature of biochar from chemical characterization methods in a feedstock independent way', *Journal of Analytical and Applied Pyrolysis*, 151, p. 104926. doi: 10.1016/j.jaap.2020.104926.

Rawat, A. P. and Singh, D. P. (2018) 'Decolourization of malachite green dye by mentha plant biochar (MPB): A combined action of adsorption and electrochemical reduction processes', *Water Science and Technology*, 77(6), pp. 1734–1743. doi: 10.2166/wst.2018.059.

Riley, J. T. (2007) *Routine Coal and Coke Analysis: Collection, Interpretation, and Use of Analytical Data*, *Routine Coal and Coke Analysis: Collection, Interpretation, and Use of Analytical Data*. doi: 10.1520/stp192-eb.

Rodriguez Correa, C. *et al.* (2019) 'Pyrolysis vs. hydrothermal carbonization: Understanding the effect of biomass structural components and inorganic compounds on the char properties', *Journal of Analytical and Applied Pyrolysis*, 140(August 2018), pp. 137–147. doi: 10.1016/j.jaap.2019.03.007.

Rodriguez, J. A. *et al.* (2020) 'Influence of pyrolysis temperature and feedstock on the properties of biochars produced from agricultural and industrial wastes', *Journal of Analytical and Applied Pyrolysis*, 149, p. 104839. doi: 10.1016/j.jaap.2020.104839.

Ronsse, F. *et al.* (2013) 'Production and characterization of slow pyrolysis biochar: Influence of feedstock type and pyrolysis conditions', *GCB Bioenergy*, 5(2), pp. 104–115. doi: 10.1111/gcbb.12018.

Sadasivam, B. Y. and Reddy, K. R. (2015) 'Adsorption and transport of methane in biochars derived from waste wood', *Waste Management*, 43, pp. 218–229. doi: 10.1016/j.wasman.2015.04.025.

Schmidt, H.-P. (2012) '55 Uses of Biochar', *Ithaka Journal*, 289, pp. 273–276.

Sethupathi, S. *et al.* (2017) 'Biochars as potential adsorbers of CH₄, CO₂ and H₂S', *Sustainability (Switzerland)*, 9(1), pp. 1–10. doi: 10.3390/su9010121.

Sewu, D. D., Boakye, P. and Woo, S. H. (2017) 'Highly efficient adsorption of cationic dye by biochar produced with Korean cabbage waste', *Bioresource Technology*, 224, pp. 206–213. doi: 10.1016/j.biortech.2016.11.009.

Shackley, S. and Sohi, S. (2010) 'An assessment of the benefits and issues associated with the application of biochar to soil', *A report commissioned by the United Kingdom Department for Environment, Food and Rural Affairs, and Department of Energy and Climate Change*, pp. 1–132. doi: 10.13140/2.1.3807.1369.

Singh, E. *et al.* (2022) 'Circular economy-based environmental management using biochar: Driving towards sustainability', *Process Safety and Environmental Protection*, 163(March), pp. 585–600. doi: 10.1016/j.psep.2022.05.056.

Smith, M. W. *et al.* (2016) 'Structural analysis of char by Raman spectroscopy: Improving band assignments through computational calculations from first principles', *Carbon*, 100, pp. 678–692. doi: 10.1016/j.carbon.2016.01.031.

Sperandio, G. *et al.* (2017) 'Increasing the value of spent grain from craft microbreweries for energy purposes', *Chemical Engineering Transactions*, 58(August), pp. 487–492. doi: 10.3303/CET1758082.

Stefaniuk, M. and Oleszczuk, P. (2015) 'Characterization of biochars produced from residues from biogas production', *Journal of Analytical and Applied Pyrolysis*, 115, pp. 157–165. doi: 10.1016/j.jaap.2015.07.011.

Stefaniuk, M., Oleszczuk, P. and Bartmiński, P. (2016) 'Chemical and ecotoxicological evaluation of biochar produced from residues of biogas production', *Journal of Hazardous Materials*, 318, pp. 417–424. doi: 10.1016/j.jhazmat.2016.06.013.

Steiner, C. *et al.* (2010) 'Reducing Nitrogen Loss during Poultry Litter Composting

Using Biochar', *Journal of Environmental Quality*, 39(4), pp. 1236–1242. doi: 10.2134/jeq2009.0337.

Stella Mary, G. *et al.* (2016) 'Production, characterization and evaluation of biochar from pod (*Pisum sativum*), leaf (*Brassica oleracea*) and peel (*Citrus sinensis*) wastes', *International Journal of Recycling of Organic Waste in Agriculture*, 5(1), pp. 43–53. doi: 10.1007/s40093-016-0116-8.

Suliman, W. *et al.* (2016) 'Influence of feedstock source and pyrolysis temperature on biochar bulk and surface properties', *Biomass and Bioenergy*, 84, pp. 37–48. doi: 10.1016/j.biombioe.2015.11.010.

Sumalinog, D. A. G., Capareda, S. C. and de Luna, M. D. G. (2018) 'Evaluation of the effectiveness and mechanisms of acetaminophen and methylene blue dye adsorption on activated biochar derived from municipal solid wastes', *Journal of Environmental Management*, 210, pp. 255–262. doi: 10.1016/j.jenvman.2018.01.010.

Sutcu, H. (2007) 'Pyrolysis of peat: Product yield and characterization', *Korean Journal of Chemical Engineering*, 24(5), pp. 736–741. doi: 10.1007/s11814-007-0035-5.

Taherymoosavi, S. *et al.* (2017) 'Characterization of organic compounds in biochars derived from municipal solid waste', *Waste Management*, 67, pp. 131–142. doi: 10.1016/j.wasman.2017.05.052.

Tanneberger, F. *et al.* (2017) 'The peatland map of Europe', *Mires and Peat*, 19(2015), pp. 1–18. doi: 10.19189/MaP.2016.OMB.264.

Tasim, B. *et al.* (2019) 'Quality Evaluation of Biochar Prepared from Different Agricultural Residues', *Sarhad Journal of Agriculture*, 35(1). doi: 10.17582/journal.sja/2019/35.1.134.143.

The global goals (2022) *The 17 goals*. Available at: <https://www.globalgoals.org/goals/>.

Troy, S. M. *et al.* (2013) 'Impact of biochar addition to soil on greenhouse gas emissions following pig manure application', *Soil Biology and Biochemistry*, 60(2013), pp. 173–181. doi: 10.1016/j.soilbio.2013.01.019.

UNFCCC Process (2007) *Global Warming Potentials (IPCC Fourth Assessment Report)*. Available at: <https://unfccc.int/process-and-meetings/transparency-and->

reporting/greenhouse-gas-data/frequently-asked-questions/global-warming-potentials-ipcc-fourth-assessment-report.

Vu, Q. D. *et al.* (2015) 'Greenhouse gas emissions from passive composting of manure and digestate with crop residues and biochar on small-scale livestock farms in Vietnam', *Environmental Technology (United Kingdom)*, 36(23), pp. 2924–2935. doi: 10.1080/09593330.2014.960475.

Wang, C. *et al.* (2013) 'Insight into the effects of biochar on manure composting: Evidence supporting the relationship between N₂O emission and denitrifying community', *Environmental Science and Technology*, 47(13), pp. 7341–7349. doi: 10.1021/es305293h.

Wang, G. *et al.* (2018) 'Structural features and gasification reactivity of biomass chars pyrolyzed in different atmospheres at high temperature', *Energy*, 147, pp. 25–35. doi: 10.1016/j.energy.2018.01.025.

Wang, J. and Wang, S. (2019) 'Preparation, modification and environmental application of biochar: A review', *Journal of Cleaner Production*, 227, pp. 1002–1022. doi: 10.1016/j.jclepro.2019.04.282.

Wang, S. *et al.* (2017) 'A novel peat biochar supported catalyst for the transesterification reaction', *Energy Conversion and Management*, 139, pp. 89–96. doi: 10.1016/j.enconman.2017.02.039.

Weidemann, E. *et al.* (2018) 'Influence of pyrolysis temperature and production unit on formation of selected PAHs, oxy-PAHs, N-PACs, PCDDs, and PCDFs in biochar—a screening study', *Environmental Science and Pollution Research*, 25, pp. 3941–3942. doi: 10.1007/s11356-017-0804-6.

Windeatt, J. H. *et al.* (2014) 'Characteristics of biochars from crop residues: Potential for carbon sequestration and soil amendment', *Journal of Environmental Management*, 146, pp. 189–197. doi: 10.1016/j.jenvman.2014.08.003.

Woolf, D. *et al.* (2010) 'Sustainable biochar to mitigate global climate change', *nature communications*, 1(1). doi: 10.1038/ncomms1053.

Xiaofeng, B. *et al.* (2017) 'Properties and applications of biochars derived from different biomass feedstock sources', *International Journal of Agricultural and*

Biological Engineering, 10(2), pp. 242–250. doi: 10.3965/j.ijabe.20171002.2878.

Xie, S. *et al.* (2017) ‘A pilot scale study on synergistic effects of co-digestion of pig manure and grass silage’, *International Biodeterioration and Biodegradation*, 123, pp. 244–250. doi: 10.1016/j.ibiod.2017.07.005.

Xu, J. *et al.* (2020) ‘Raman spectroscopy of biochar from the pyrolysis of three typical Chinese biomasses: A novel method for rapidly evaluating the biochar property’, *Energy*, 202, p. 117644. doi: 10.1016/j.energy.2020.117644.

Yang, H. *et al.* (2016) ‘Biomass-Based Pyrolytic Polygeneration System for Bamboo Industry Waste: Evolution of the Char Structure and the Pyrolysis Mechanism’, *Energy and Fuels*, 30(8), pp. 6430–6439. doi: 10.1021/acs.energyfuels.6b00732.

Yang, S. S. *et al.* (2019) ‘Generation of high-efficient biochar for dye adsorption using frass of yellow mealworms (larvae of *Tenebrio molitor* Linnaeus) fed with wheat straw for insect biomass production’, *Journal of Cleaner Production*, 227, pp. 33–47. doi: 10.1016/j.jclepro.2019.04.005.

Yang, Y. *et al.* (2020) ‘Compost supplementation with nitrogen loss and greenhouse gas emissions during pig manure composting’, *Bioresource Technology*, 297(September), p. 122435. doi: 10.1016/j.biortech.2019.122435.

Yinxin, Z., Jishi, Z. and Yi, M. (2015) ‘Preparation and Application of Biochar from Brewery’s Spent Grain and Sewage Sludge’, *The Open Chemical Engineering Journal*, 9(1), pp. 14–19. doi: 10.2174/1874123101509010014.

Yu, J. *et al.* (2018) ‘Influence of temperature and particle size on structural characteristics of chars from Beechwood pyrolysis’, *Journal of Analytical and Applied Pyrolysis*, 130(August 2017), pp. 249–255. doi: 10.1016/j.jaap.2018.01.018.

Zaccone, C., Miano, T. M. and Shotyk, W. (2007) ‘Qualitative comparison between raw peat and related humic acids in an ombrotrophic bog profile’, *Organic Geochemistry*, 38(1), pp. 151–160. doi: 10.1016/j.orggeochem.2006.06.023.

Zhang, H. *et al.* (2017) ‘Effect of feedstock and pyrolysis temperature on properties of biochar governing end use efficacy’, *Biomass and Bioenergy*, 105, pp. 136–146. doi: 10.1016/j.biombioe.2017.06.024.

Zhang, X. *et al.* (2020) 'Effect of pyrolysis temperature and correlation analysis on the yield and physicochemical properties of crop residue biochar', *Bioresource Technology*, 296, p. 122318. doi: 10.1016/j.biortech.2019.122318.

Zhang, Y. *et al.* (2021) 'Environmental sustainability assessment of pig manure mono- and co-digestion and dynamic land application of the digestate', *Renewable and Sustainable Energy Reviews*, 137(October 2020), p. 110476. doi: 10.1016/j.rser.2020.110476.

Zhao, B. *et al.* (2018) 'Effect of pyrolysis temperature, heating rate, and residence time on rapeseed stem derived biochar', *Journal of Cleaner Production*, 174, pp. 977–987. doi: 10.1016/j.jclepro.2017.11.013.

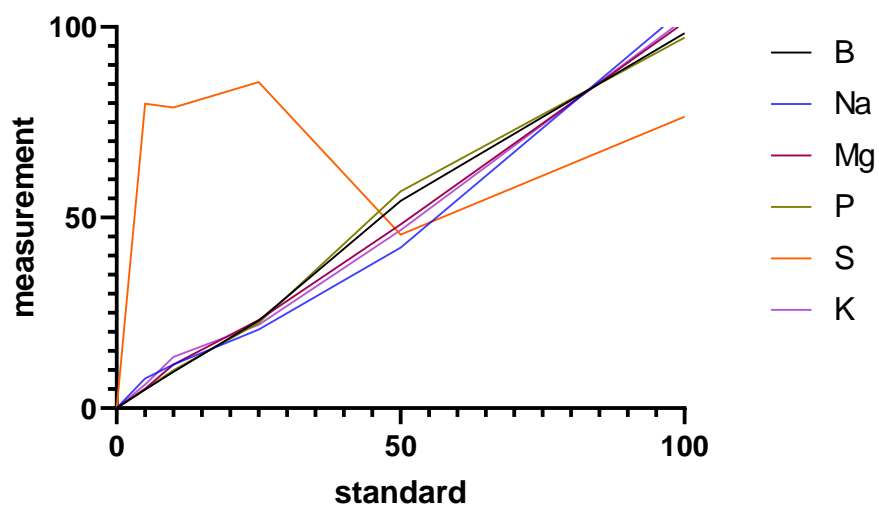
Zhao, L. *et al.* (2013) 'Heterogeneity of biochar properties as a function of feedstock sources and production temperatures', *Journal of Hazardous Materials*, 256–257, pp. 1–9. doi: 10.1016/j.jhazmat.2013.04.015.

Zhao, R., Coles, N. and Wu, J. (2015) 'Soil carbon mineralization following biochar addition associated with external nitrogen', *Chilean journal of agricultural research*, 75(4), pp. 465–471. doi: 10.4067/S0718-58392015000500012.

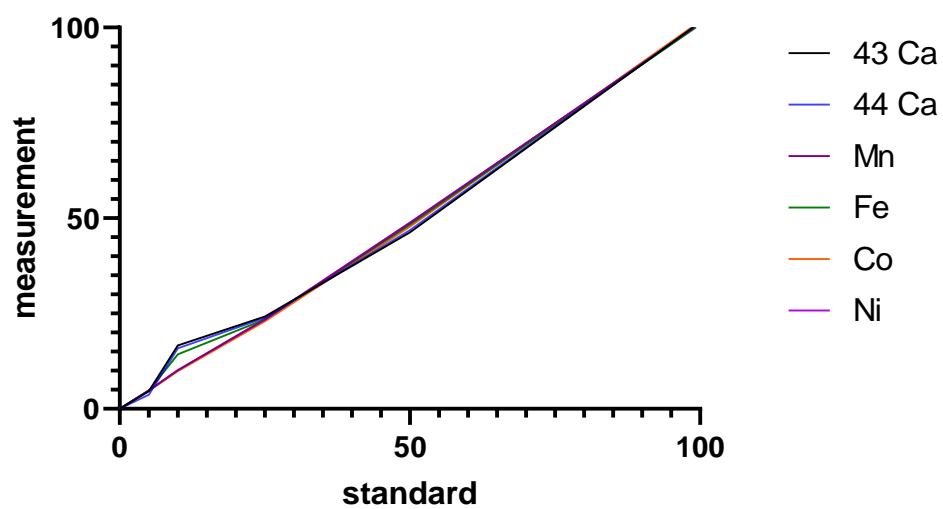
Zhou, Y. *et al.* (2021) 'Production and beneficial impact of biochar for environmental application: A comprehensive review', *Bioresource Technology*, 337(June), p. 125451. doi: 10.1016/j.biortech.2021.125451.

Appendix

ICP-MS calibration curve



ICP-MS calibration curve



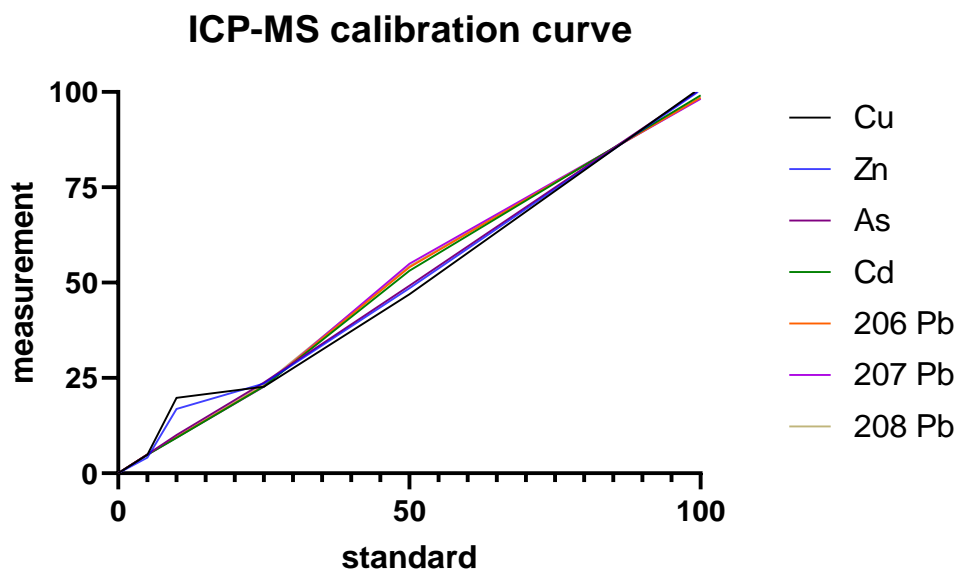


Table 37: D- and G- band values of biochars obtained through Raman analysis

Material	Temperature (°C)	D band (cm ⁻¹)	G band (cm ⁻¹)
Peat	450	1368.08	1582.39
	550	1357.2	1590.32
	650	1346.09	1587.24
	750	1341.32	1591.87
Peat fibre	450	1364.91	1587.02
	550	1358.79	1590.32
	650	1339.5	1596.27
	750	1341.32	1590.32
Fine ugw	450	1366.72	1570.25
	550	1358.57	1587.02
	650	1355.62	1594.95
	750	1344.27	1582.39
B black	450	1379.39	1591.87
	550	1358.79	1588.78

	650	1350.85	1594.95
	750	1350.63	1590.11
B white	450	1355.62	1582.61
	550	1360.38	1584.15
	650	1344.27	1587.02
	750	1350.85	1581.06

b black

